THE UNIVERSITY OF CHICAGO

SEMAPHORIN SIGNALING COORDINATES THE COLLECTIVE MIGRATION OF EPITHELIAL CELLS IN THE *DROSOPHILA* EGG CHAMBER

A DISSERTATION SUBMITTED TO
THE FACULTY OF THE DIVISION OF THE BIOLOGICAL SCIENCES
AND THE PRITZKER SCHOOL OF MEDICINE
IN CANDIDACY FOR THE DEGREE OF
DOCTOR OF PHILOSOPHY

COMMITTEE ON DEVELOPMENT, REGENERATION, AND STEM CELL BIOLOGY

BY

CLAIRE STEDDEN

CHICAGO, ILLINOIS

MARCH 2019

DEDICATION

This dissertation is dedicated to my parents, for their never-ending support and encouragement in all of my endeavors.

TABLE OF CONTENTS

LIST OF FIGURES

LIST OF TABLES

ACKNOWLEDGEMENTS

I would like to thank Sally for her mentorship and support. I am grateful that she always makes time for her students, especially for the care she takes with teaching us how to present and write, and that she is supportive of each individual's goals, allowing me to complete two internships during graduate school. I've learned a lot from my time in her lab.

I would also like to thank the lab for creating an interesting and fun place to work, especially Darcy for supporting me when I first joined the lab, Maureen for her rigor and critical insights, Adam for keeping things lighthearted, Kari for demonstrating how to be efficient at bench work, Audrey for scientific discussions, Kristen for being a great bay-mate, and Allison for her constant enthusiasm about everyone's work and willingness to help us all out, it really kept my spirits up and made my project what it is today.

I would like to thank my committee, Ilaria, Ed, and Vicky for thoughtful guidance and feedback throughout this work. Also, Kristine Gaston, for always being someone I could turn to, and Abby Stayart, for creating an amazing program that kept me going.

I would also like to thank Younan, Louesa, Kamil, Chris, Jon, and Rebeccah, for their friendship, it would have been hard to make it without them. And importantly, I want to thank my family. First my parents, Marilyn and David, for their constant encouragement, support, patience, and belief in me, which have made it possible for me to be where I am today. Also, my sister, Holly, for always being upbeat and positive. And finally, Will for his insights, perspective, sense of adventure, and humor.

ABSTRACT

Collective migration of epithelial cells is essential for tissue morphogenesis, wound repair, and the spread of many cancers, yet how individual cells signal to one another to coordinate their movements is poorly understood. My dissertation work introduces a paradigm for regulating collective cell migration via semaphorin signaling. Semaphorins are transmembrane guidance cues that typically regulate the motility of neuronal growth cones and other migrating cells by acting as repulsive cues within the migratory environment to activate the plexin family of receptors, which are expressed in the motile cells. Studying the follicular epithelium of *Drosophila* revealed that a transmembrane semaphorin, Semaphorin-5c (Sema-5c), promotes collective cell migration by acting within the migrating cells themselves, not the surrounding environment.

My work focused on how Sema-5c could promote migration in this unconventional manner. Here I show that Sema-5c is planar polarized within the follicular epithelium, such that it is enriched at the leading edge of each cell. This location places it in a prime position to send a signal to the trailing edge of the cell ahead, and thus communicate directional information between neighboring follicle cells during migration. My data demonstrate that Sema-5c can signal across cell-cell boundaries and this activity suppress protrusions in neighboring cells. I also find that Plexin A (PlexA) is the receptor that transduces this signal and that it is enriched at the trailing edge of each cell, the correct location to receive a signal from Sema-5c. PlexA interacts with the actin disassembly factor Mical, and I present data that are suggestive of Mical acting downstream of PlexA during follicle cell migration. Together, these data suggest that Sema-5c promotes collective motility by providing a repulsive signal from the leading edge of each cell to the trailing edge of the cell ahead.

My work also revealed that Sema-5c interacts with another factor that promotes migration of the follicular epithelium, the receptor tyrosine phosphatase Lar. Like Sema-5c and PlexA, Lar is known for its role in nervous system development. Overall, my studies have uncovered a system in which multiple transmembrane guidance cues work in concert to coordinate individual cell movements for collective motility.

CHAPTER 1: INTRODCUTION TO COLLECTIVE CELL MIGRATION DURING DEVELOPMENT

1.1 PREFACE

Embryonic development requires a complex set of cellular behaviors that creates the shape of tissues. Collective cell migration plays a key role during these shape changes, and it is increasingly recognized that semaphorin signaling can guide such migration events. This dissertation explores the role of semaphorin signaling during collective migration of follicular epithelial cells in the *Drosophila* egg chamber. This chapter will introduce collective cell migration, semaphorin signaling, and discuss our current understanding of follicle cell migration.

1.2 COLLECTIVE CELL MIGRATION

Collective cell migration is an essential biological process. During embryonic development, it is required for the complex tissue remodeling events that shape the organism (Mayor and Etienne-Manneville, 2016; Scarpa and Mayor, 2016). In adults, it is involved in wound healing and the metastasis of many tumor types (Friedl and Gilmour, 2009; Friedl et al., 2012; Lintz et al., 2017; Shaw and Martin, 2016). When cells move collectively, every cell must regulate its migration to move in the same direction as all the neighboring cells in the tissue. How cells move individually has been extensively studied, but less is known about how they coordinate their motility to move as a coherent group. Here I will introduce single cell motility, then discuss the commonly occurring types of collective cell migration and our current understanding of the mechanisms cells use to coordinate their movement.

Mechanisms underlying single cell migration

In order to appreciate the high level of coordination required for collective cell migration, we first need to understand what it takes for a single cell to migrate, as collectively migrating cells utilize the same migration machinery as individual cells. When a cell migrates, it polarizes in the direction of migration, forming a leading and trailing edge (Figure 1.1). Actin-rich protrusions, adhesions with the extracellular environment, and stress fibers are often key players in the migratory process (Ridley, 2003).

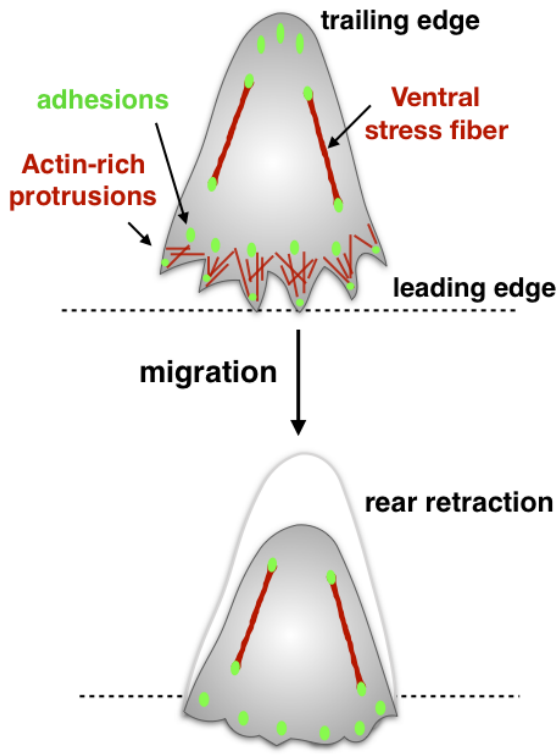

Figure 1.1. Mechanisms underlying individual cell migration A schematic of a single migrating cell. When a cell migrates, it becomes polarized in the direction of migration. From its leading edge, it extends actin-rich protrusions and forms new adhesions with the substrate. These adhesions grow as the cell migrates forward, with some persisting until the rear of the cell. The adhesions are disassembled as the cell moves forward and the rear of the cell retracts. Many migrating cells also contain stress fibers that run the length of the cell. Adapted from Ridley et al., 2003, DePascalis et al., 2017.

Cells can extend a variety of actin-rich protrusions from their leading edge, including lamellipodia and filopodia (Ridley, 2011); here I will focus on lamellipodia because they are often formed in collectively migrating cells. Lamellipodia are composed of branched actin networks that are formed in large part by the Arp2/3 complex, which is activated by

SCAR/WAVE proteins (Pollitt and Insall, 2009; Ridley, 2011). Rho GTPases also play an important role in lamellipodia, in particular Rac, which activates the SCAR/WAVE proteins (Pollitt and Insall, 2009; Ridley, 2011). Upon extension, actin-based protrusions are stabilized through forming new adhesions with the extracellular environment, which is often an extracellular matrix (ECM) (Ridley, 2003).

Cells adhere to the ECM through focal adhesions, and integrin family proteins are a major player in these adhesions. Integrins are receptors that bind the ECM on their extracellular side and connect to the actin cytoskeleton on their cytoplasmic domain, via adaptor proteins such as talin and vinculin, thereby linking the external ECM with the internal actin network (De Pascalis and Etienne-Manneville, 2017; Ridley, 2003). Focal adhesions are vital to cell migration because they enable the cell to adhere to a substrate and generate traction forces on it (Ridley, 2003; Scarpa and Mayor, 2016). As a cell moves forward, new adhesions are formed at the leading edge. At the trailing edge, older adhesions are disassembled, which enables the rear of the cell to detach from the ECM and retract. This retraction relies on actomyosin-mediated contraction and the GTPase RhoA (Ridley, 2003; Rørth, 2009; Zegers and Friedl, 2014).

A major structure that binds to and regulates focal adhesions is the stress fibers. There are many types of stress fibers but I will focus on the ventral stress fibers, since they are most relevant to my work. Ventral stress fibers are contractile actomyosin structures composed of actin filaments and Myosin II that have focal adhesions at their ends (Figure 1.1) (Tojkander et al., 2012). Force transmission in a cell relies on the interaction of Myosin II with the actin filaments, and though this generation of tension they regulate assembly, growth, and maintenance of focal adhesions (Ridley, 2003; Tojkander et al., 2012). Stress fibers are not present in all migrating cells and their role in movement is still being elucidated, but they are

thought to provide force generation and communication between the cell and the ECM via focal adhesions (De Pascalis and Etienne-Manneville, 2017; Tojkander et al., 2012).

Overview of collective cell migration

Collective motility during development

In many cases, cells move not individually, but in groups that coordinate their movements. This collective behavior keeps tissues intact during remodeling, ensures the proper distribution of cells in newly shaped tissues, and can contribute to tumor metastasis (Friedl and Gilmour, 2009; Lintz et al., 2017; Michaelis, 2014; Rørth, 2009). In order for collective movement to occur, the polarity of the migration machinery within each cell needs to be organized across the entire group of moving cells (Mayor and Etienne-Manneville, 2016; Rørth, 2012; Scarpa and Mayor, 2016). How individual cells coordinate their polarities is a fascinating area of investigation. In the subsequent sections I will give an overview of collective migration, and then go into the mechanisms underlying this complex cellular coordination.

Collective migration encompasses a specific set of cell behaviors. Collectively migrating cells move together and make contact with each other in loosely or closely associated groups. Importantly, there is organization between these cells and they influence the polarity of one another to maintain this organization (Rørth, 2009; Rørth, 2012; Scarpa and Mayor, 2016). This is a key feature of collective migration because it distinguishes it from a group of cells that are each moving independently in the same direction at the same time.

Collective cell migration can be divided into a variety of categories, depending on how adherent the cells are to one another and the shape of the tissue involved (Figure 1.2). Cells that are loosely associated can move together in streams or chains, such as during migration of neural

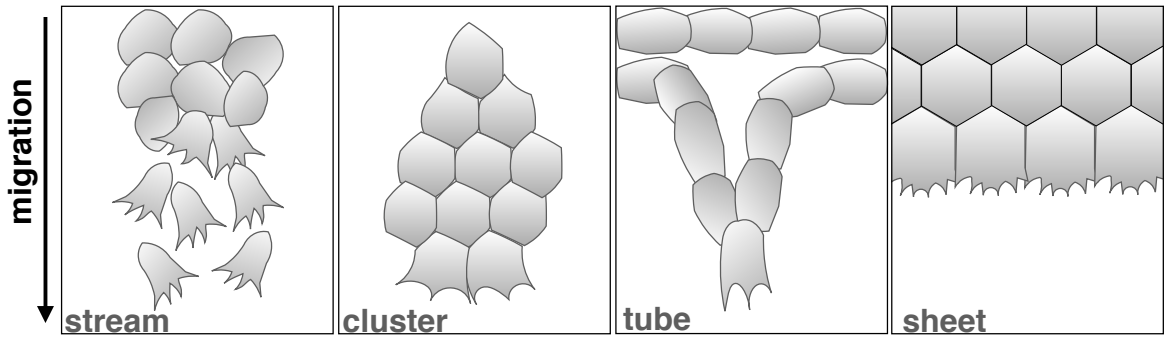

Figure 1.2. Collective migration requires coordinated polarity across the tissue and can occur in streams, tubes, clusters and sheets Schematics of collectively migrating cells. When cells migrate as a group, they become polarized in the same direction with leading edges aligned across the tissue. When cells are loosely adhered, they migrate in streams. When cells are tightly adhered, they can migrate in clusters, tubes, or sheets. Adapted from Scarpa and Mayor, 2016.

crest cells (Rørth, 2009; Theveneau and Mayor, 2012) or mesodermal cells during gastrulation in zebrafish and *Xenopous* (Theveneau et al., 2013). Cells that are tightly adhered to one another can migrate in clusters, tubes and sheets (Rørth, 2009).

Two well studied examples of migratory clusters are the posterior lateral line primordium in zebrafish and the border cells in the *Drosophila* egg chamber (Friedl et al., 2012; Rørth, 2009; Scarpa and Mayor, 2016). The posterior lateral line primordium is a group of cells that originates as an epithelial placode and then migrates posteriorly to lay down sensory organs (Haas and Gilmour, 2006; Scarpa and Mayor, 2016). The border cells are a cluster that delaminates from an epithelium at the anterior of the egg chamber and migrates posteriorly toward the oocyte as a tightly associated group (Montell, 2003; Rørth, 2009). In both of these cases, the cluster is polarized with a front and rear (Cai et al., 2014; Haas and Gilmour, 2006).

Collective migration in tubes is observed during sprouting and branching morphogenesis, which is required for the formation of many organs including the vasculature and lungs (Scarpa and Mayor, 2016; Vasilyev et al., 2009). During angiogenesis, endothelial cells migrate to form

new blood vessels. In the *Drosophila* trachea, cells sprout from epithelial placodes to form the tracheal braches (Mayor and Etienne-Manneville, 2016; Rørth, 2009; Scarpa and Mayor, 2016). Tube migration has also recently been reported during morphogenesis of the kidney nephron in zebrafish (Vasilyev et al., 2009).

Collective migration in sheets can be seen in a variety of situations. When a gap is generated in a monolayer of cultured epithelial or endothelial cells, such as though a scratch wound, the cells migrate in response to the free space in order to fill the gap (Rørth, 2009). Similar behavior occurs during wound healing *in vivo* (Liu and Kao, 2015; Shaw and Martin, 2016). Sheet migration can also occur without the trigger of free space, such as during formation of the optic cup in zebrafish (Sidhaye and Norden, 2017) or when cultured cells are plated on circular micropatterns (Doxzen et al., 2013).

Collective motility plays a role in metastasis

The migration of cell streams and clusters also contributes to the metastasis of solid tumors (Friedl et al., 2012; Lintz et al., 2017). Metastases were traditionally thought to be due to the invasion of single tumor cells, but recent studies have shown that groups of cells are also a major player in this process (Friedl et al., 2012; Lintz et al., 2017). An organotypic culture model was used to investigate the migration of squamous cell carcinoma (SCC) cells and revealed that they collectively migrate in streams (Gaggioli et al., 2007). In this *in vitro* model, SCC cells always invade in groups and retain their epithelial characteristics, such as expressing E-cadherin. These groups follow leading fibroblasts, a fibroblast is always in the front of the stream, and activity of the fibroblasts is required for the SCC cells to invade. Additionally, a mouse model of breast cancer was used to show that tumor cells move in clusters, not just as single cells, throughout

metastasis (Cheung et al., 2016). In this study, mosaic tumor organoids, containing a mixture of cells that expressed either a red or green fluorescent marker, were injected into mice. The tumor cells migrated away from the primary tumor, causing metastases in other areas. If the resulting metastases arose from single cells, then they should be a single color, but if they arose from a cluster then they should be multicolored. Multicolored metastases were observed and, in this model, it was estimated that multicellular clusters contributed to 97% of metastases. Multicolored tumors could also result from serial seeding, but subsequent experiments showed that this was unlikely to be the case. Further observations supported this, as the authors observed multicolored groups of cells at five stages of metastasis, including invasive streams at the primary tumor as well as in disseminated tumor cell clusters. Interestingly, invasion in clusters has been observed to increase the viability of the resulting metastases (Cheung et al., 2016; Duda et al., 2010). Since the mechanisms underlying collective motility are likely to be conserved between development and pathological conditions, studies of collective cell migration in developing tissues will contribute to our understanding of the role these processes play during metastasis (Friedl and Gilmour, 2009).

Coordinating individual cell motility for collective movement

A variety of mechanisms are utilized to coordinate migratory behaviors between neighboring cells. Here I will highlight examples from each category that demonstrate how they feed into generating collective movement.

Cues in the environment

Chemotactic cues in the migratory environment often play a role in guiding collective cell migration. For example, the *Drosophila* border cells respond to a gradient of Pvf1, a ligand for the receptor tyrosine kinase PVR, and Spitz and Keren, both EGFFR ligands, coming from the oocyte (Duchek and Rørth, 2001; McDonald et al., 2003; McDonald et al., 2006). In the mouse retina, endothelial cells are guided by a gradient of VEGF-A (Gerhardt et al., 2003). The organizing role of chemotactic cues has nicely been shown during collective migration of the zebrafish posterior lateral line primordium, which migrates in response to an external cue, the chemokine SDF-1. When the receptor for SDF-1 is knocked out, cells in the lateral line primordium are each individually capable of migrating, but since they are tightly adhered to one another and have lost their directional migratory cue, the net displacement of the cluster is greatly reduced (Haas and Gilmour, 2006). This shows that a cue in the migratory environment can play a key role in coordinating polarity across a group of cells.

Leading the way

During collective migration, the cells at the front of the group often act as leaders to guide the way (Mayor and Etienne-Manneville, 2016). For example, leader cells play an important role during migration of the border cells in the *Drosophila* egg chamber. The border cells have polarity across the entire cluster, with Rac having highest activity in the leading cell (Cai et al., 2014). When Rac is photoinhibited in the leading cell, the follower cells lose their sense of direction and send out protrusions away from the leading edge (Cai et al., 2014). Additionally, photoactivating Rac in a single cell of the group is able to determine the migration direction for

the entire cohort (Wang et al., 2010). These data suggest that polarity information is specifically communicated from the leader cell to the follower cells.

It has been shown that, in some systems, only the leading cells need to be able to sense guidance cues in order for the whole group to migrate. During development of the *Drosophila* trachea, cells migrate in response to a cue from the surrounding tissue, the FGF homolog *branchless,* which activates the receptor *breathless.* In a *breathless* mutant, tracheal migration is greatly reduced, but a single cell clone of *breathless* expression is sufficient to rescue movement of the entire cluster (Lebreton and Casanova, 2014). Such ability to organize and influence the behavior of neighboring cells is a hallmark of collective migration and is seen in many additional cases including migration of neural crest cells in *Xenopus* and the posterior lateral line in zebrafish (Mayor and Etienne-Manneville, 2016; Scarpa and Mayor, 2016).

Followers don't just follow

Despite the role of the leader cells in guiding migration, the follower cells can also play important roles, and without them the leaders don't effectively migrate. Followers can respond to soluble cues, help to polarize the leader cells, and can even help generate the gradients of chemokines. For example, during migration of the lateral line in zebrafish, the follower cells are required to generate the gradient along which the group migrates. The lateral line primordium migrates posteriorly along a stripe of SDF-1, but SDF-1 has a uniform distribution; it is not a gradient. The lateral line cells can generate their own gradient because the cells at the rear of the group act as a sink for SDF-1 (Donà et al., 2013; Scarpa and Mayor, 2016). The power of the rear cells to guide this migration is demonstrated by the fact that the stripe of SDF-1 can even act

as a “two-way street”; if it terminates prematurely, the lateral line primordium can turn around migrate anteriorly back along the same stripe of SDF-1 (Haas and Gilmour, 2006).

Another example of follower cells promoting migration of the entire group is seen during neural crest cell migration. When the follower cells come into contact with the leader cells, they polarize the leader cells and promote protrusion away from the region of contact (Stramer and Mayor, 2016). This type of behavior is called contact inhibition of locomotion and will be discussed in more detail below.

Migration in the absence of a leading edge

It is being increasingly recognized that follower cells play a large role in collective cell migration, and in fact some cell populations collectively migrate with no leader cells at all. When MDCK cells are plated on circular micropatterns of fibronectin, they collectively rotate, migrating in a circle with no leading edge (Doxzen et al., 2013). A critical density must be reached for this behavior to be seen; at low density, the cells migrate randomly. It seems that cell-cell adhesion plays a role in the ability to achieve stable collective rotation, as cells with reduced E-cadherin levels only transiently rotate. It is possible that reduced cell-cell adhesions prevent the stable transmission of guidance cues between neighboring cells (Doxzen et al., 2013). Collective migrations in the absence of a free leading edge have been shown to be involved in morphogenesis *in vivo*, during formation of the optic cup and kidney nephron in zebrafish and in the *Drosophila* egg chamber, (Haigo and Bilder, 2011; Sidhaye and Norden, 2017; Vasilyev et al., 2009).

Coordinating cell movements via mechanical cues

The above examples demonstrate that polarity information is transmitted throughout a tissue during collective migration. Leader cells transmit polarity information to followers, while followers can transmit polarity information back to the leaders and amongst themselves. An active area of investigation is determining how this information is communicated and studies show that mechanical cues between cells play an important role.

When cells migrate in tubes, clusters or sheets they are mechanically coupled to one another though cell-cell adhesions. These physical connections, particularly adherens junctions, allow cells to exert pulling forces on their neighbors, which transmits information from one cell to another via mechanosensing. The force induces conformational changes in proteins at the adhesions, which then exert downstream signaling effects (Ladoux and Mège, 2017; Mayor and Etienne-Manneville, 2016).

The ability of pulling forces to lead to cell polarization was nicely shown in *Xenopus* mesendoderm cells. During *Xenopus* gastrulation, presumptive mesendoderm cells reside on the outer surface of the embryo and migrate inward to their correct location along a substrate of fibronectin, a component of the ECM (Davidson et al., 2002). When single mesendoderm cells are isolated *in vitro*, pulling on C-cadherin with optical tweezers at one side of a cell induced protrusions to form at the opposite side (Weber et al., 2012). It was proposed that a similar mechanism could operate during collective migration of mesendoderm cells *in vivo*. In this model, the cells at the trailing side of the mesendoderm sheet provide resistance to the forward movement, effectively generating a pulling force on those cells in front of them, which could induce protrusions across the entire sheet in the direction of migration.

Another example of the mechanical cues involved in collective movement occurs during migration of cultured epithelial cells. In these cells, Merlin, a regulator of the Hippo pathway, is responsive to pulling forces and helps direct migration (Das et al., 2015). In stationary cells, Merlin localizes to cell-cell junctions. However, when leader cells begin to migrate they cause a pulling force on the follower cells, as they are mechanically coupled though their cell-cell adhesions, and a proportion of the junctional Merlin relocalizes to the cytoplasm. This allows for activation of Rac1 and protrusion formation in the direction of migration. These studies suggest that mechanical coupling between cells provides a means to communicate polarity information across a group.

Cell-cell coordination via contact inhibition of locomotion

Biochemical cues also play a role in organizing polarity information across cells, particularly in migrating neural crest cells (Stramer and Mayor, 2016). These cells migrate collectively, but make transient cell-cell contacts instead of being tightly adhered to one another. When *Xenopus* neural crest cells are cultured *in vitro*, leading-edge cells from an explant have a higher directional persistence than individual cells, suggesting that the directional migration is driven by cell-cell contacts (Carmona-Fontaine et al., 2008).

One mechanism that contributes to the collective behavior of these cells is called contact inhibition of locomotion (CIL). CIL occurs when a migrating cell, upon contact with another cell, stops and repolarizes to migrate away from the point of contact (Stramer and Mayor, 2016). CIL happens in concert with other cues that together foster collective migration, including a constrained migration path (Scarpa and Mayor, 2016), a chemotactic cue in the environment (Theveneau et al., 2010; Theveneau et al., 2013) and ‘coattraction’ between the cells via a

secreted chemoattractant (Carmona-Fontaine et al., 2011). It has been proposed that CIL generates collective migration by polarizing the group; it promotes protrusions in the leader cells, away from their points of contact with follower cells, and prevents protrusions at other points of cell-cell contact. This organization, with large protrusions in the leading cells and reduced protrusions at cell-cell contacts within the group, is seen in many examples of collective cell migration, and it has been suggested that CIL is a fundamental process underlying collective movement (Mayor and Etienne-Manneville, 2016).

CIL can be broken down into three phases: establishing cell-cell contact, transmitting a signal into the cell, and changing behavior in response to that signal, which in this case is to retract protrusions away from the site of contact and repolarize in the opposite direction (Mayor and Etienne-Manneville, 2016). Many cell-surface molecules have been shown to be involved in CIL, including planar cell polarity (PCP) proteins (Carmona-Fontaine et al., 2008; Mayor and Etienne-Manneville, 2016). In neural crest cells, knocking down the PCP protein Dishevelled disrupts CIL, decreasing directional migration and causing mis-orientation of protrusions away from the leading edge (Carmona-Fontaine et al., 2008). Upon contact between Xenopus neural crest cells, the PCP factors Dishevelled, Frizzled 7 and Wnt 11 accumulate at the newly formed cell-cell interface and activation of these proteins leads to intracellular signaling that repolarizes the cell (Carmona-Fontaine et al., 2008). Specifically, RhoA is activated at the site of cell-cell contact, while Rac1 is inhibited at the contact but activated away from it (Mayor and Etienne-Manneville, 2016; Stramer and Mayor, 2016; Theveneau and Mayor, 2012). The role of CIL in migrating neural crest cells is a clear example of how internal biochemical signals play a role in organizing cells for collective movement.

It is possible that CIL behaviors represent a broader class of mechanisms by which repulsive cues can be deployed to guide collective movement. A recent study showed that CIL can promote directional collective migration through a 'chase and run' mechanism. In this case, a leading cohort of cells secretes a chemotactic cue that attracts a follower cohort, then when the follower cohort reaches the leader cohort and makes contact, this induces CIL and propels the leader cohort forward, and the cycle repeats (Theveneau et al., 2013). This suggests that there is still much to be learned about how repulsive cues guide collective movement in multiple cell types, and it is likely that further biochemical cues remain to be elucidated. Semaphorins are one of the most well-studied families of repulsive cues and their roles in collective motility will be discussed below.

1.3 THE ROLE OF SEMAPHORINS IN CELL MIGRATION AND TISSUE MORPHOGENESIS

The semaphorins are a large family of signaling proteins that play key roles during embryonic development (Alto and Terman, 2017; Jongbloets and Pasterkamp, 2014; Tran et al., 2007). They were first recognized for their role in axon guidance, but have since been found to regulate the morphology and behavior of a variety of cell types in many organisms, ranging from flies to mammals (Alto and Terman, 2017). Through my dissertation work, I have found that a transmembrane semaphorin coordinates the collective migration of epithelial cells during development. Although transmembrane semaphorins have been found to act in an epithelial context, they had not been implicated in epithelial motility (Xia et al., 2015; Yoo et al., 2016). Additionally, there have been indications that transmembrane semaphorins can guide migration, but our understanding of how they are deployed to do this is still in the early stages (Kerjan et

al., 2005; Toyofuku et al., 2004b). My studies have uncovered a paradigm by which transmembrane semaphorins organize motility within a migrating cohort that has not yet been described for any semaphorin, but which could be broadly applicable to this family of proteins. To set the stage for this work, here I will introduce semaphorins and their signaling mechanisms, describe the roles transmembrane semaphorins play in epithelia, and then discuss what is known about the role of semaphorins in cell migration during development.

Overview of semaphorins and their signaling mechanism

The semaphorin (sema) family contains eight classes, all of which share a conserved extracellular Sema domain (Figure 1.3) (Yazdani and Terman, 2006). These classes primarily represent exclusively invertebrate, vertebrae, or vial semaphorins. The exception is class 5, which has homologs in both invertebrates and vertebrates. Semaphorins include secreted (classes 2, 3 and V), cell surface-attached (class 7), and transmembrane proteins (classes 1, and 4-6) (Yazdani and Terman, 2006).

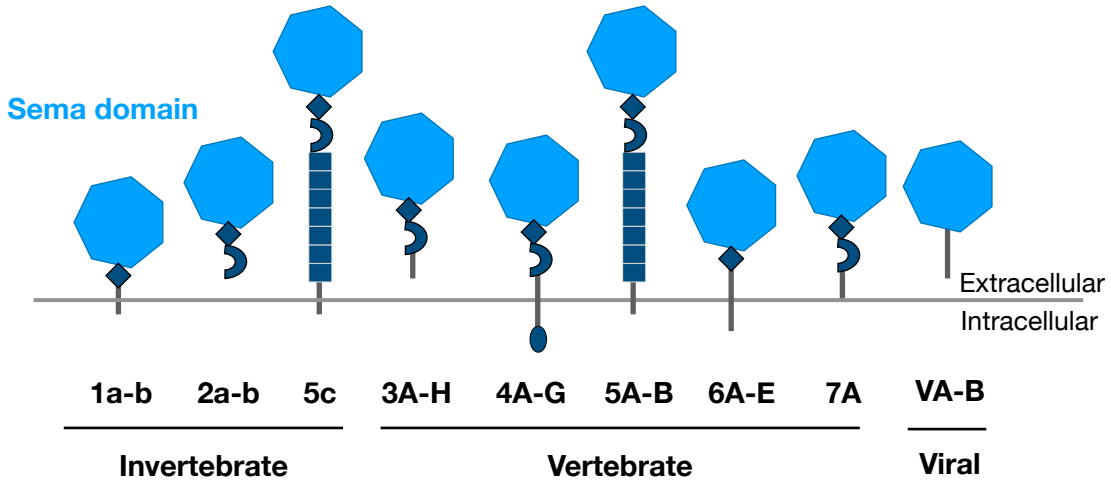

Figure 1.3. The semaphorins A schematic of the eight classes of semaphorins. Classes 1, 2 and 5 are invertebrate semaphorins, classes 3-7 are vertebrate semaphorins, and VA-B are vial semaphorins. Class 5 is the only class with homologs in both invertebrates in vertebrates. All semaphorins share a conserved Sema domain on the extracellular side (Tran et al., 2007; Yadzi and Terman, 2006; Hung and Terman, 2011).

Semaphorins are best known as ligands for the Plexin family of receptors (Figure 1.4). Like semaphorins, plexins also have an extracellular Sema domain. Semaphorins and plexins bind via their Sema domains, which activates the plexin by inducing conformational changes (Alto and Terman, 2017; Tran et al., 2007; Yazdani and Terman, 2006). There are four classes of Plexins: PlexA-B in invertebrates and PlexA-D in vertebrates. In many cases, each class of semaphorin activates a specific class of plexins. Co-receptors can also associate with plexins and affect their signaling; the best studied are neuropilins, which are required as co-receptors by class 3 semaphorins (Alto and Terman, 2017; Tran et al., 2007). More recently, it has been found that specific classes of semaphorins can also signal via their cytoplasmic domain, which is referred to as reverse signaling (Battistini and Tamagnone, 2016).

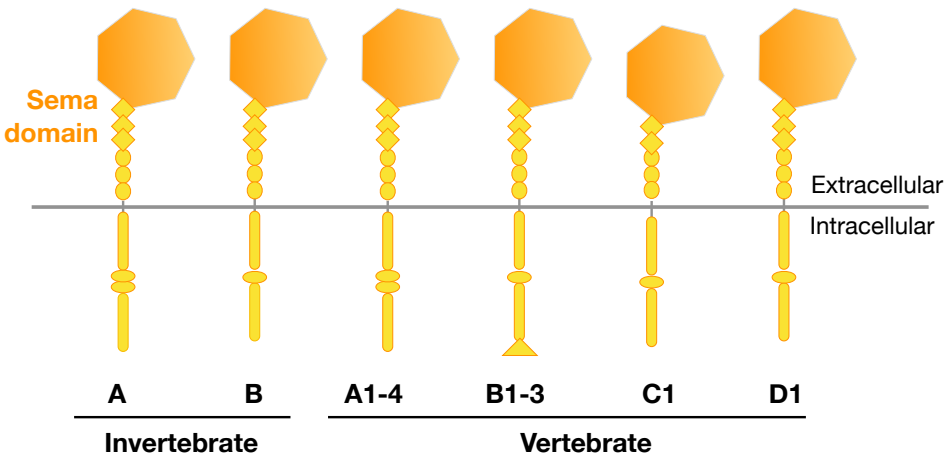

Figure 1.4 The plexins A schematic of the four classes of plexins, Classes A and B are invertebrate plexins, while classes A-D are vertebrate plexins. All share a conserved Sema domain on the extracellular side, though which they bind to semaphorins. (Tran et al., 2007; Yadzi and Terman, 2006; Hung and Terman, 2011).

Semaphorins were initially recognized as repulsive cues for axon guidance (Kolodkin et al., 1992; Luo et al., 1993). In the developing nervous system, plexin receptors are expressed within axonal growth cones and these growth cones are steered toward their targets by

semaphorin-expressing cells present in specific regions of the environment (Figure 1.5A). Upon contact with the repulsive semaphorin cue, the plexin-expressing growth cone will collapse its protrusions and turn away (Alto and Terman, 2017; Casazza et al., 2007; Tran et al., 2007). Studies have now shown that semaphorins can also act as an attractive cue, depending on co-receptors and environmental factors, which reveals the complexity of this field (Artigiani et al., 2004; Barberis et al., 2004; Giordano et al., 2002; Li and Lee, 2010a; Li et al., 2012; Toyofuku et al., 2004a).

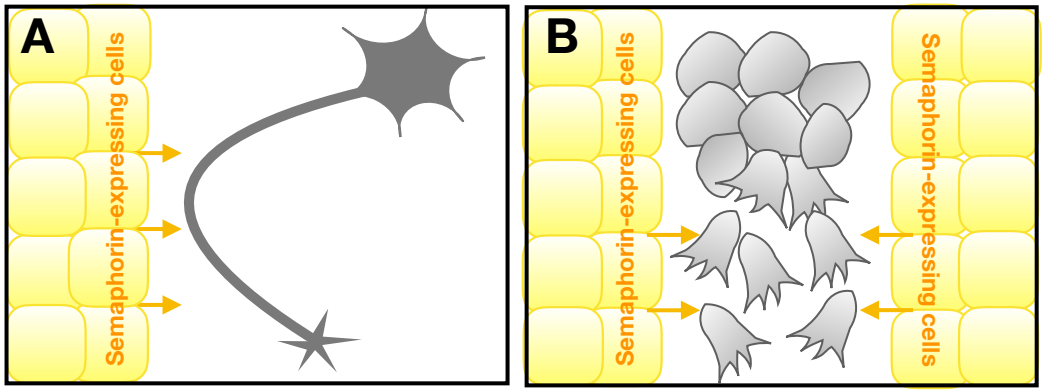

Figure 1.5. Semaphorins act as repulsive cues in the migratory environment (A) A schematic of axon guidance, the axon (gray) is prevented from entering the yellow region by a repulsive cue from semaphorin-expressing cells. (B) A schematic of neural crest cell migration. When neural crest cells (gray) migrate, they are kept on the correct migratory path by repulsive semaphorin cues in the surrounding tissue (yellow), adapted from Scarpa and Mayor., 2016.

The ability to collapse cellular protrusions is a well-established outcome of semaphorin activity and is caused by a variety of downstream plexin effectors that target small GTPases, microtubules, and F-actin (Alto and Terman, 2017). Although the intracellular domains of the plexin classes vary slightly, they all contain a GAP homology domain for Ras and Rap family GTPases. When activated by a semaphorin, the plexin GAP domain for R-Ras is activated, leading to reduced R-Ras activity and decreased integrin activation (Alto and Terman, 2017;

Oinuma et al., 2004; Oinuma et al., 2006; Tran et al., 2007). Plexin B is also able to activate Rho, by recruiting a Rho-GEF to the C-terminus, and inhibit Rac, by sequestering it from its effector PAK (Pasterkamp et al., 2003). Semaphorin-plexin signaling also acts on the microtubule cytoskeleton through CRMP-2, which promotes microtubule polymerization; CRMP-2 is inactivated by Sema3A activity (Tran et al., 2007). Since the semaphorins are a large and varied protein family, it is often suggested that more mechanisms underlying their activity remain to be uncovered.

Despite these findings, an interaction that eluded researches for many years was a direct connection between semaphorin-plexin signaling and the actin cytoskeleton. In 2002, it was discovered that the protein Mical could provide this link (Terman et al., 2002). The Mical family is composed of one *Drosophila* Mical and three mammalian MICALs (Alto and Terman, 2017). Mical is a Redox enzyme that direcly binds to and disassembles bundled F-Actin (Hung et al., 2010; Hung et al., 2011). It also binds to class A plexins through a Mical interacting region on their cytoplasmic domain. Mical was found to act downstream of semaphorin signaling during formation of the *Drosophila* bristle (Hung et al., 2010), showing for the first time that semaphorin-plexin signaling can directly destabilize the actin cytoskeleton.

Transmembrane semaphorins in an epithelial context

Recent studies suggest that semaphorin-plexin signaling can regulate epithelial dynamics during morphogenesis and wound repair in mouse, *Drosophila* and zebrafish. These studies demonstrate that semaphorins and plexins can play wider roles than have previously been recognized. They also reveal that a transmembrane semaphorins and its plexin receptor can be expressed in the

same tissue, which is in contrast to the classic model that they are expressed in separate tissues and only signal when these tissues come into contact.

In renal tubular epithelial cells of the mouse kidney, semaphorins and plexins are required to orient the cell division plane during morphogenesis and tissue repair (Xia et al., 2015). Renal tubules in mouse strongly express Plexin-B2. Mice deficient for Plex-B2 and Plex-B1 develop renal tubules with a multilayered morphology, instead of having a single layer of cells surrounding a lumen, suggesting plexin signaling is required for kidney morphogenesis. The renal tubule cells normally divide within the plane of the tissue, but in these knockout mice a large proportion of cells now have a division plane that is shifted perpendicular to the tissue plane, likely leading to the multi-layering. To further study this phenotype, the authors also utilized a kidney injury model in adult mice. In this context, they only needed to remove PlexB2, as Plex-B1 is not expressed in the adult kidney. Following injury, healing did not occur properly in Plexin-B2 deficient mice; there was multilayering and occlusion of the tubules, suggesting plexin signaling is also required during tissue repair. Plexin-B2 is known to be activated by class 4 semaphorins. Sema-4A, Sema-4B, Sema-4C, Sema-4D, and Sema-4G are all expressed in the renal tubules and a triple-knockout mouse also had multilayered tubules following injury. However, this didn't fully recapitulate the Plex-B2 knockdown phenotype, suggesting another Plex-B2 ligand is likely involved. This was the first study to implicate semaphorin-plexin signaling in the orientation of cell division and the authors suggest that it could play a similar role in other contexts.

Semaphorins and plexins also play a role during wound healing in *Drosophila* wing imaginal discs (Yoo et al., 2016). These larval epithelial structures form the adult wings, and knocking down PlexA in the discs causes a large proportion of the resulting wings to have

healing defects following injury. Overexpression of PlexA lacking its cytoplasmic domain also caused healing defects, suggesting it is acting as a DN to compete for PlexA ligands, and that PlexA's role in tissue repair involves cell-cell signaling. The ligands for PlexA are Sema-1a and Sema-1b, and double knock down of these proteins also results in healing defects, although not to the same extent as PlexA knockdown, suggesting that additional PlexA ligands are involved. Data suggest that PlexA is cell-autonomously required for the epithelial rearrangements that occur during wound healing, including basal extrusion of dying cells, by facilitating junctional remodeling. This same study found a similar role for Plexin A1 during tail fin regeneration in zebrafish, suggesting that the role of semaphorin-plexin signaling during wound repair may be conserved.

Overall, these studies show that transmembrane semaphorins and their plexin receptors can coordinate epithelial dynamics when they are expressed in the same epithelium. This expression pattern is intriguing because it suggests that semaphorin-plexin signaling is occurring within a single tissue. This is contrary to the well-studied role of semaphorin-plexin signaling during axon guidance, where the plexin is expressed in the axon and the semaphorin in the environment. Going forward, it will be interesting to see if this mode of semaphorin-plexin signaling plays a role in other contexts.

The role of semaphorins in collective cell migration during development

Semaphorins play a role in cell migration in many developing tissues, and the role they play is often similar to their role during axon guidance (Casazza et al., 2007; Kruger et al., 2005; Tamagnone and Comoglio, 2004). The growth cone that pioneers axonal extension is similar in structure to the protrusive front of a migrating cell (Huber et al., 2003). During axon guidance,

growth cone protrusions are collapsed by semaphorin cues in the environment. Semaphorins also regulate cell migration by suppressing protrusions, likely by promoting disassembly of the actin cytoskeleton and regulating adhesion to the ECM (Barberis et al., 2004; Li and Lee, 2010a; Oinuma et al., 2006; Sadanandam et al., 2010; Serini et al., 2003).

Despite uncovering mechanisms by which semaphorins act on the migration machinery, this does not indicate how semaphorins are deployed to affect collective cell migration *in vivo.* Of the semaphorins, the secreted class 3 semaphorins have been best studied in this context, where they often act as repulsive cues in the migratory environment. In contrast, the role of transmembrane semaphorins in collective cell migration is much less studied, and the manner in which they operate is still fairly mysterious. I will review what is known about each of these topics below.

Secreted semaphorins are well-established to act as cues in the migratory environment

Secreted semaphorins guide collective cell migration by providing repulsive cues in the migratory environment, similar to their role during axon guidance (Casazza et al., 2007; Kruger et al., 2005; Tamagnone and Comoglio, 2004; Tran et al., 2007). One of the best studied examples is the role of class 3 semaphorins in the migration of both cranial and trunk neural crest cells. This was one of the first cases showing that semaphorins can regulate cell migration outside of their role in axon guidance (Eickholt et al., 1999). During neural crest cell migration, the secreted semaphorins line the migratory route to keep the neural crest cells confined to a specific path (Figure 1.5B) (Gammill et al., 2006; Ruhrberg and Schwarz, 2010; Theveneau and Mayor, 2012; Yu and Moens, 2005). A similar role has also been found for class 3 semaphorins during collective migration of endothelial cells to guide formation of the vasculature (Gu and

Giraudo, 2013; Hamm et al., 2016). During endothelial migration, class 3 semaphorins also signal in an autocrine manner, signaling from the leading edge of the cohort of cells to regulate actin dynamics or cell-ECM adhesion (Hamm et al., 2016; Serini et al., 2003).

How transmembrane semaphorins are deployed to guide migration is not well understood

Studies indicate that transmembrane semaphorins may also play a role in collective cell migration during development, but how they do so is not yet clear. A few nice studies demonstrate that transmembrane semaphorins can promote cell migration *in vivo*, but they also demonstrate gaps in our understanding of how these proteins guide cell migration.

In chick embryos, Sema6D is required for the migration of myocardial cells during cardiac development (Toyofuku et al., 2004b). The developing myocardium contains multiple layers, one of which, the trabeculaer layer, contains a population of migratory cells that express Sema6D. The receptor, PlexA1, is expressed in an adjacent layer. The Sema6D-expressing trabecular cells migrate away from the PlexA1-expressing cells. This requires reverse signaling by Sema6D's cytoplasmic domain, upon activation by PlexA1. However, this study failed to explain how this signaling polarizes the cells to migrate away from the PlexA1 source and what maintains the migration after the Sema6D-expressing cells have lost contact with the PlexA1-expressing cells.

Another case in which transmembrane semaphorins affect cell migration is during cerebellar development in mouse. Cerebellar granule cells express Sema6A, which is required for their radial migration, but interestingly, it is turned off in these cells right before the radial migration begins (Kerjan et al., 2005). Further, Sema6A acts non-cell-autonomously during this process. This leaves the mechanism by which Sema6A promotes the movement of these cells a

mystery, but it has been proposed that Sema6A may signal between granule cells as they migrate radially away from the main population, either by acting as a de-adhesion molecule or by being involved in contact mediated repulsion, with an unknown receptor that is expressed in the radially migrating cells (Kerjan et al., 2005; Tran et al., 2007).

These studies demonstrate that the involvement of transmembrane semaphorins in cell migration is likely to be complex, and that further studies will be required to determine the breadth of ways in which they can guide cell migration. In both of these cases, there appears to be a cue in one cell population that signals to another population to migrate away, which is reminiscent of how secreted semaphorins have been show to guide neural crest cells and endothelial cells. However, a repulsive cue doesn't have to be in the migratory environment to guide migration; during CIL repulsive cues act within the migrating cells themselves to help organize and polarize the cohort, as I discussed in the previous section. Interestingly, a transmembrane semaphorin has been shown to elicit CIL between osteoclasts and osteoblasts (Deb Roy et al., 2017). Thus, it is conceivable that a semaphorin and a plexin could coordinate collective cell migration by both being deployed within the migrating cohort, but such a mechanism has not yet been described.

1.4 COLLECTIVE MIGRATION OF THE FOLLICULAR EPITHILIUM IN THE *DROSOPHILA* EGG CHAMBER

The *Drosophila* egg chamber has become an important model system for studies of tissue morphogenesis and collective cell migration. One of the major migratory populations in the egg chamber is a sheet of epithelial cells called the follicular epithelium. My work examined the role of semaphorin signaling during the migration of this tissue. In this section, I will provide an

overview of the structure and development of the egg chamber, introduce the timing and purpose of the migration of the follicular epithelium, and discuss our understanding of how the migration of these cells is organized.

Overview of egg chamber structure and development

The *Drosophila* egg chamber is an organ-like structure that develops in to the fly egg. Each egg chamber consists of a central cluster of 16 germ cells surrounded by a layer of epithelial cells, called follicle cells (Figure 1.6) (Horne-Badovinac and Bilder, 2005). The germ cell population is made up of 15 supporting nurse cells and one oocyte. The follicular epithelium has its apical surface facing inward toward the germ cells and its basal surface facing outward. The basal surface of the epithelium is in contact with a basement membrane extracellular matrix that surrounds the entire structure.

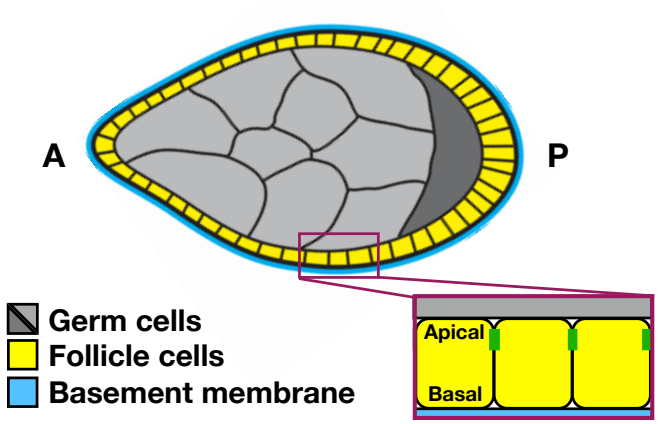

Figure 1.6. Structure of the *Drosophila* egg chamber Schematic of a cross section through the anterior-posterior (A-P) axis of an egg chamber. This small, organ-like structure consists of a central cluster of germ cells, including nurse cells (light gray) and 1 oocyte (dark gray), surrounded by a layer of epithelial cells, called follicle cells (yellow). A basement membrane extracellular matrix surrounds the entire structure (blue). Egg chamber ilustration courtesy of Adam Isabella (Isabella and Horne-Badovinac, 2015).

Egg chambers are located in the *Drosophila* ovary where they are connected in developmental arrays, called ovarioles (Figure 1.7) (Horne-Badovinac and Bilder, 2005; Duhart et al., 2017). Newly-formed egg chambers are assembled in an anterior region of the ovariole

called the germarium, which contains both germline and somatic stem cells, and move posteriorly as they develop (Horne-Badovinac and Bilder, 2005). Each egg chamber remains connected to those that come after it though stalk cells until it develops into the mature egg. Each ovary contains 16-20 ovarioles.

As the egg chamber develops, it passes through 14 stages, which are largely based on morphology (Figure 1.7). It begins as a roughly spherical structure that is 20 µm in diameter, then increases over 1000-fold in volume as it elongates along its anterior-posterior axis to form an elliptical structure that is over 500 µm long (Horne-Badovinac, 2014; Horne-Badovinac and Bilder, 2005). Investigating how the egg chamber elongates from a spherical structure into an elliptical one has provided a highly-tractable model for studies of tissue morphogenesis (Duhart et al., 2017; Horne-Badovinac, 2014).

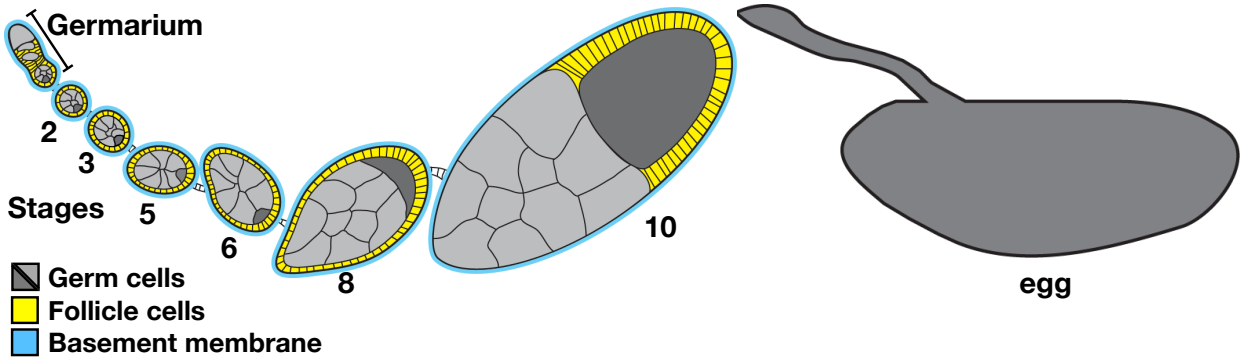

Figure 1.7. Egg chamber development Schematic of cross sections through an ovariole and a mature egg. Egg chambers progress through 14 stages, a subset of which are shown here, until they develop into a mature egg. The oocyte (dark gray) will ultimately form the final egg. Ovariole illustration courtesy of Adam Isabella (Isabella and Horne-Badovinac, 2015).

During stages 1-8 a uniform monolayer of cubodial follicle cells surround the central germ cell cluster. These cells undergo multiple rounds of cell division during stages 1-6, then division ceases and the cells endoreplicate and increase in size (Horne-Badovinac and Bilder, 2005). Starting at stage 9, the follicular epithelium undergoes dramatic morphological changes

and rearrangements. This results in the majority of follicle cells becoming columnar and spreading over the expanding oocyte, while a smaller proportion become squamous and stretch over the nurse cells. The nurse cells then dump their contents into the oocyte, which will form the final egg. For this remainder of this chapter I will focus on stages 1-8, when the follicle cells remain a cuboidal epithelium.

Egg chamber elongation relies on planar polarity

Early studies of egg chamber elongation focused on highly organized structures at the outer surface of the egg chamber, the basal actin bundles, actin-rich protrusions, and basement membrane fibrils. During stages 1-8, the basal surface of each follicle cell contains a parallel array of actin bundles that lies perpendicular to the anterior-posterior axis, as well as actin-rich protrusions that extend from one side of each cell in this same direction (Cetera et al., 2014; Gutzeit et al., 1991). The organization of the actin bundles results in a circumferential arrangement of actin at the outer surface of the egg chamber (Figure 1.8). The basement membrane also contains linear structures, fibrils of basement membrane proteins, which are aligned along anterior-posterior axis starting around stage 5 and persist throughout development (Figure 1.8) (Gutzeit et al., 1991; Isabella and Horne-Badovinac, 2016).

The organization of the actin bundles, actin-rich protrusions, and basement membrane fibrils is an arrangement known as planar polarity. Planar polarity describes a scenario in which the polarities of individual cells all lie in the same direction within the tissue plane, and it is well known to play a role in the organization of many types of epithelial tissues (Goodrich and Strutt, 2011; Munoz-Soriano et al., 2012). A classic example of PCP is found in the *Drosophila* wing, where a single trichrome extends only from the distal side of each cell, resulting in an

arrangement where all trichromes point in the same direction across the wing (Goodrich and Strutt, 2011). A similar situation occurs in the follicular epithelium, protrusions extend from just one side of each follicle cell, which leads to them all pointing in a uniform direction across the tissue plane.

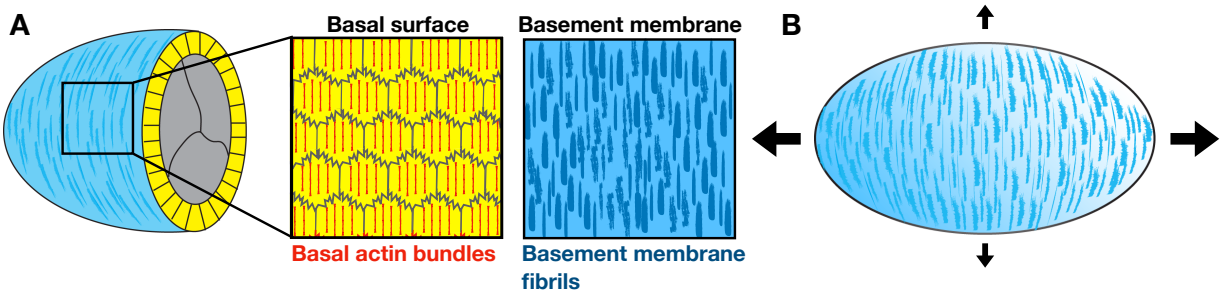

Figure 1.8. The molecular corset model (A) Schematic of a sagittal section through an egg chamber, showing how the epithelial cells (yellow) wrap around the germ cells (gray) and the whole structure is enclosed within the basement membrane (blue). Schematic of a zoomed in view of the basal epithelial surface, showing how the basal actin bundles (red) that lie along the basal surface of each follicle cell (outlined in gray) all are aligned in the same direction across the tissue and how the fibrils in the basement membrane (dark blue) also are all aligned in this same direction. (B) Schematic of the molecular corset model. The circumferential arrangement of the actin bundles and basement membrane fibrils as they wrap around the egg chamber are proposed to constrain growth perpendicular to the axis of elongation (small arrows) and therefore channel expansion along the anterior-posterior axis (large arrows).

The planar polarity found in the follicle cells is different from classic PCP in a couple of ways. A well-studied mechanism for achieving planar polarity is the planar cell polarity (PCP) pathway, which relies on the polarized asymmetric distribution of core signaling cassettes, Frizzled/Strabismus and Fat/Dachsous (Goodrich and Strutt, 2011). Despite the striking level of planar polarity seen in the follicle cells, the canonical PCP proteins are not required to achieve this organization (Viktorinova et al., 2009). Additionally, the planar polarized structures of the follicular epithelium are found at the basal side of the cells, whereas the canonical PCP proteins

localize to the apical region. These differences suggest that studying the unusual form of PCP found in the follicle cells will bring to light new facets of how planar polarity can be achieved.

Egg chamber elongation is tightly correlated with the planar polarity of the basal actin bundles and basement membrane fibrils; in egg chambers that fail to elongate, the planar polarity of these structures is often disrupted (Bateman et al., 2001; Cetera et al., 2014; Frydman and Spradling, 2001; Gutzeit et al., 1991; Haigo and Bilder, 2011; Horne-Badovinac et al., 2012; Isabella and Horne-Badovinac, 2016; Lewellyn et al., 2013; Viktorinova et al., 2009). It is proposed that these planar polarized arrays act as a molecular corset to constrain growth perpendicular to axis of elongation and channel it along the anterior-posterior axis (figure 1.8) (Gutzeit et al., 1991).

Many studies have demonstrated that this unusual form of planar polarity plays an important role in egg chamber elongation, but the molecular mechanisms underlying it are not well understood. Since the canonical PCP proteins are not involved, it suggests that additional factors exist which help to coordinate the polarities of the follicle cells. And indeed, roughly 20 years after the description of planar polarity at the basal surface of the follicular epithelium, a discovery was made that shed light on how this pattern arises: the follicle cells collectively migrate.

Introduction to collective migration of the follicle cells

From the time an egg chamber forms through stage 8 of development, the follicle cells collectively migrate within the egg chamber (Cetera et al., 2014; Haigo and Bilder, 2011). They crawl along the basement membrane in a direction that is perpendicular to the A-P axis (Figure 1.9A). Since the apical surface of the follicle cells is connected to the inner cluster of germ cells,

this migration causes the entire cohort of follicle cells and germ cells to rotate within the surrounding basement membrane. This migration is tightly linked to egg chamber elongation, which will be discussed in the next section.

Collective migration of the follicle cells is similar to other epithelial migrations. Each follicle cell is polarized in the direction of movement (Figure 1.9B). At the basal surface, the planar polarized actin-based protrusions that I described earlier are actually leading edge

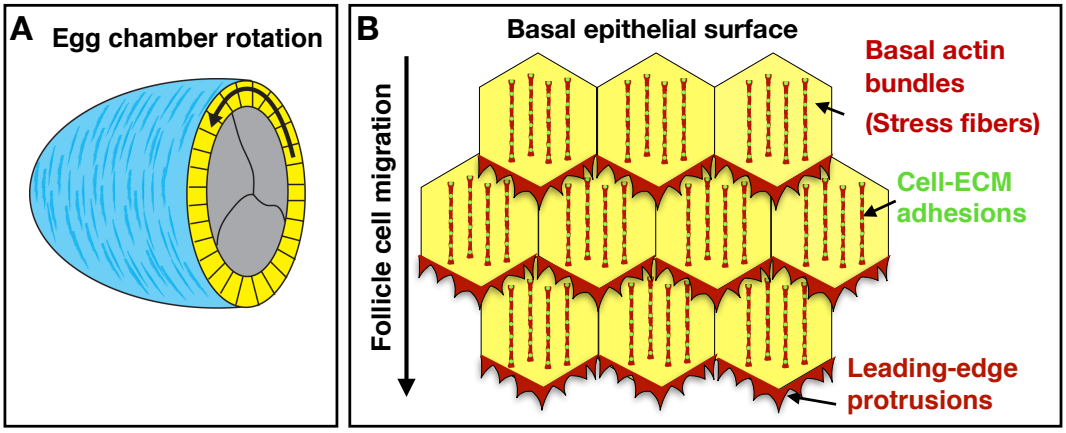

Figure 1.9. Follicle cell migration (A) Schematic of a sagittal section through an egg chamber, arrow indicates the path of follicle cell migration. (B) Schematic of the basal epithelial surface showing that each cell has actin rich protrusions at its leading edge, stress fiber-like structures that extend along the basal surface and adhesions along these stress fibers that link them to the surrounding basement membrane.

protrusions and are required for migration (Cetera et al., 2014). In addition, the actin bundles that lay along each cell's basal surface are contractile structures with myosin and adhesions that link the actin cytoskeleton to the basement membrane, similar to stress fibers (Cetera et al., 2014; Delon and Brown, 2009; Haigo and Bilder, 2011; Lewellyn et al., 2013; Viktorinová and Dahmann, 2013). As the cells crawl forward, their trailing edges need to retract, and proteins localize specifically to this region to promote the release of adhesions and tail retraction (Barlan

et al., 2017; Lewellyn et al., 2013). Since the migration machinery is localized to the basal side of the follicle cells, which lie at the outer surface of the egg chamber, this tissue is highly amenable to both fixed and live cell imaging. Studies of this highly tractable system have provided new insights into what coordinates the collective migration of epithelial cells and will be discussed in more detail below.

Notably, the follicle cells migrate without a free leading edge. Unlike a migrating cluster or sheet of cells, which have leader cells and follower cells that make different contributions to migration, the follicle cells exist in a topologically constrained system where all migrating cells appear to make equal contributions to the migration (Cetera et al., 2014; Lewellyn et al., 2013). Since the follicle cells essentially migrate in a circle, there is no way for a chemotactic cue from the environment to guide this movement nor is there free space to provide a polarity cue for the tissue. Cultured cysts of mammalian epithelial cells display a similar motion, as they rotate within 3 dimensional ECMs (Tanner et al., 2012; Wang et al., 2013). This rotation was suggested to play a role in establishing proper tissue architecture and was linked to malignancy. The mechanisms that drive this rotation remain unknown. This suggests that rotational motion in the absence of a leading edge is a conserved phenomenon and it will be interesting to elucidate the mechanisms which drive these collective movements. I will further discuss our current understanding of the mechanisms underlying follicle cell migration, but first I want to touch back on egg chamber elongation, because migration plays a key role in that process.

Follicle cell migration is tightly linked to planar polarity and egg chamber elongation

Follicle cell migration is tightly linked to planar polarity of the stress fibers and basement membrane fibrils across the epithelium and proper elongation of the egg chamber. In a majority

of cases, lack of migration leads to disrupted planar polarity of the stress fibers and fibrils and leads to failure to fully elongate (Barlan et al., 2017; Cetera et al., 2014; Haigo and Bilder, 2011; Lewellyn et al., 2013; Viktorinová and Dahmann, 2013). Migration is thought to promote elongation by building the molecular corset, which then persists into post-migration stages. Notably, the actin bundles and basement membrane fibrils are aligned in the direction of migration.

Evidence suggests that migration plays a role in construction of the molecular corset in party by maintaining planar polarity across the follicular epithelium. Global alignment of the actin bundles across the tissue is high when an egg chamber first forms and increases throughout the migratory period (Cetera et al., 2014). Blocking migration causes the global alignment to decrease over time; it still starts out high at stage 1 but then rapidly falls off (Cetera et al., 2014). This suggests that migration is required to maintain planar polarity that is inherited from the germarium, which also displays planar polarized actin bundles (Cetera et al., 2014; Frydman and Spradling, 2001). The mechanism by which the planar polarity of actin bundles is set up in the germarium remains unknown. It is also of note that the germarium also contains polarized microtubules whose organization has been linked to the initiation of migration, (Chen et al., 2016).

Migration also plays a key role in building the polarized fibrils of the basement membrane. The follicle cells synthesize basement membrane proteins and secrete them as they migration. Protein secretion synergizes with tissue movement, causing the secreted proteins to be drawn out into fibrils that lie in the direction of migration (Haigo and Bilder, 2011; Isabella and Horne-Badovinac, 2016). When migration is blocked, the polarized fibrils fail to form and

basement membrane proteins become more uniformly distributed in the matrix (Haigo and Bilder, 2011; Isabella and Horne-Badovinac, 2016; Lewellyn et al., 2013).

Planar polarized proteins at the basal surface drive collective migration

One of the big questions underlying studies of collective cell migration is how cells coordinate their motility across a tissue, and the follicular epithelium provides a highly tractable system in which to identify cues that coordinate this collective movement. While many studies demonstrated that follicle cell migration plays an important role in maintaining planar polarity in the egg chamber, what governs the organization of this migration was not well understood. Recent work has identified proteins that are planar polarized across the follicular epithelium, localizing specifically to the leading or trailing edge of each cell, and play a key role driving their migration. Here I will focus on the roles of Fat2, an atypical cadherin, and Lar, a receptor tyrosine phosphatase, which interacts with Fat2.

Fat2, also known as *Kugelei*, is a Fat-like cadherin. Its mammalian homologs are Fat1-3 (Horne-Badovinac, 2017; Sadeqzadeh et al., 2014). Fat cadherins are extremely large, approximately 500-7600kDa, single-pass transmembrane proteins with 32-34 cadherin repeats on their extracellular side (Sadeqzadeh et al., 2014). Their size has made work on them difficult, but recently roles for them are emerging in development and disease, including in modulating cell polarity and motility (Horne-Badovinac, 2017; Sadeqzadeh et al., 2014).

Kugelei was the first gene identified to be required for egg chamber elongation, and was later mapped to *fat2* (Gutzeit et al., 1991; Viktorinova et al., 2009). Fat2 is required for migration of the follicular epithelium and localizes along leading-trailing cell-cell interfaces at the basal epithelial surface, specifically to each cell's trailing edge, such that it adopts a planar polarized

distribution across the tissue (Barlan et al., 2017; Chen et al., 2016; Squarr et al., 2016; Viktorinová and Dahmann, 2013; Viktorinova et al., 2009).

Lar, is a member of the leukocyte common antigen-related (Lar) subfamily of receptor tyrosine phosphatases (LAR-RPTPs). Its mammalian homologs are LAR, RPTP-sigma and RPTP-delta (Chagnon et al., 2004). LAR-RPTPs are known to play a role in neuronal development, especially synapse formation (Han et al., 2016).

Studies on Lar in the egg chamber revealed similar phenotypes to studies of Fat2. Lar is required for egg chamber elongation and also localizes to leading-trailing cell-cell interfaces the basal surface of the follicular epithelium (Bateman et al., 2001; Frydman and Spradling, 2001). Recent work showed that Lar plays a role in follicle cell migration and that Fat2 and Lar likely work together to coordinate this motility (Barlan et al., 2017; Squarr et al., 2016).

One study suggested that Fat2 and Lar drive migration by promoting the formation of protrusions at tri-cellular contacts (Squarr et al., 2016). Fat2 interacts with the WAVE regulatory complex (WRC), which is required for protrusion formation, via WIRS (WRC interacting receptor sequence) motifs on its intracellular domain. Fat2 and Abi, a component of the WRC, colocalize at tricellular contacts and Fat2 was required for Abi's localization. Lar also interacts with the WRC, and it was suggested that Lar and Fat2 pathways were linked via their interaction with the WRC. This group's model proposed that Fat2 cell-autonomously promotes protrusion formation by acting at the leading edge of each follicle cell. However, this conflicts with results from other groups, showing that Fat2 localizes specifically to the trailing edge of each follicle cell (Barlan et al., 2017; Viktorinová and Dahmann, 2013; Viktorinova et al., 2009).

Work by a former post-doc from our lab, Kari Barlan, showed that Fat2 and Lar promote follicle cell migration by signaling across leading-trailing cell-cell interfaces (Barlan et al.,

2017). At the basal surface, Fat2 and Lar localize to juxtaposing membrane domains, with Fat2 on the trailing edge of each cell and Lar on the leading edge of each cell (Figure 1.10), such that puncta of Fat2 and Lar colocalize where these leading-trailing cell-cell interfaces meet. Fat2 is required for Lar to localize to the basal surface, which demonstrates that they interact across cell-cell boundaries. At the trailing edge, Fat2 promotes protrusion formation non-cell-autonomously; in a mosaic tissue loss of *fat2* causes loss of protrusions from the cells behind the null clone. At the leading edge, Lar cell autonomously promotes protrusion formation, leading to the suggestion that Fat2 promotes protrusions by signaling though Lar. Lar does not affect protrusions to the same extent as Fat2, loss of Lar only causes a partial loss of protrusions, suggesting that an additional factor in involved in this pathway. Fat2 also has a cell autonomous role during follicle cell migration. Long tails extend from the rear of *fat2* null cells, suggesting Fat2 promotes retraction of the trailing edge. Lar has a complementary non-cell-autonomous phenotype, it promotes rear retraction of the cell ahead, suggesting that Fat2 and Lar work together in this process as well. Overall, this suggests that Fat2 and Lar mediate short-range planar cell-cell signaling that plays a key role in coordinating migration between the leading and trailing edges in a migrating epithelium.

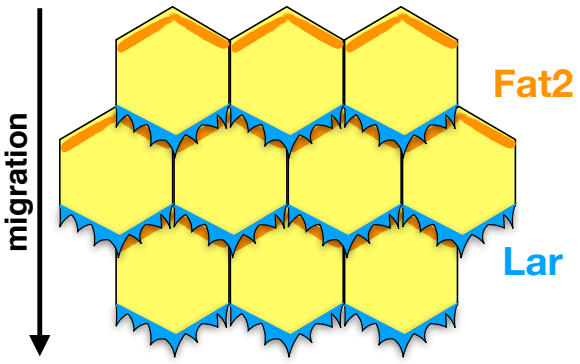

Figure 1.10. Fat2 and Lar are planar polarized at the basal surface of the follicular epithelium Schematic of the follicle cells showing the localization of Fat2 and Lar at the basal surface. Fat2 (orange) localizes to the trailing edge of each cell, and Lar (blue) to the leading edge.

Interestingly, the work from Barlan and colleagues demonstrates that there is a high level of coordination between leading and trailing edge dynamics during epithelial migration. Since epithelial cells are tightly adhered to one another during migration, protrusion formation at the leading edge of one cell needs to be tightly linked to trailing-edge retraction of the cell ahead. This work also suggests that planar cell-cell signaling at the basal epithelial surface plays a role in coordinating these dynamics. Notably, Fat2 likely interacts with at least one other factor besides Lar. This suggests that additional proteins are involved, and that this work is just the first step in understanding how the dynamics of leading and trailing edges are coordinated during epithelial migration.

My work identifies another set of planar polarized cues that act of the basal surface of the follicular epithelium to promote migration, but in this case, it is a semaphorin-plexin pair, Sema-5c and PlexA. I further uncovered that the activity of these two signaling systems, Fat2 – Lar and Sema-5c – PlexA, may converge during follicle cell migration. Interestingly these four factors are all known for their role in the developing nervous system. Overall, this work reveals that neuronal guidance cues can be deployed in a planar polarized manner to promote epithelial motility.

CHAPTER 2: PLANAR POLARIZED SEMAPHORIN-5C AND PLEXIN A PROMOTE THE COLLECTIVE MIGRATION OF EPITHELIAL CELLS IN *DROSOPHILA*

2.1 PREFACE

This chapter was accepted for publication at Current Biology with the following authors: Claire G. Stedden (Stevenson), William Menegas, Allison L. Zajac, Audrey M. Williams, Shouqiang Cheng, Engin Özkan, and Sally Horne-Badovinac.

William Menegas, a former undergraduate in the lab, mapped the *Sema-5c* lesion and performed early phenotypic analysis. Allison L. Zajac, a postdoc in the lab, created the *UAS-Sema-5c-GFP* line and assisted with design of the *Sema-5c*-3xGFP line. Audrey M. Williams, a graduate student in the lab, provided Figure 2.12J. Shouqiang Cheng, a post doc in Engin Özkan's lab, provided Figures 2.10A and 2.10B.

2.2 ABSTRACT

Collective migration of epithelial cells is essential for morphogenesis, wound repair, and the spread of many cancers, yet how individual cells signal to one another to coordinate their movements is largely unknown. Here we introduce a tissue-autonomous paradigm for semaphorin-based regulation of collective cell migration. Semaphorins typically regulate the motility of neuronal growth cones and other migrating cell types by acting as repulsive cues within the migratory environment. Studying the follicular epithelial cells of *Drosophila*, we discovered that the transmembrane semaphorin, Sema-5c, promotes collective cell migration by acting within the migrating cells, themselves, not the surrounding environment. Sema-5c is planar polarized at the basal epithelial surface, such that it is enriched at the leading edge of each

cell. This location places it in a prime position to send a repulsive signal to the trailing edge of the cell ahead to communicate directional information between neighboring cells. Our data show that Sema-5c can signal across cell-cell boundaries to suppress protrusions in neighboring cells and that Plexin A is the receptor that transduces this signal. Finally, we present evidence that Sema-5c antagonizes the activity of Lar, another transmembrane guidance cue that operates along leading-trailing cell-cell interfaces in this tissue, via a mechanism that appears to be independent of Plexin A. Together our results suggest that multiple transmembrane guidance cues can be deployed in a planar polarized manner across an epithelium and work in concert to coordinate individual cell movements for collective migration.

2.3 INTRODUCTION

Collective migration of epithelial cells underlies numerous tissue remodeling events (Friedl and Gilmour, 2009; Mayor and Etienne-Manneville, 2016). In embryos, epithelial migration shapes organs including the mammary gland, vasculature, kidney, and eye (Ewald et al., 2008; Michaelis, 2014; Sidhaye and Norden, 2017; Vasilyev et al., 2009). In adults, it closes wounds in the skin and cornea, and facilitates metastasis (Friedl et al., 2012; Liu and Kao, 2015; Shaw and Martin, 2016). For epithelial cells to migrate collectively, each cell must coordinate its movements with those of its neighbors. It is likely that both mechanical and biochemical signals are used to achieve this goal (Ladoux and Mège, 2017). To date, however, few biochemical signals have been identified.

The *Drosophila* egg chamber provides a tractable system in which to identify these coordinating biochemical signals and the principles underlying their activity (Horne-Badovinac and Bilder, 2005). Egg chambers are organ-like structures that will each develop into one egg

(Figure 2.1A). They have an inner germ cell cluster surrounded by follicular epithelial cells (follicle cells), whose basal surfaces contact the basement membrane (BM) ECM that ensheaths the organ. From the time an egg chamber forms through stage 8 of oogenesis, the follicle cells collectively migrate along the BM (Cetera et al., 2014; Haigo and Bilder, 2011). This motion causes the egg chamber to rotate within the BM (Figure 2.1B), and helps to create the ellipsoid shape of the egg. Each migrating follicle cell extends leading edge protrusions and has a parallel array of stress fibers along its basal surface that mediates adhesion to the BM. These actin-based structures all align in the direction of tissue movement, revealing a high degree of coordination among the cells (Figure 2.1C).

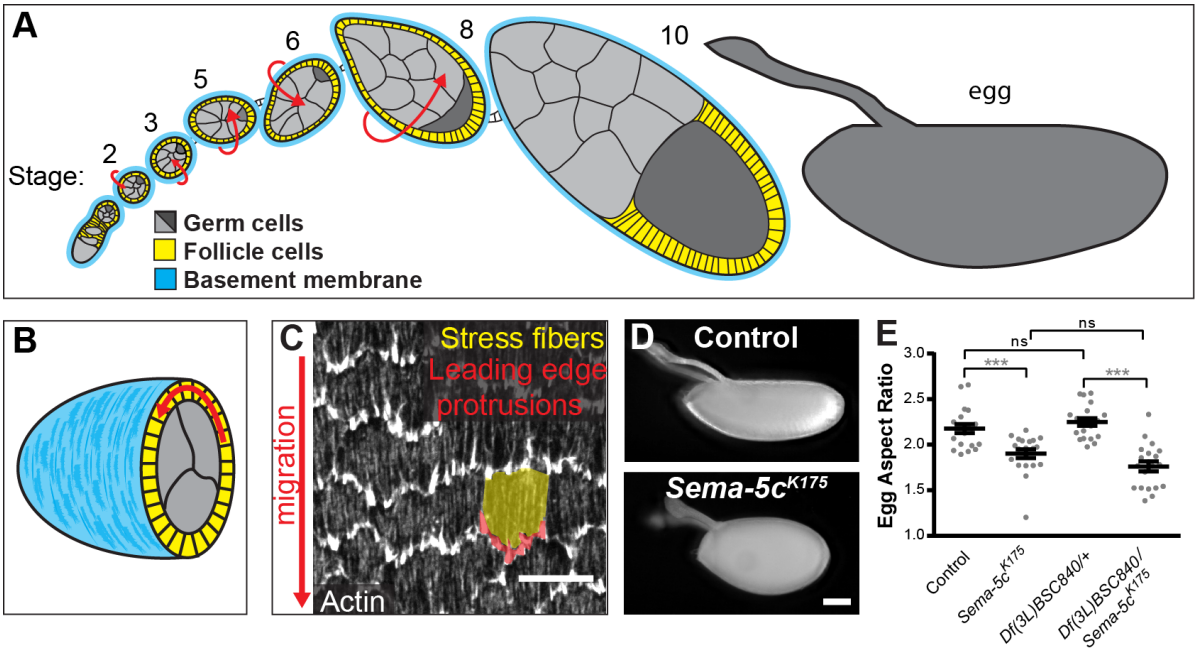

Figure 2.1. Sema-5c is required for egg chamber elongation (A) Illustration of a sagittal section through a developmental array of egg chambers. Arrows indicate rotation stages. (B) Illustration of a transverse section through an egg chamber. Arrow indicates rotation. (C) Image of the basal epithelial surface highlighting protrusions and stress fibers in one cell. (D) Images of eggs from control and *Sema-5c*^{K175} females. (E) Quantification of egg aspect ratio. Eggs from *Sema-5c*^{K175} females are rounder than controls. Data in (E) represent mean ± SEM. Unpaired t-test. ns, not significant ($p > 0.05$), ***$p < 0.001$. Scale bars, 10 µm (C); 100 µm (D).

The migration of the follicular epithelium requires the receptor protein tyrosine phosphatase (RPTP) Lar and the cadherin Fat2, which are planar polarized at the basal epithelial surface along leading-trailing cell-cell interfaces (Barlan et al., 2017; Bateman et al., 2001; Viktorinová and Dahmann, 2013; Viktorinova et al., 2009). Lar localizes to each cell's leading edge and Fat2 localizes to the trailing edge, allowing them to mediate signaling between the leading and trailing edges of neighboring cells (Barlan et al., 2017). Whether other signaling systems also operate along these critical cell-cell interfaces is unknown.

The Semaphorins are a family of both secreted and membrane-associated proteins that activate plexin receptors (Jongbloets and Pasterkamp, 2014; Yazdani and Terman, 2006). They were first identified as repulsive cues for axon guidance, but also regulate the motility of other cell types, including collectively migrating neural crest and endothelial cells (Gu and Giraudo, 2013; Theveneau and Mayor, 2012). Typically, the plexin is expressed by the migrating cells and the semaphorin is expressed by cells within the migratory environment. When a plexin-expressing cell encounters a source of semaphorin, it is repelled, and thus confined to a particular migration path. *Drosophila* have three classes of semaphorins (Sema-1a/1b, Sema-2a/2b, and Sema-5c) and two plexins (PlexA and PlexB) (Yazdani and Terman, 2006). It is conceivable that a transmembrane semaphorin and a plexin could be coexpressed within an epithelium, similar to Lar and Fat2, to allow each cell to influence the migratory behavior of its neighbors. However, no such signaling system involving a semaphorin has yet been found.

Here we show that the transmembrane semaphorin, Sema-5c, functions within the follicle cells, not the migratory environment, to promote their collective motility. We further show that Sema-5c is planar polarized at the basal epithelial surface, and enriched at each cell's leading edge. This location places it in a prime position to signal to the trailing edge of the cell ahead,

which could coordinate migration direction between neighboring cells. Indeed, we find that Sema-5c can signal across cell-cell boundaries to suppress protrusions and that Plexin A appears to transduce this signal. Finally, we present evidence that Sema-5c also interacts with Lar. Altogether, these results show that diverse guidance cues can be deployed within an epithelium to coordinate cellular movements for collective motility.

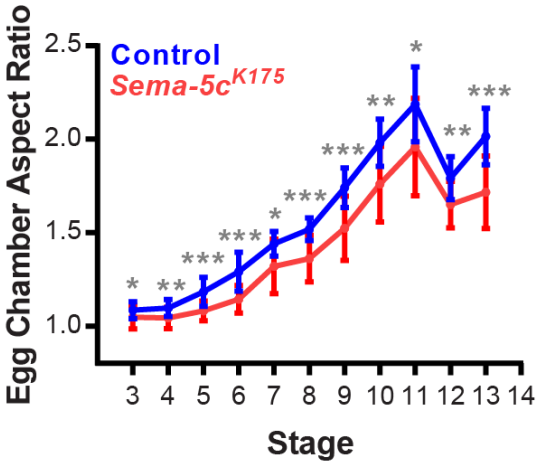

Figure 2.2. Further analysis of Sema-5c's role in egg chamber elongation
Quantification of egg chamber aspect ratios. Egg chambers from *Sema-5c*^{K175} females are rounder than controls. n ≥ 10 for all conditions. Data represent mean ± SEM. Unpaired t-test. *p < 0.05; **p < 0.01; ***p < 0.001.

2.4 RESULTS

Semaphorin-5c is required for egg chamber elongation

We previously performed a genetic screen to identify genes required in the follicle cells to produce the elongated shape of the egg (Horne-Badovinac et al., 2012). The *K175* allele found in this screen is homozygous viable. However, in homozygous females, the aspect ratio (length/width) of egg chambers and eggs is reduced (Figures 2.1D, 2.1E and 2.2). Using deficiency mapping to identify the mutated gene, we found that females with *K175 in trans* to *Df(3L)BSC840* produce rounded eggs similar to those of *K175* homozygotes (Figure 2.1E). This deficiency contains the *Semphorin-5c* (*Sema-5c*) gene, which is non-essential for viability (Bahri et al., 2001). Sequencing *Sema-5c* coding regions in *K175* animals identified a point mutation, T393-to-A, which produces a premature stop codon near the protein's N-terminus. Together,

these data suggest that *K175* is a nonsense mutation in *Sema-5c (Sema-5c^{K175})*, and that Sema-5c is required for egg chamber elongation.

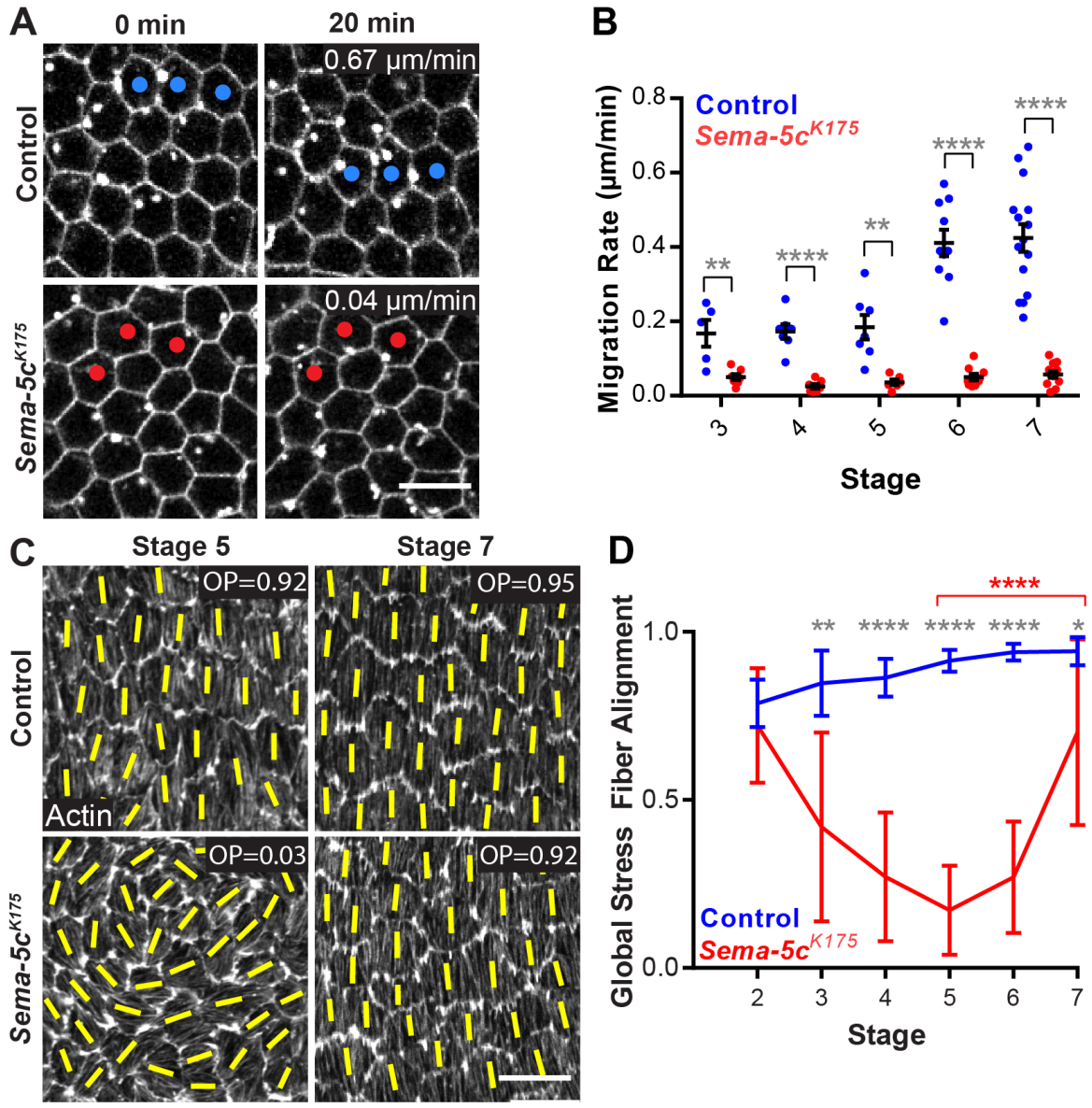

Figure 2.3. Loss of Sema-5c disrupts epithelial migration and global stress fiber alignment (A) Still images from videos of control and *Sema-5c* ^{K175} epithelia, stage 7. Dots mark the same cells over time. (B) Quantification of migration rates for control and *Sema-5c* ^{K175} epithelia. (C) Images of global stress fiber alignment in control and *Sema-5c* ^{K175} epithelia. Yellow lines show the primary stress fiber direction in each cell. OP = order parameter. (D) Quantification of global stress fiber alignment in control and *Sema-5c* ^{K175} epithelia. Grey asterisks compare control to *Sema-5c* ^{K175}. Red asterisks compare *Sema-5c*^{K175} stage 5 to stage 7. n ≥ 8 for all conditions. Data represent mean ± SEM in (B) and mean ± SD in (D). Unpaired t-test. *p < 0.05, **p < 0.01, ****p < 0.0001. Scale bars, 10 µm.

Loss of Semaphorin-5c slows the rate and onset of epithelial migration

Defects in egg chamber elongation are often associated with impaired follicle cell migration (Cetera and Horne-Badovinac, 2015), so we investigated if Sema-5c is required for this process. *Ex vivo* live imaging showed that *Sema-5c* epithelia appear to be non-migratory (Figures 2.3A and 2.3B). However, careful analysis of the actin cytoskeleton in fixed tissue, as discussed below, indicated that *Sema-5c* epithelia might have cryptic migratory ability.

The stress fibers at the basal surfaces of the follicle cells are aligned globally across the tissue, such that they all run parallel to the direction of movement (Cetera et al., 2014; Gutzeit, 1990). We quantify this global alignment with an order parameter, where zero represents no alignment and one represents perfect alignment. Global stress fiber alignment is high in wild-type epithelia when migration begins, and increases until the end of migration at stage 8. By contrast, when migration is blocked, the alignment starts at the same high level, but then decreases until the order parameter is near zero at stage 8 (Cetera et al., 2014).

Because *ex vivo* live imaging revealed no obvious migration in *Sema-5c* epithelia, we expected to see a consistent decrease in global stress fiber alignment, similar to other non-migratory conditions. Instead, the alignment decreases until stage 5, but then recovers, such that many *Sema-5c* epithelia are indistinguishable from controls at stage 7 (Figures 2.3C and 2.3D). This observation suggested that *Sema-5c* epithelial might migrate extremely slowly, and that the onset of motility might be delayed to stage 5/6. Given that *ex vivo* live imaging can only be performed for hours, and follicle cell migration lasts ~2 days (Cetera et al., 2014; Horne-Badovinac and Bilder, 2005), these subtle tissue dynamics could be missed by live imaging alone.

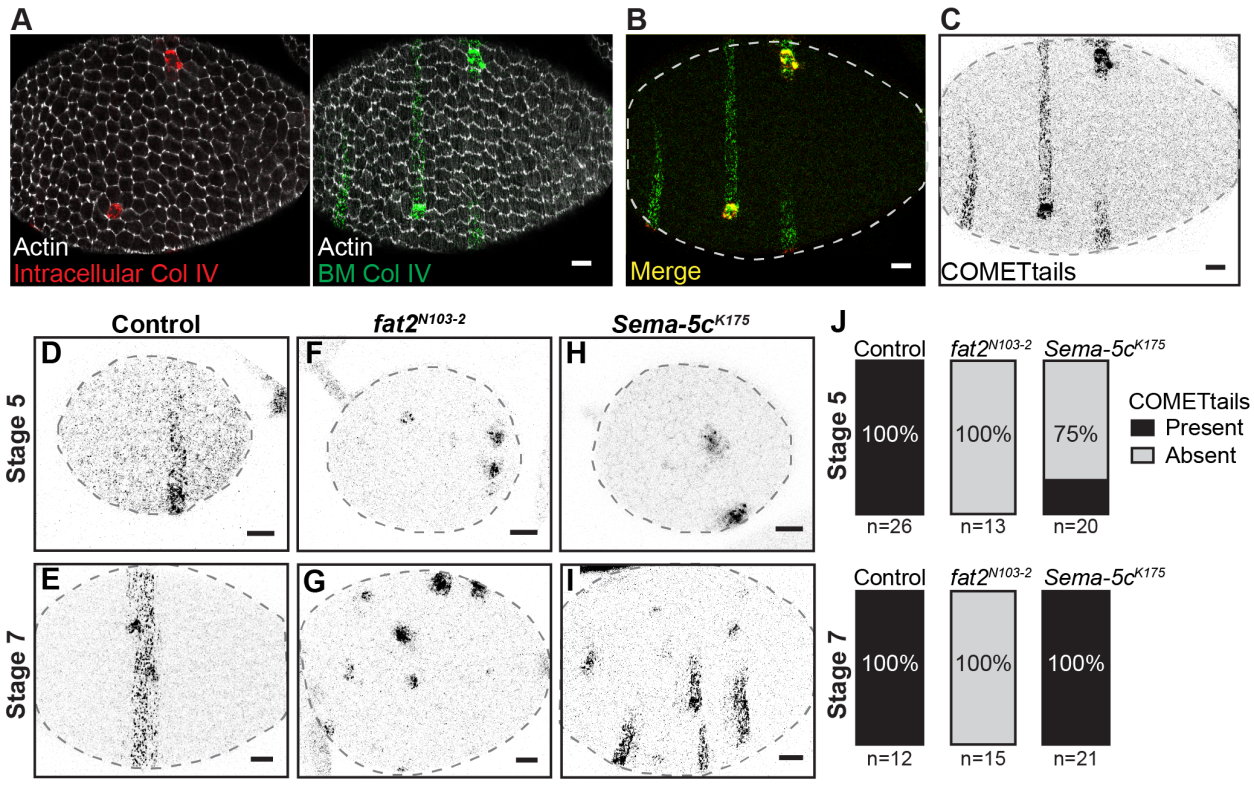

Figure 2.4. Loss of Sema-5c slows the onset and rate of epithelial migration (A-C) The COMETtail method. Clones expressing Col IV-mRFP are detected by the intracellular signal. Clones deposit stripes of Col IV-mRFP into the BM as they migrate (false-colored green). (B) Overlay of Col IV-mRFP images in (A). (C) Image from (B) in grayscale. (D-I) Images of COMETtails from control, non-migratory *fat2*$^{N103-2}$, and *Sema-5c* ^{K175} epithelia. (J) Quantification of COMETtail data. n = number of egg chambers examined. Scale bars, 10 µm.

To test this, we developed an *in vivo* method to track epithelial migration over longer time periods, which leverages the fact that these cells secrete new matrix proteins into the BM as they migrate (Haigo and Bilder, 2011; Isabella and Horne-Badovinac, 2016). We induced small clones of cells to express an mRFP-tagged version of the BM protein type IV collagen (Col IV-mRFP), and identified them by the fluorescent collagen within the secretory pathway of the expressing cells (Figure 2.4A). In a migratory epithelium, these clones deposit stripes of Col IV-mRFP into the BM behind them, creating a permanent record that migration occurred (Figures 2.4A-2.4E). By contrast, clones in a non-migratory *fat2*$^{N103-2}$ epithelium only deposit spots of Col

IV-mRFP into the BM directly adjacent to the expressing cells (Figures 2.4F and 2.4G). We call the BM stripes COMETtails (Clonal Overexpression of Matrix proteins for Epithelial cell Tracking). A similar method was recently published (Chen et al., 2017).

Using COMETtails, we found that *Sema-5c* epithelia display a phenotype that is intermediate between control and $fat2^{N103\text{-}2}$ epithelia. At stage 7, when global stress fiber alignment has largely recovered, all egg chambers have COMETtails (Figures 2.4I and 2.4J), which indicates that these *Sema-5c* epithelia do migrate. However, because *Sema-5c* COMETails are shorter than controls, and *ex vivo* live imaging reveals almost no movement (Figure 2.3B), the migration must be extremely slow. At stage 5, when stress fibers are maximally mis-aligned, only 25% of *Sema-5c* epithelia have COMETtails (Figures 2.4H and 2.4J). This observation is consistent with migration initiating in the majority of *Sema-5c* epithelia around stage 5/6. Altogether, these data show that loss of Sema-5c slows the rate of epithelial migration and often delays its onset.

Semaphorin-5c localizes to each cell's leading edge

To explore how Sema-5c promotes epithelial migration, we determined its localization in the egg chamber. We used the CRISPR-Cas9 system to insert three copies of GFP into the *Sema-5c* locus (*Sema-5c-3xGFP*). The resulting C-terminal protein fusion appears to be functional, as eggs from *Sema-5c-3xGFP* females elongate normally (Figure 2.5A). Sema-5c-3xGFP is expressed strongly in the follicle cells through stage 7, with little signal in the germ cells (Figure 2.6A). Optical sections through the epithelium reveal that Sema-5c-3xGFP is on apical and lateral cell membranes, and intracellular puncta that may represent endosomes (Figure 2.6B).

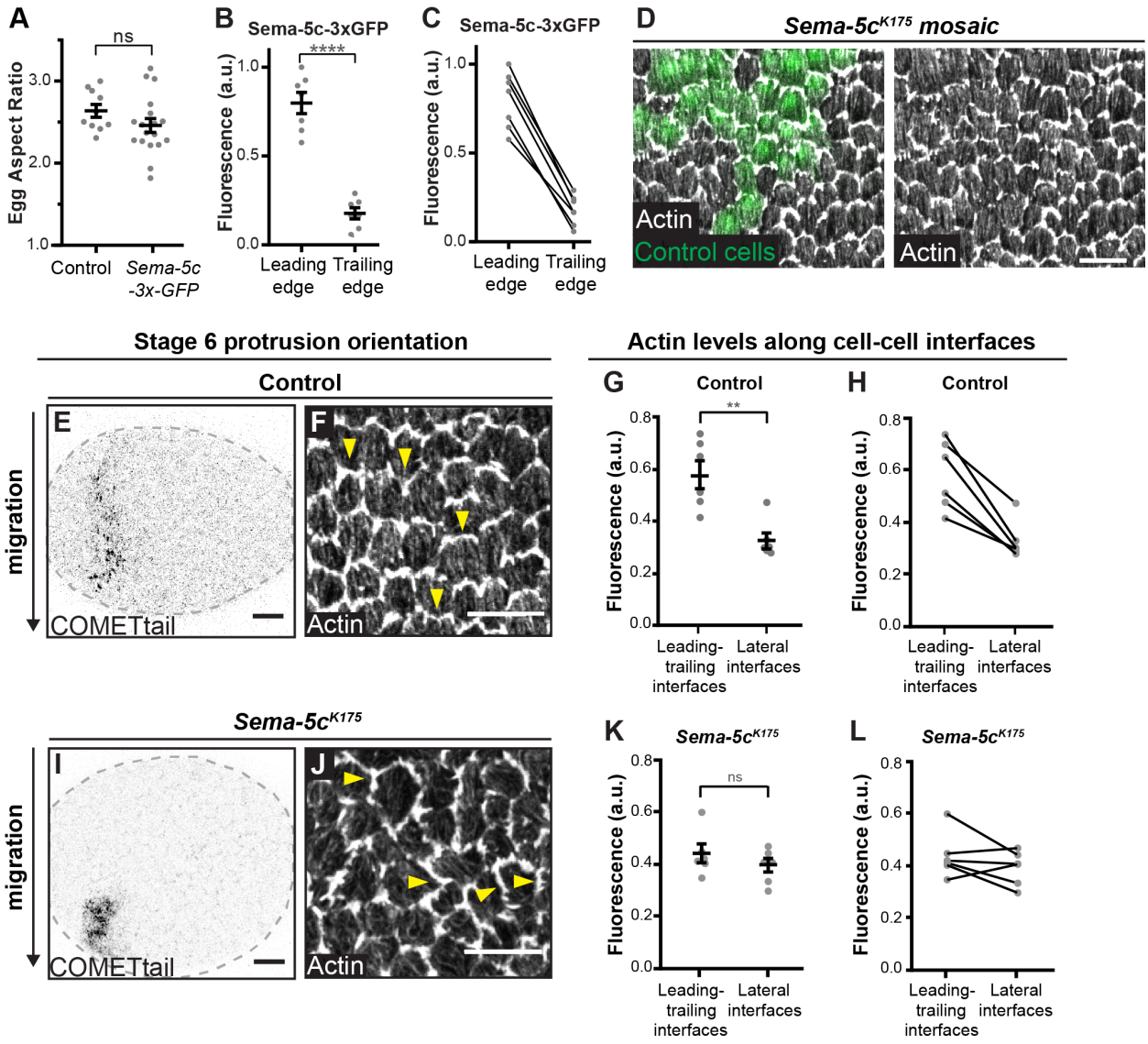

Figure 2.5. Characterization of Sema-5c-3xGFP and effect of Sema-5c loss of function on protrusions (A) Quantification of egg aspect ratios. The 3xGFP tag on Sema-5c does not cause a defect in egg shape. (B and C) Quantification of fluorescence intensity of Sema-5c-3xGFP at leading versus trailing edges of *Sema-5c-3xGFP* clones, stage 7. Each data point is one epithelium in which line scans were preformed along 3-8 leading or trailing cell-cell interfaces. (B) The first graph shows the data for statistical purposes. (C) The second graph links the leading and trailing measurements for each egg chamber with a line. (D) Images of the basal surface of a *Sema-5c* ^{K175} mosaic epithelium, stage 7. Loss of Sema-5c has no obvious effect on cellular protrusions at this stage. (E and F) Images of the basal surface of a wild-type egg chamber. The COMETtail image shows that the epithelium was migrating prior to fixation (E), and the image showing the actin cytoskeleton at the basal surface is from the same egg chamber (F). The protrusions are primarily oriented in the direction of migration (closed triangles). Legend continued on next page.

Figure 2.5. continued (G and H) Quantification of protrusion orientation along opposing cell-cell interfaces in wild-type epithelia (see STAR methods). Because actin levels are particularly high in protrusions, actin levels can be used as a proxy for protrusion position. (G) The first graph shows the data for statistical purposes. (H) The second graph links the two measurements for each egg chamber with a line. (I and J) Images of the basal surface of a *Sema-5c* egg chamber. The COMETtail image shows that the epithelium was migrating prior to fixation (I), and the image showing the actin cytoskeleton at the basal surface is from the same egg chamber (J). The protrusions are often oriented away from the direction of migration (open triangles). (K and L) Quantification of protrusion orientation along opposing cell-cell interfaces in *Sema-5c* epithelia (see STAR methods). Because actin levels are particularly high in protrusions, actin levels can be used as a proxy for protrusion position. (K) The first graph shows the data for statistical purposes. (L) The second graph links the two measurements for each egg chamber with a line. Data represent mean ± SEM. Unpaired t-test. ns, not significant ($p > 0.05$), ** $p < 0.01$, ****$p < 0.0001$. Scale bars, 10 μm (D-F, I and J).

Because the migration machinery is at the tissue's basal surface, we were particularly interested in Sema-5c's localization along this plane. We found that Sema-5c-3xGFP is both punctate and planar polarized along leading-trailing cell-cell interfaces (Figures 2.6C-2.6F). To determine if this localization corresponds to the leading edge, trailing edge, or both, we generated mosaic epithelia wherein some cells express *Sema-5c-3xGFP* and the remainder express untagged *Sema-5c*. Using leading edge protrusions to indicate migration direction, we found that *Sema-5c-3xGFP*-expressing cells migrating directly behind unmarked cells have GFP at their leading edges, whereas *Sema-5c-3xGFP*-expressing cells migrating directly ahead of unmarked cells largely lack GFP at their trailing edges (Figures 2.6G-2.6I, 2.5B and 2.5C). Hence, Sema-5c is enriched at each cell's leading edge.

Semaphorin-5c can suppress protrusions in neighboring cells

One way that semaphorins regulate cell motility is by signaling non-cell-autonomously to suppress protrusions (Hung and Terman, 2011). This activity was first identified in axon guidance, where semaphorins "collapse" the protrusive growth cone that pioneers the migration

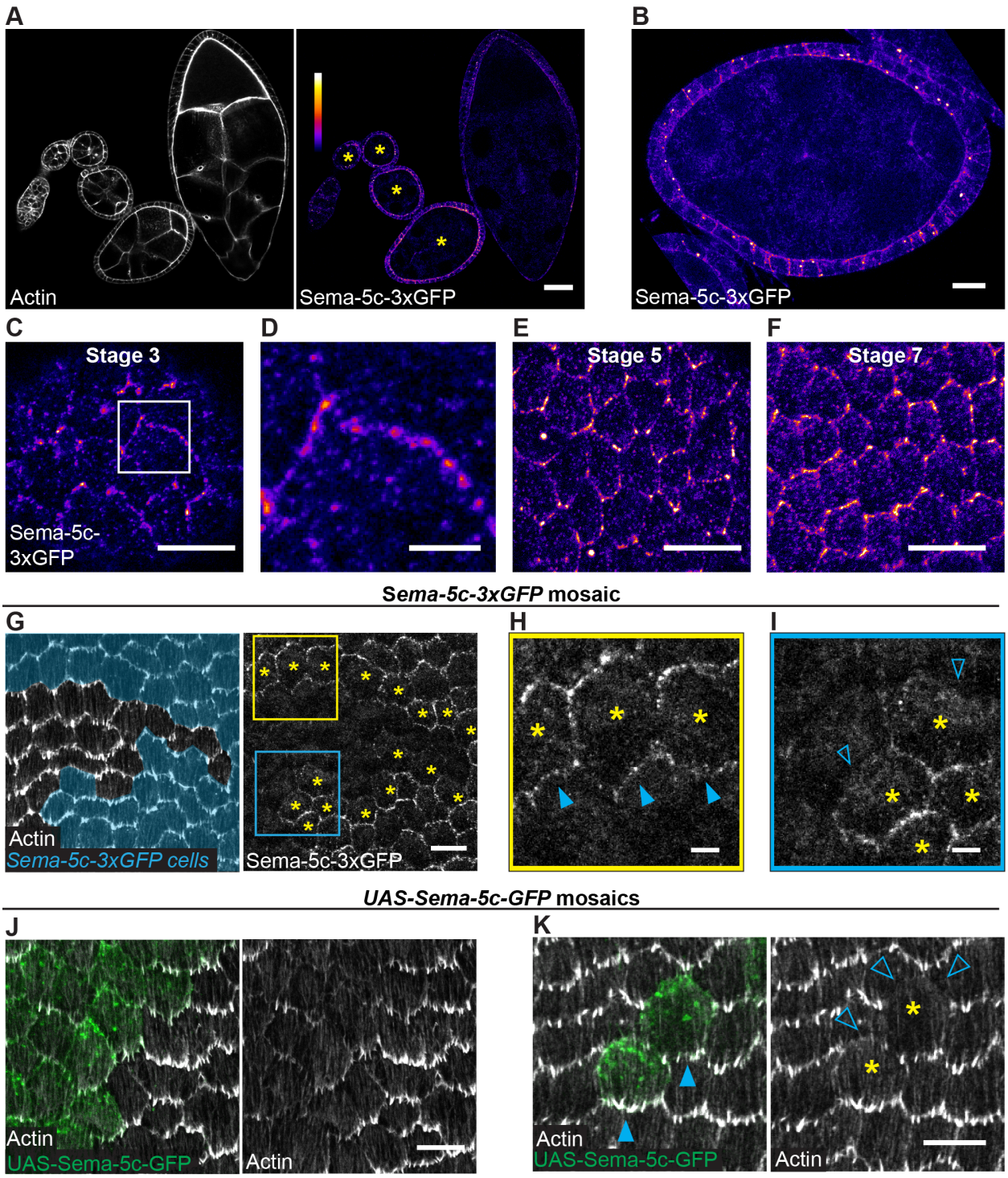

Figure 2.6. Sema-5c localizes to the leading edge and can suppress protrusions in neighboring cells (A) Images of a sagittal section through an ovariole expressing Sema-5c-3xGFP. Asterisks mark migratory stages. Heat map index applies to (A-F). (B) Image of a sagittal section through an egg chamber, stage 6. Sema-5c-3xGFP is on apical and lateral cell membranes, and intracellular puncta. Legend continued on next page.

Figure 2.6. continued (C-F) Images of the basal epithelial surface at indicated stages. Sema-5c-3xGFP is punctate along leading-trailing cell-cell interfaces. (D) Zoom of boxed region in (C). (G-I) Images of the basal surface of a *Sema-5c-3xGFP* mosaic epithelium, stage 7. (G) Cells expressing Sema-5c-3xGFP are pseudocolored cyan. Asterisks mark Sema-5c-3xGFP-expressing cells at the clone boundary. (H) Zoom of the yellow boxed region in (G). Sema-5c-3xGFP-expressing cells have GFP at their leading edge (solid triangles). (I) Zoom of the blue boxed region in (G). Sema-5c-3xGFP-expressing cells lack GFP at their trailing edge (open triangles). (J-K) Images of the basal surface of *UAS-Sema-5c-GFP* mosaic epithelia, stage 7. (J) Protrusions are reduced in the clone. (K) Protrusions are present at the front of the clone (closed triangles) but are lost from cells directly behind the clone (open triangles). Asterisks mark the clone. Scale bars, 100 μm (A); 10 μm (B,C, E-G, J and K); 3 μm (D, H and I).

of an axon toward its target, but it also applies to other migratory cell types (Barberis et al., 2004; Li and Lee, 2010b; van Rijn et al., 2016). Although the level and location of protrusions appear normal in *Sema-5c* clones at stage 7 (Figure 2.5D), there is an abundance of mis-oriented protrusions in *Sema-5c* epithelia at stage 6 (Figures 2.5E-2.5L). Moreover, the presence of short COMETtails in *Sema-5c* epithelia at this stage indicates that the mis-oriented protrusions can occur in conjunction with the early stages of epithelial motility. Together with the localization data above, these observations suggest that Sema-5c might signal from each cell's leading edge to regulate the site of protrusion formation in the cell ahead.

To examine whether Sema-5c can suppress protrusions in neighboring cells, we overexpressed *Sema-5c* (*UAS-Sema-5c-GFP*) in follicle cell clones, which causes Sema-5c's localization to expand to the trailing edge (Figure 2.7A). In this overexpression condition, Sema-5c signals non-cell-autonomously to suppress leading edge protrusions in the cells directly behind the overexpressing cells (Figures 2.6J and 2.6K). The leading edge localization of the actin assembly factor SCAR is also reduced (Figures 2.7B and 2.7C). These phenotypes are only seen along cellular interfaces that directly contact the overexpressing cell, denoting an extremely short-range signal. Although Sema-5c is not normally localized to the trailing edge, this

overexpression system demonstrates that Sema-5c can suppress protrusions, and that it does so by signaling across cell-cell boundaries.

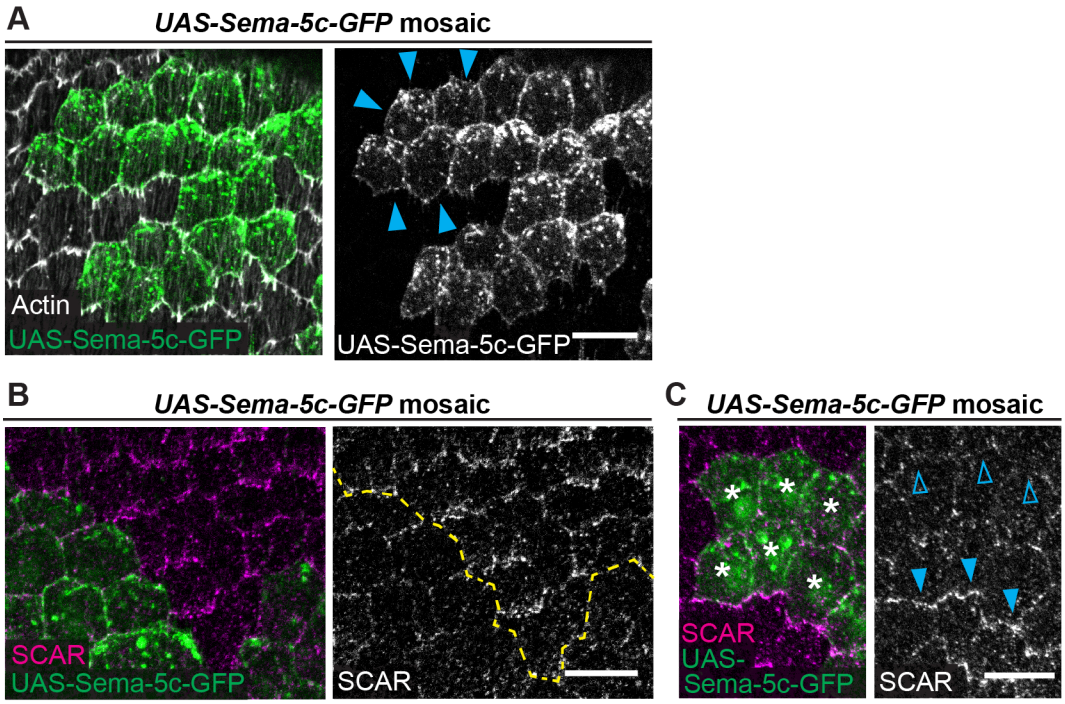

Figure 2.7. Effect of Sema-5c overexpression on protrusions (A) Images of the basal surface of a *UAS-Sema-5c-GFP* mosaic epithelium, stage 7. Sema-5c localizes all around the plasma membrane when overexpressed (blue triangles). (B and C) Images of the basal surface of *UAS-Sema-5c-GFP* mosaic epithelia with SCAR immunostaining, stage 7. (B) The larger clone shows that SCAR is reduced when *Sema-5c* is overexpressed. Dashed line marks the clone boundary. (C) The smaller clone (asterisks) shows that SCAR is lost from the leading edge of cells directly behind *Sema-5c* overexpressing cells (open triangles), but not from the leading edge of the *Sema-5c* overexpressing cells themselves (closed triangles). Scale bars, 10 µm.

Plexin A mediates Semaphorin-5c signaling

Our data suggest that Sema-5c promotes epithelial migration via intercellular signaling. To identify Sema-5c's receptor, we expressed RNAi against the *Drosophila's* plexins. Two *PlexB RNAi* transgenes, previously validated in other tissues, do not affect egg elongation (Figure 2.8A). By contrast, two independent *PlexA RNAi* transgenes strongly deplete PlexA from the follicle cells and produce round eggs (Figures 2.9A, 2.8B and 2.8C). Moreover, global stress

fiber alignment in *PlexA-RNAi* epithelia decreases until stage 5, but then recovers through stage 7, and we detected no obvious migration in *PlexA RNAi* epithelia by *ex vivo* live imaging (Figures 2.9B-2.9D). Thus, depletion of PlexA causes migration-associated phenotypes that are strikingly similar to those caused by loss of Sema-5c.

We then mapped PlexA's localization pattern. Using both a BAC transgene wherein *PlexA* is tagged with *myc* (*BAC-PlexA-myc*) and a PlexA antibody, we found that PlexA is punctate at the basal epithelial surface, and planar polarized along leading-trailing cell-cell interfaces (Figures 2.9E and 2.8D). To determine PlexA's subcellular localization, we then used a mosaic method similar to that described for Sema-5c above (STAR Methods). This experiment revealed that, although some PlexA is at the leading edge, most PlexA is at the trailing edge (Figures 2.9F-2.9H and 2.8E-2.8G). Thus, PlexA is in the right position to receive a Sema-5c signal from the leading edge of the cell behind.

To determine if PlexA binds to Sema-5c, we probed their interaction *in vitro* and *in vivo*. First, we employed an ELISA-type assay using the ectodomains of PlexA and the five *Drosophila* semaphorins (Figures 2.10A and 2.10B). This assay revealed robust binding between PlexA and Sema-5c. Additionally, PlexA binds to its known ligands, Sema-1a and 1b (Winberg et al., 1998), but not to Sema-2a and 2b, which are PlexB ligands (Ayoob, 2006; Wu et al., 2011). Second, we asked whether Sema-5c and PlexA are required for each other's localization. Although PlexA levels appear normal in *Sema-5c* epithelia (Figure 2.10C), Sema-5c-3xGFP is reduced at the basal surface of *PlexA-RNAi* epithelia (Figures 2.11A, 2.11B, and 2.10D). Despite this stabilizing effect of PlexA on Sema-5c, PlexA puncta are sparser and only sometimes colocalize with Sema-5c puncta (Figures 2.11C-2.11G) Altogether, these data indicate that PlexA and Sema-5c do interact, but that their interaction *in vivo* may be transient.

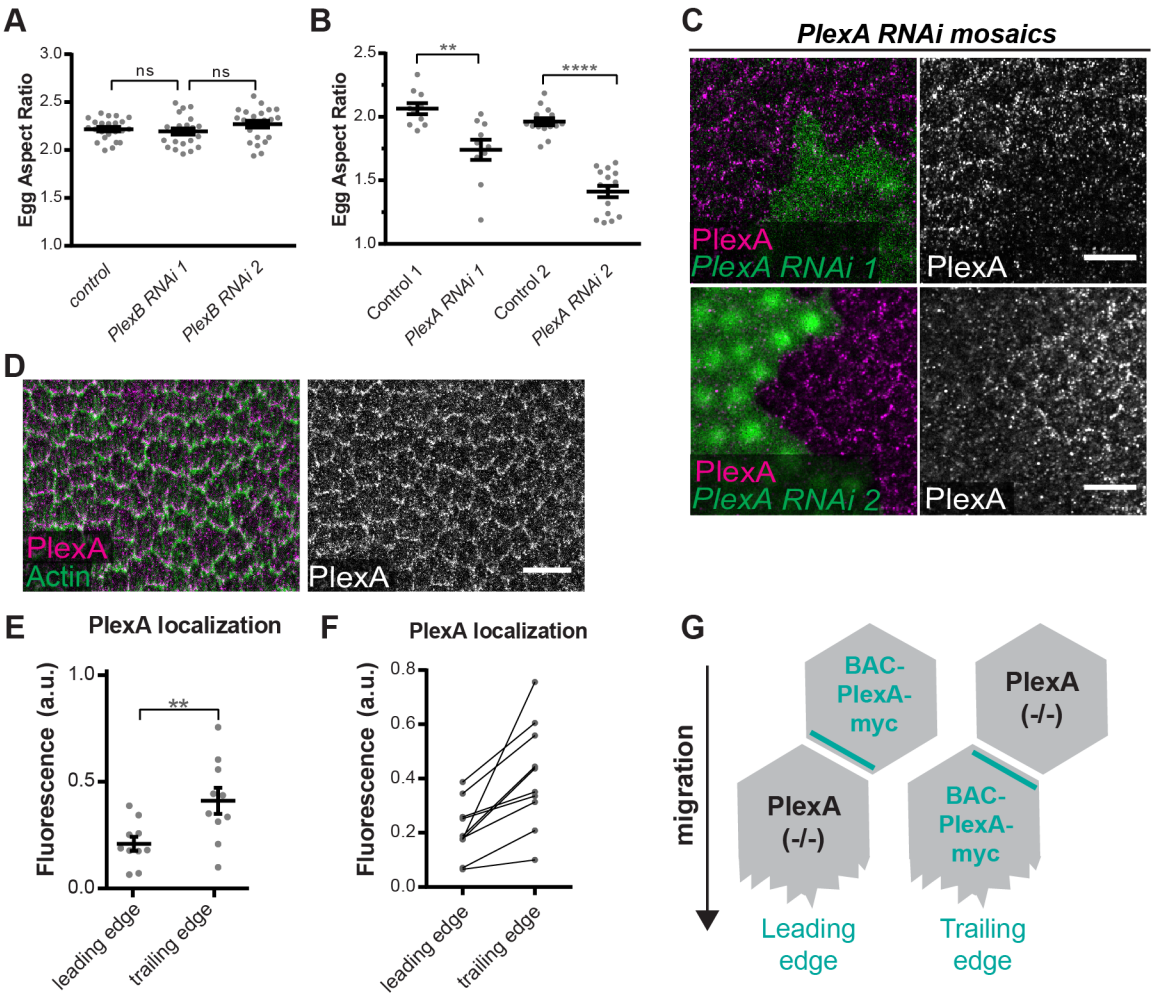

Figure 2.8. Analysis of Plexin reagents and PlexA localization (A) Quantification of egg aspect ratios. Expressing either of two previously validated *PlexB RNAi* transgenes in the follicular epithelium fails to affect egg shape. (B) Quantification of egg aspect ratios. Expressing ether of two independent *PlexA RNAi* transgenes in the follicular epithelium results in eggs that are rounder than controls. (C) Images of the basal surface of *PlexA RNAi* mosaic epithelia, stage 7. PlexA immunostaining is reduced by two independent *PlexA RNAi* transgenes. (D) Image of PlexA immunostaining at the basal epithelial surface, stage 7. PlexA is punctate along leading-trailing cell-cell interfaces. (E and F) Quantification of fluorescence intensity of BAC-PlexA-myc, anti-myc and anti-PlexA immunostaining, at leading versus trailing interfaces of *BAC-PlexA-myc* clones in a *PlexA* null background, stage 7. Each point is one epithelium in which line scans were preformed along 6-15 leading or trailing cell-cell interfaces. (E) The first graph shows the data for statistical purposes. (F) The second graph links the leading and trailing measurements for each egg chamber with a line. (G) Illustration depicting the populations of BAC-PlexA-myc quantified in (E and F). Data represent mean ± SEM. Unpaired t-test. ns, not significant ($p > 0.05$), **$p < 0.01$; ****$p < 0.0001$. Scale bars, 10 µm.

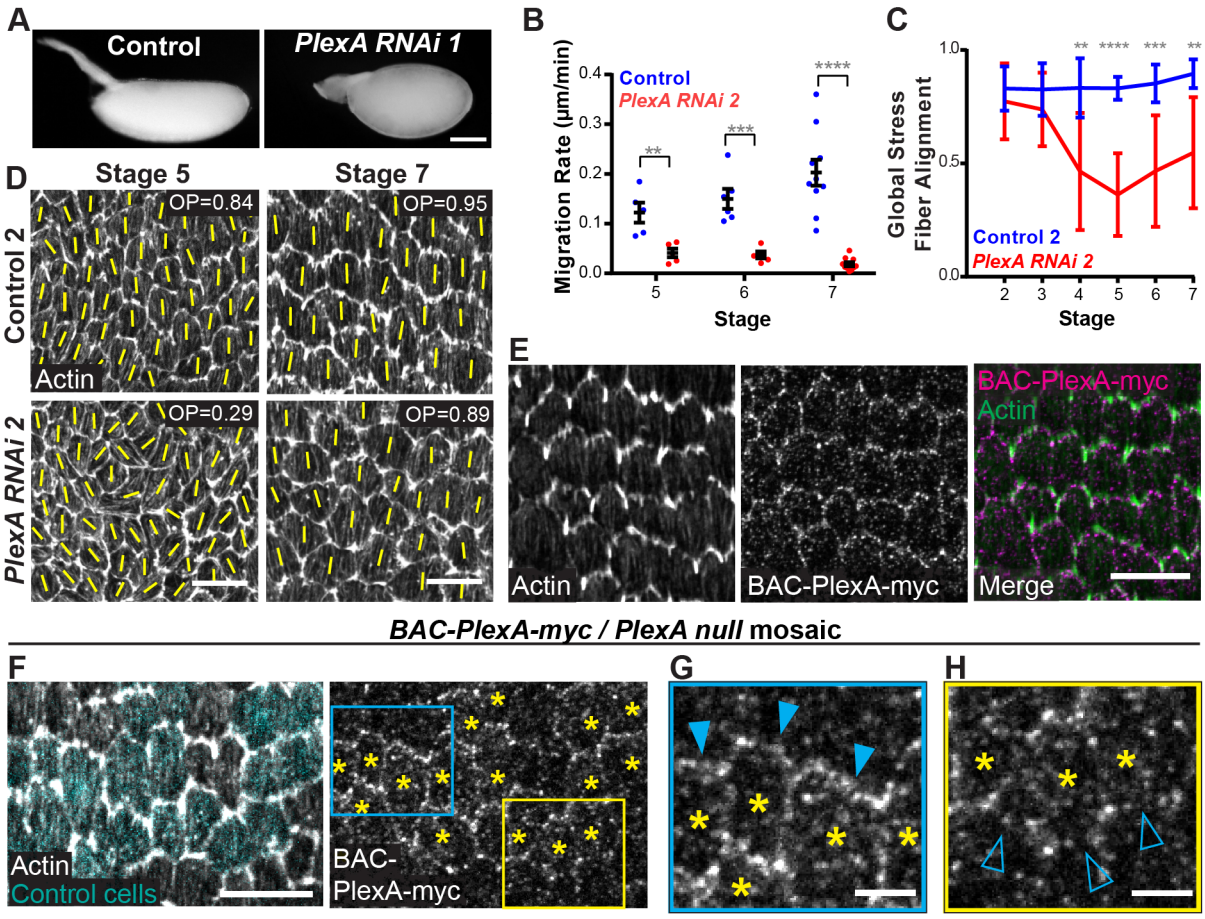

Figure 2.9. Loss of PlexA phenocopies loss of Sema-5c and PlexA is enriched at the trailing edge (A) Images of eggs from a control female and a female expressing *PlexA RNAi* in the follicular epithelium. (B) Quantification of migration rates from control and *PlexA RNAi* epithelia. (C) Quantification of global stress fiber alignment in control and *PlexA RNAi* epithelia. n ≥ 8 for all conditions. (D) Images of global stress fiber alignment in control and *PlexA RNAi* epithelia. Yellow lines show the primary stress fiber direction in each cell. OP = order parameter. (E) Images of the basal surface of a *BAC-PlexA-myc* epithelium, myc immunostaining, stage 7. PlexA is punctate along leading-trailing cell-cell interfaces. (F-H) Images of the basal surface of a mosaic epithelium with *BAC-PlexA-myc* clones in a *PlexA* null background, PlexA and myc immunostaining, stage 7. (F) Control cells are marked in cyan. (F-H) Asterisks mark cells expressing *BAC-PlexA-myc* at the clone boundary. (G) Zoom of the blue boxed region in (F). *BAC-PlexA-myc*-expressing cells primarily have PlexA enriched at their trailing edge (solid triangles). (H) Zoom of the yellow boxed region in (F). *BAC-PlexA-myc*-expressing cells also have some PlexA at their leading edge (open triangles). Data represent mean ± SEM in (B) and mean ± SD in (C). Unpaired t-test. **p < 0.01; ***p < 0.001; ****p < 0.0001. Scale bars, 100 µm (A); 10 µm (D-F); 3 µm (G and H)

Finally, we revisited our Sema-5c overexpression condition to ask if PlexA mediates Sema-5c's ability to suppress protrusions. Because there is some PlexA at each cell's leading edge, overexpressed *Sema-5c* may inhibit protrusions in the cell behind by signaling through this population of the receptor. Indeed, depleting PlexA from *UAS-Sema-5c-GFP* clones abrogates Sema-5c's ability to suppress protrusions (Figures 2.10E-2.10H), which shows that PlexA is required for Sema-5c activity. We further found that expressing either *UAS-HA-PlexA* or a low level of *UAS-Sema-5c-GFP* in the entire epithelium has only a minor effect on protrusions, whereas expressing both transgenes together strongly suppresses protrusions (Figures 2.11H-2.11K). Thus, overexpressed PlexA can also enhance Sema-5c's ability to signal. Altogether, these data suggest that PlexA acts as a receptor for Sema-5c in the follicular epithelium.

Semaphorin-5c interacts with Lar

The localization patterns of Sema-5c and PlexA resemble those of Lar and Fat2, which suggests that these four proteins might work together to promote epithelial motility. However, neither *Sema-5c* clones (Figure 2.5D), nor *PlexA RNAi* clones (Figure 2.10F), show the defects in leading edge protrusions and/or trailing edge retraction caused by loss of Lar or Fat2 (Barlan et al., 2017). This observation argues against Sema-5c and PlexA being part of the Lar/Fat2 signaling system; yet, there may still be crosstalk between the two signaling pathways.

We therefore explored if Sema-5c/PlexA and Lar/Fat2 interact at the genetic level. Removing one copy of *Lar* substantially rescues the egg shape defect in *Sema-5c* females (Figures 2.12A, 2.13A and 2.13B). Reduced Lar dosage may allow migration to begin earlier in *Sema-5c* epithelia, as global stress fiber alignment is higher in the rescued epithelia than in

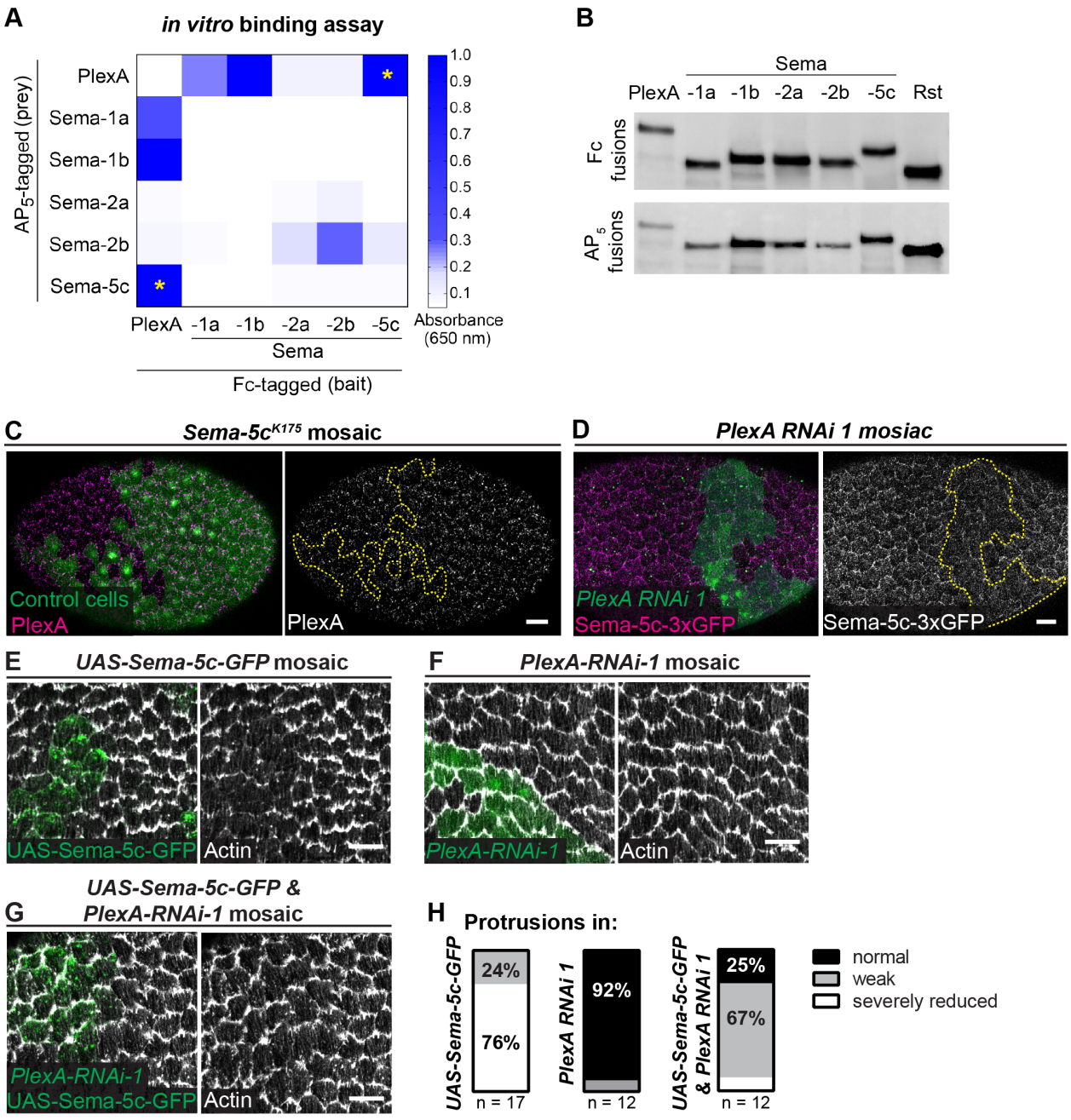

Figure 2.10. Further investigation of Sema-5c – PlexA interactions (A) Interaction grid for the binding between the PlexA ectodomain and the ectodomains of the five *Drosophila* semaphorins. Binding of prey to bait was detected using the BluePhos colorigenic substrate (KPL) for Alkaline Phosphatase (see STAR Methods). Sema-1a and Sema-1b are PlexA ligands and thus serve as positive controls. Sema-2a and Sema-2b are PlexB ligands and serve as negative controls. The yellow asterisks highlight strong binding between PlexA and Sema-5c. The binding seen between some of the Sema ligands was unexpected, but may be consistent with a previous report of a possible Sema-1a - Sema-2a interaction (Sweeny et al., 2011). Legend continued on next page.

Figure 2.10. continued (B) Western blot showing the expression levels of the ectodomains used in (A), Roughest (Rst) was used as a positive control. (C) Image of PlexA immunostaining at the basal surface of a *Sema-5c* ^{K175} mosaic epithelium, stage 7. PlexA levels are not affected by loss of Sema-5c. (D) Image of the basal surface of a *PlexA RNAi* mosaic epithelium, stage 7. *PlexA RNAi* cells pseudocolored green. Sema-5c-3XGFP levels are reduced by loss of PlexA. (E-G) Depletion of PlexA abrogates Sema-5c's ability to suppress protrusions. Images of the basal epithelial surface, stage 8. (E) Clones of cells expressing *UAS-Sema-5c-GFP* have strongly reduced protrusions. (F) Clones of cells expressing *UAS-PlexA-RNAi* have largely normal protrusions. (G) Co-expressing *UAS-PlexA-RNAi* with *UAS-Sema-5c-GFP* partially rescues the protrusion defect induced by *Sema-5c* overexpression. (H) Quantification of the data presented in (E-G). n = number of

Sema-5c epithelia (Figures 2.12B-2.13D and 2.13C). Reduced *Lar* dosage does not rescue the migration rate, however, as we detected no directional motility in rescued epithelia by *ex vivo* live imaging (Figure 2.13D). Removing one copy of *fat2* does not rescue the egg shape defect in *Sema-5c* females (Figure 2.13E), nor does removing one copy of *Lar* in *PlexA-RNAi* females (Figure 2.13F). Altogether, these data suggest that Sema-5c antagonizes Lar activity, and that this interaction may be independent of Fat2 and PlexA.

Since Sema-5c and Lar both localize to the leading edge, we next asked if they colocalize. The density of Sema-5c and Lar puncta is similar along the leading-trailing cell-cell interfaces, and they consistently overlap (Figures 2.12E-2.12I). Moreover, although Lar levels appear normal in *Sema-5c* and *PlexA RNAi* clones, Sema-5c levels are reduced in *Lar* clones (Figures 2.12J, 2.13G and 2.13H). This reduction is not due to an effect on PlexA, as PlexA levels are normal in *Lar* clones (Figure 2.13I). Altogether, these data suggest that Sema-5c has a second function that involves a cis interaction with Lar.

2.5 DISCUSSION

Here we introduce a tissue-autonomous model for semaphorin signaling in collective cell migration (Figure 2.12K). Our data show that Sema-5c acts as a migratory cue within the

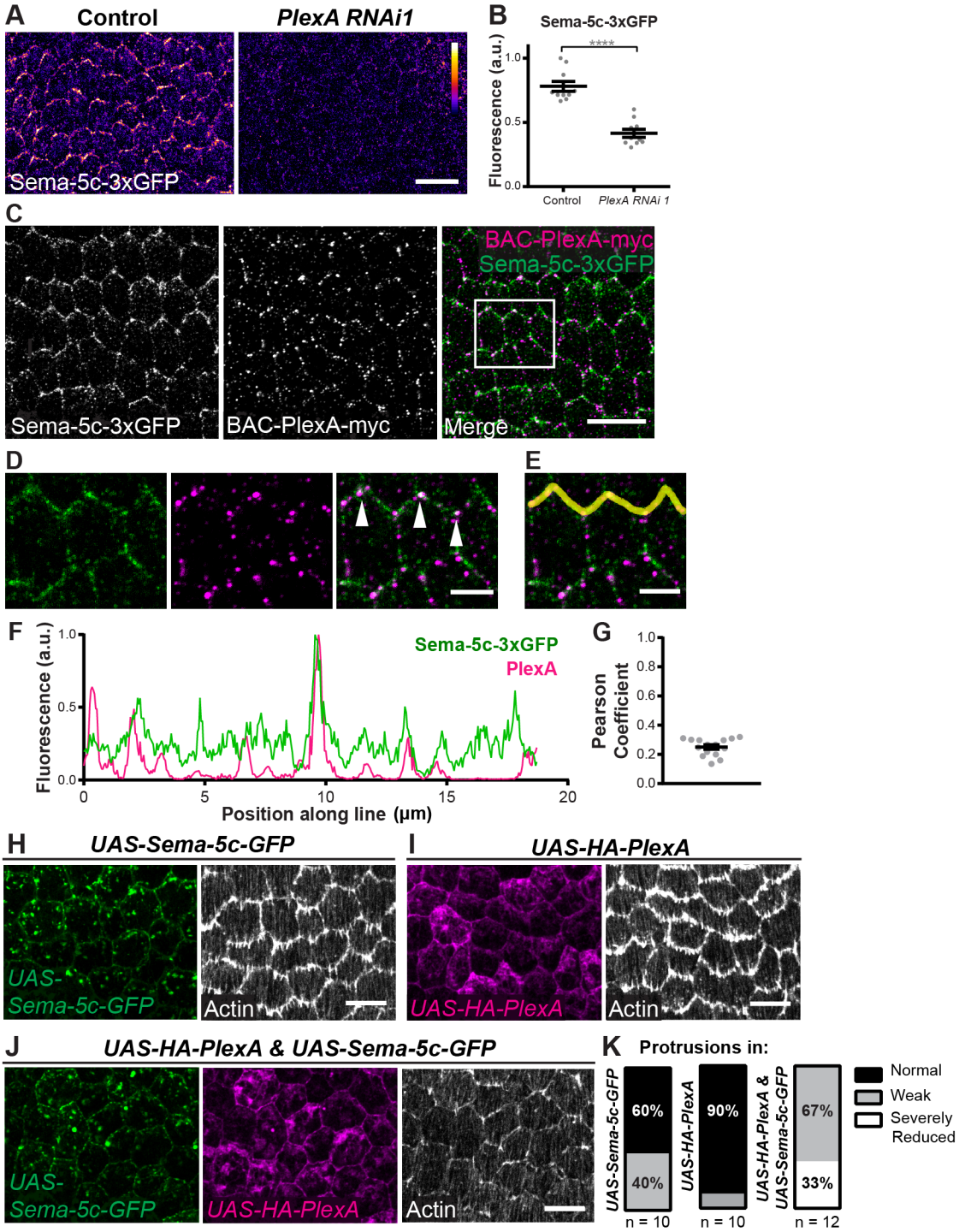

Figure 2.11. PlexA is the likely receptor for Sema-5c (A) Images of the basal epithelial surface, stage 7. *PlexA RNAi* reduces Sema-5c-3xGFP levels. (B) Quantification of Sema-5c-3xGFP levels at cell-cell interfaces in control and *PlexA RNAi* epithelia, stage 7. (C-E) Images of the basal surface of an epithelium expressing *Sema-5c-3xGFP* and *BAC-PlexA-myc*, myc immunostaining, stage 7. (D and E) Zoom of boxed region in (C). Legend continued on next page.

Figure 2.11. continued White triangles indicate colocalization between Sema-5c and PlexA. (F) Quantification of fluorescence intensities of Sema-5c-3xGFP and BAC-PlexA-myc along the cell-cell interfaces marked by the yellow line in (E). (G) Pearson correlation coefficient for Sema-5c-3xGFP and BAC-PlexA-myc fluorescence intensities along leading-trailing cell-cell interfaces, stage 7. Each point is one epithelium in which a line scan was performed along 5-8 cell-cell interfaces. (H-J) Coexpression of *PlexA* enhances the *Sema-5c* overexpression phenotype. Images are of the basal epithelial surface, stage 8. (H) A low level of *UAS-Sema-5c-GFP* mildly reduces protrusions. (I) *UAS-HA-PlexA* has little effect on protrusions. (J) Coexpressing both transgenes strongly reduces protrusions. (K) Quantification of data in (H-J). n = number of egg chambers examined. Data in (B) represent mean ± SEM. Unpaired t-test. ****$p < 0.0001$. Scale bars, 10 μm (A, C and H-J); 3 μm (D and E).

collectively migrating epithelial cells, themselves, instead of acting in the migratory environment. Sema-5c is planar polarized at the basal epithelial surface, localizing to each cell's leading edge. We envision that this placement allows Sema-5c to activate PlexA on the trailing edge of the cell ahead, and thus communicate directional information between neighboring cells. We further identify an interaction between Sema-5c and Lar, which suggests that Sema-5c may play a second role in the Lar/Fat2 signaling pathway. Together these results highlight how multiple guidance cues work in concert within an epithelium to coordinate cell movements for collective motility.

Semaphorin-5c may promote collective motility by acting as a repulsive cue for neighboring cells

Given that overexpressing Sema-5c collapses protrusions in neighboring cells, we propose that Sema-5c may promote collective motility via contact inhibition of locomotion (CIL). CIL describes a set of behaviors exhibited by a migrating cell when it collides with another cell (Stramer and Mayor, 2016). Specifically, the cell retracts its protrusions from the point of contact and repolarizes to migrate away in a new direction. CIL is mediated by signaling proteins on the cells' surfaces, including semaphorins and plexins (Deb Roy et al., 2017; Hung and Terman,

2011). Although CIL is often used to disperse cells, cases exist where CIL appears to organize cells for collective movement (Stramer and Mayor, 2016). We propose that the Sema-5c at each cell's leading edge could signal to suppress protrusions at the trailing edge of the cell ahead, and thus direct the signal-receiving cell to polarize away from this point of contact, such that both cells then migrate in the same direction. In this scenario, the semaphorin is a repulsive cue, similar to the most common function of semaphorins in axon guidance. Supporting this notion, we see an abundance of mis-oriented protrusions in *Sema-5c* epithelia at stages 5 and 6. Determining if Semaphorin-based CIL is operating in the follicular epithelium will be an important area for future work.

The role we have identified for Sema-5c in promoting collective migration may be conserved. Sema-5c is the only *Drosophila* semaphorin with direct homologs in vertebrates (Sema5A and Sema5B). Moreover, similar to Sema-5c, the vertebrate class 5 semaphorins promote the migration of multiple cell types (Artigiani et al., 2004; Li and Lee, 2010b; Li et al., 2012; Sadanandam et al., 2010), and can collapse protrusions non-cell-autonomously (Artigiani et al., 2004; Li and Lee, 2010b). Given that three of the five classes of vertebrate semaphorins are integral membrane proteins (classes 4, 5, and 6), any one of these family members could promote collective migration similarly to Sema-5c, which opens the possibility that Sema-5c's mechanism of action could be widely used.

Semaphorin-5c likely signals through Plexin A

Four pieces of evidence suggest that PlexA is a Sema-5c receptor. First, the follicle cells require PlexA to migrate normally. Second, the dynamics of the global stress fiber pattern in *PlexA RNAi* epithelia is similar to that of *Sema-5c* epithelia. Third, PlexA and Sema-5c interact both *in vitro*

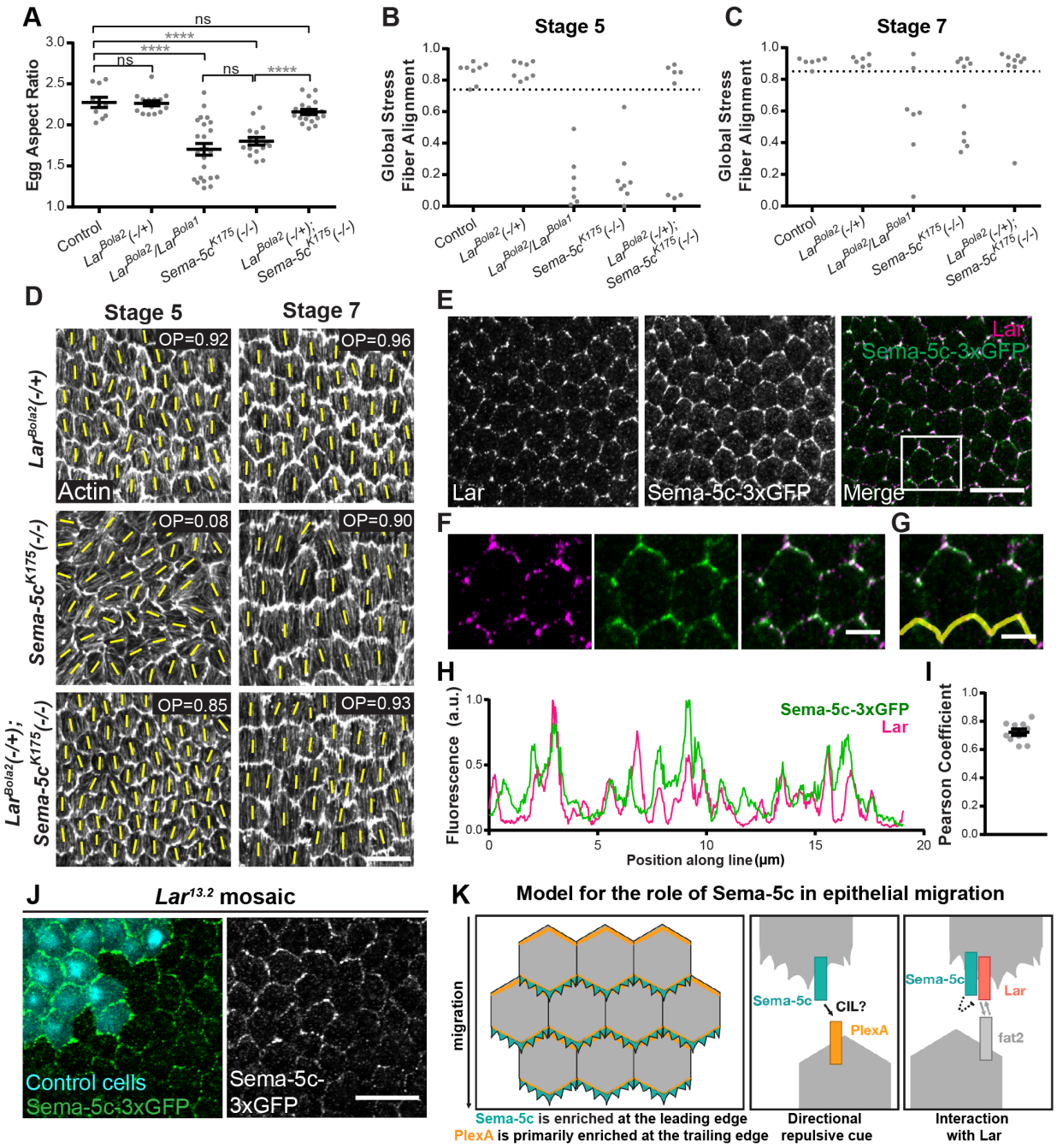

Figure 2.12. Sema-5c interacts with Lar (A) Quantification of egg aspect ratios. Removing one copy of *Lar* rescues the *Sema-5c*^{K175} egg shape defect. (B and C) Quantification of global stress fiber alignment. Removing one copy of *Lar* partially rescues the defect in *Sema-5c*^{K175} epithelia. (D) Images of global stress fiber alignment for some conditions analyzed in (B and C). Yellow lines show the primary stress fiber direction in each cell. OP = order parameter. Legend continued on next page.

Figure 2.12. continued (E-G) Images of the basal surface of a *Sema-5c-3xGFP* epithelium with Lar immunostaining, stage 7. Sema-5c and Lar colocalize. (F-G) Zoom of the boxed region in (E). (H) Quantification of fluorescence intensities of Sema-5c-3xGFP and Lar along the cell-cell interfaces marked by the yellow line in (G). (I) Pearson correlation coefficient for Sema-5c-3xGFP and Lar along leading-trailing cell-cell interfaces, stage 7. Each point represents one epithelium in which a line scan was performed along 5-8 cell-cell interfaces. (J) Images of the basal surface of a $Lar^{13.2}$ mosaic epithelium, stage 7. Sema-5c-3xGFP is reduced in mutant cells. (K) Illustration of our working model for Sema-5c's role in follicle cell migration. Data in (A) represent mean ± SEM. Unpaired t-test. ns, not significant ($p > 0.05$); ****$p < 0.0001$. Scale bars, 10 μm (D, E and J); 3μm (F and G).

and *in vivo*. Fourth, PlexA primarily localizes to each cell's trailing edge, placing it in the right position to receive a Sema-5c signal from the leading edge of the cell behind. This observation is particularly intriguing, as a vertebrate homolog of PlexA, Plexin A1, functions at the trailing edge of migrating dendritic cells (Takamatsu et al., 2010).

Given that PlexA is required for Sema-5c's localization, we were surprised to find that they only rarely colocalize. We are not aware of other studies that report colocalization of a semaphorin-plexin pair at the sub-cellular level, so the dynamics of the ligand-receptor interaction *in vivo* are mysterious. It is interesting to speculate that the repulsive nature of the semaphorin signal may necessitate a transient interaction with its receptor.

Although our data strongly suggest that Sema-5c signals through PlexA, more complex models are possible. For example, vertebrate class 5 semaphorins signal through both A- and B-type plexins (Artigiani et al., 2004; Duan et al., 2014; Li and Lee, 2010b; Matsuoka et al., 2011). Thus, Sema-5c could also signal through PlexB. There may also be reverse signaling through Sema-5c's intracellular domain (Battistini and Tamagnone, 2016). Future work will determine if these alternate modes of Sema-5c signaling also contribute to epithelial motility.

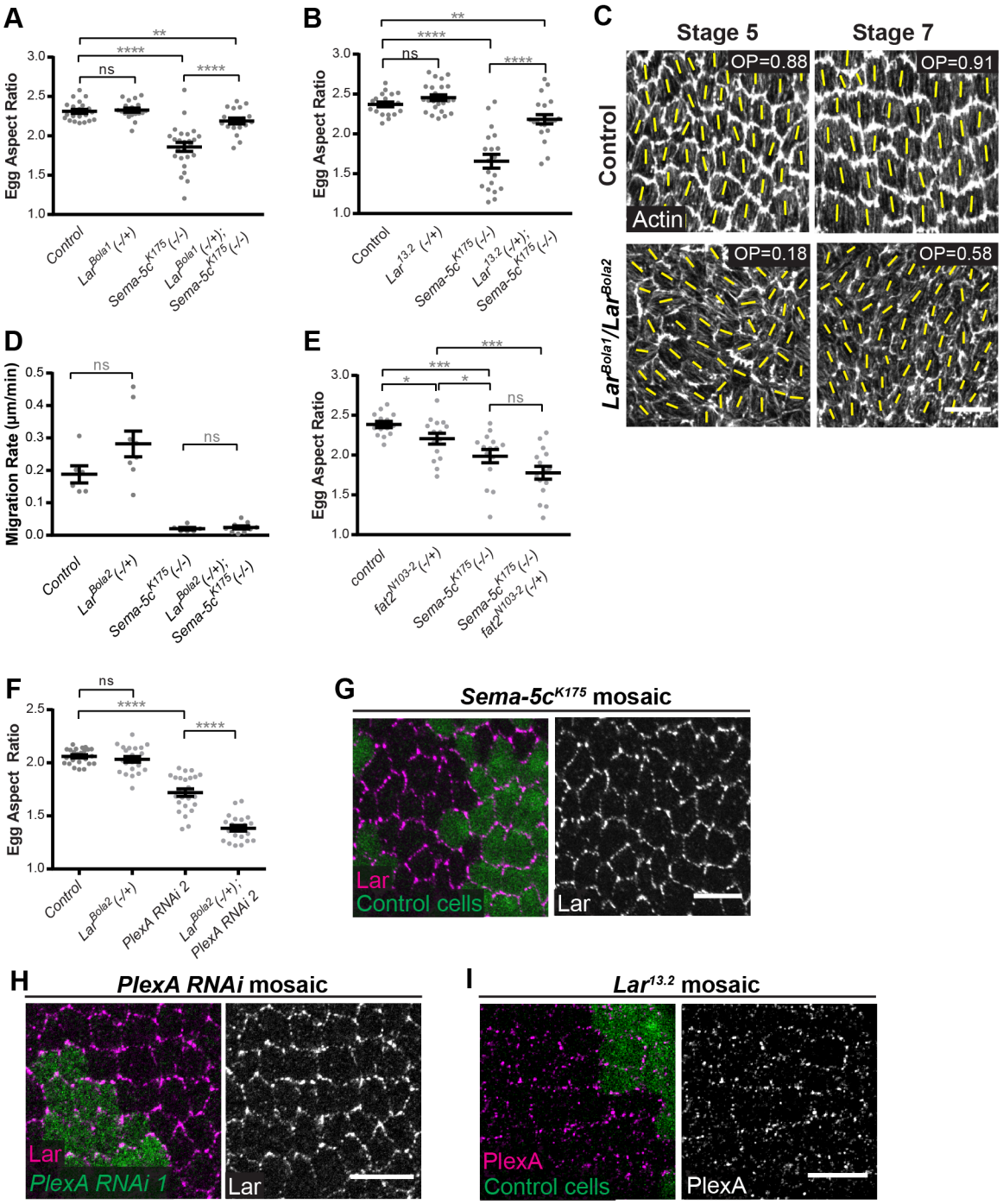

Figure 2.13. Investigating the interaction between Sema-5c, PlexA, Lar, and Fat2 (A and B) Quantification of egg aspect ratios. Removing one copy of *Lar* largely rescues the egg shape defect in *Sema-5c* ^{K175} females. Data are shown for two independent alleles of *Lar*. (C) Images of global stress fiber alignment for the control and *Lar*^{Bola}/*Lar*^{Bola2} conditions analyzed in Figures 2.12B and 2.12C. Yellow lines show the primary stress fiber direction in each cell. OP = order parameter. Legend continued on next page.

Figure 2.13. continued (D) Quantification of migration rates. Removing one copy of *Lar* in the *Sema-5c*^{K175} background does not rescue the migration rate, stage 7. (E and F) Quantification of egg aspect ratios. Elongation is neither rescued by loss of one copy of *fat2* in a *Sema-5c*^{K175} background (E), nor by loss of one copy of *Lar* in a *PlexA RNAi* background (F). (G) Image of Lar immunostaining at the basal surface of a *Sema-5c*^{K175} mosaic epithelium, stage 7. Lar levels are not affected by loss of Sema-5c. (H) Image of Lar immunostaining at the basal surface of a *PlexA RNAi* mosaic epithelium, stage 7. Lar levels are not affected by loss of PlexA. (I) Image of PlexA immunostaining at the basal surface of a *Lar*$^{13.2}$ mosaic epithelium, stage 7. PlexA levels are not affected by loss of Lar. Data represent mean ± SEM. Unpaired t-test. ns, not significant ($p > 0.05$), *$p < 0.05$; **$p < 0.01$; ***$p < 0.001$; ****$p < 0.0001$. Scale bars, 10 μm.

Multiple guidance cues work in concert to promote epithelial migration

The Sema-5c/PlexA and Lar/Fat2 signaling systems both operate along leading-trailing cell-cell interfaces to promote collective motility. Although phenotypic differences argue against all four proteins acting in one pathway, three pieces of evidence indicate that Sema-5c interacts with Lar. First, Sema-5c and Lar colocalize at the basal epithelial surface. Second, Lar is required for Sema-5c's localization. Third, reducing *Lar* dosage rescues the global stress fiber alignment and egg shape phenotypes caused by loss of Sema-5c. These data suggest that Sema-5c antagonizes Lar activity, and further imply that Lar may inhibit cell migration under some circumstances. It is possible that Sema-5c plays two roles in the follicle cells – one with PlexA and one with Lar. Alternatively, the interaction between Sema-5c and Lar may represent a point of convergence between two otherwise separate signaling pathways.

Given that Sema-5c and Lar both localize to the leading edge, they likely interact *in cis*. We envision two non-mutually-exclusive models by which this could occur. Class 5 semaphorins and Lar both bind heparin sulfate proteoglycans (Johnson et al., 2006; Kantor et al., 2004), making it possible that glycan chains could bridge an interaction between their ectodomains. Alternatively, the interaction could occur downstream of their intracellular domains (Battistini and Tamagnone, 2016). A recent study showed that semaphorins interact with Lar-family RPTPs

in the nervous systems of *C. elegans* and mice (Nakamura et al., 2017). However, the mechanism described therein is different, with Lar functioning *in cis* with the plexin to amplify a secreted semaphorin signal. Thus, there may be crosstalk between Lar and semaphorins in multiple contexts.

The protein families to which Sema-5c, PlexA, Lar, and Fat2 belong are all known for their roles in nervous system development. Semaphorins and plexins are one of the canonical families of axon guidance cues (Kolodkin and Tessier-Lavigne, 2011), and Lar-family RPTPs function in both axon guidance and synapse formation (Han et al., 2016). Although less studied, Fat-like cadherins also help to wire the nervous system (Avilés and Goodrich, 2017). The steering of a growth cone toward its target represents a system in which a guidance cue from the cellular environment modulates the behavior of a migrating cell. We have now identified a situation wherein these same guidance cues are planar polarized across an epithelium to allow each cell within the tissue to modulate the migratory behavior of their neighbors for collective motility. A recent study noted that the appearance of the semaphorin and plexin families predates the evolution of the nervous system in metazoans (Yoo et al., 2016). The same is true for Fat-like cadherins (Hulpiau and van Roy, 2011). Thus, the ancestral role for these guidance cues may be to regulate epithelial dynamics, with their role in guiding axons arising later.

Collective migration of the follicle cells can begin late in development from a disordered state

Finally, this work elucidates the cellular parameters required for the follicular epithelium to migrate. The follicle cells typically begin migrating shortly after an egg chamber forms, and their stress fibers always show a high degree of global alignment (Cetera et al., 2014). We have

discovered that neither of these features is strictly required for epithelial motility. Moreover, our observations that epithelial migration can begin later in development, and can do so after the stress fiber pattern has become disordered, show that the ability of this epithelium to break symmetry and polarize is more robust than previously appreciated.

There is a *fat2* partial-loss-of-function condition that is phenotypically similar to *Sema-5c* (Aurich and Dahmann, 2016; Chen et al., 2017). In this condition, epithelial migration is so slow that it cannot be detected by *ex vivo* live imaging. Moreover, migration is likely delayed, as the global stress fiber pattern is disordered at stage 6, but recovers by stage 8. Future work will determine the extent to which these two mutant conditions phenocopy, and whether these similarities indicate yet more points of convergence between the Sema-5c/PlexA and Lar/Fat2 signaling systems.

The observation that some mutant epithelia polarize and begin migrating at stage 5/6 suggests that there may be developmentally programmed changes in the egg chamber that create a more favorable environment for epithelial motility. We previously noted that global stress fiber alignment and migration rate both increase in wild-type epithelia around this time (Cetera et al., 2014). This improved migratory ability could be due to higher BM stiffness, as stiffer matrices promote cell migration (Mason et al., 2012), and the stiffness of the follicular BM increases over time (Chlasta et al., 2017; Crest et al., 2017). Determining if the cells are responding to mechanical changes in the BM, and how they do so, will be fertile areas for future research.

Conclusion

This work introduces a tissue-autonomous role for semaphorins in guiding the collective migration of epithelial cells. Moreover, our observation that Sema-5c and PlexA act alongside

Lar and Fat2 to promote epithelial motility highlights the complex signaling interactions that occur along leading-trailing cell-cell interfaces to allow these cells to coordinate their individual movements for collective motility.

2.6 METHODS

Drosophila genetics

D. melanogaster was cultured on cornmeal molasses agar food using standard techniques. All experiments were performed on adult females. For most experiments, crosses were raised at 25°C and experimental females were aged on yeast with males for 2-3 days at the same temperature. Experimental genotypes for each figure panel are in Table S1. The culturing conditions for the females in each experiment are detailed in Table S2.

Clones of either S*ema-5c*^{K175} mutant cells or *Sema-5c-3xGFP* expressing cells were produced using *FRT80B* with *e22c-Gal4* driving *FLP* recombinase expression (Duffy et al., 1998). For Flp out clones, *UAS* lines were crossed to flies with FLP recombinase under a heat shock promoter and an *Act5c>>Gal4* Flp out cassette with or without *UAS-GFP* or *UAS-RFP*. Heat shock was induced by incubating pupae and adults at 37°C for 1 hour, followed by 1 hour of recovery at 25°C, and then another hour at 37°C. This heat shock procedure was performed 3 times over the course of 2 days. Females that eclosed during the period were placed on yeast with males overnight and dissected the next day.

For the studies of the Plexin receptors, the following RNAi lines were used: *UAS-PlexA-RNAi* 1 (v27240, GD14483), *UAS-PlexA-RNAi* 2 (TRiP.HM05221), *UAS-PlexB-RNAi* 1 (v27220, GD14473), and *UAS-PlexB-RNAi* 2 (v12167, GD3150) (Meltzer et al., 2016).

Stocks are from Bloomington *Drosophila* Stock Center with the following exceptions. *UAS-PlexA-RNAi*^{GD14483}, *UAS-PlexB-RNAi*^{GD14473}, and *UAS-PlexB-RNAi*^{GD3150} are from the Vienna *Drosophila* Resource Center. *Traffic jam-Gal4* (104055) is from the *Drosophila* Genetic Resource Center in Kyoto. *Lar*^{Bola1} and *Lar*^{Bola2} are a gift from Allan Spradling (Frydman and Spradling, 2001). *UAS-Col4a1-mRFP* is a gift from Jose Pastor-Pareja (Zang et al., 2015). *Lar*$^{13.2}$*, FRT40A* is a gift from David Van Vactor (Bateman et al., 2001). The *BAC-PlexA-myc* strain is a gift from Alex Kolodkin (Pecot et al., 2013; Yoo et al., 2016). *UAS-HA-PlexA* is a gift from Johnathan Terman (Terman et al., 2002). Both *w;; BAC-PlexA-myc, ubi-GFP, h, FRT80B/TM6; Df(4)C3/CiD* and *yw, hsFLP;; FRT80B, e, ca/TM6; PlexA*^{MB}*/CiD* are gifts from Trudi Schüpbach. *Sema-5c*^{K175} and *fat2*$^{N103-2}$ are from (Horne-Badovinac et al., 2012) and *Fat2-3xGFP* is from (Barlan et al., 2017)**.**

Time lapse video acquisition and microscopy

Ex vivo live imaging of egg chambers was performed largely as described (Cetera et al., 2016; Prasad et al., 2007), with the exact procedure outlined below. Experimental females were collected 1-2 days after eclosion and aged on yeast for 2 days. Ovaries were dissected in live imaging media (Schneider's *Drosophila* medium containing 15% FBS and 200 µg/ml insulin) containing CellMask Deep Red Plasma Membrane Stain (Thermo-Fisher; 1:1000). After carefully removing the muscle sheathes with forceps, individual ovarioles were transferred to fresh live imaging media to wash out excess CellMask. The ovarioles and media were transferred to a glass slide; 51 µm Soda Lime Glass beads (Cospheric LLC) were added to support a 22 x 22 µm No. 1.5 coverslip. The edges of the coverslip were sealed with Vaseline to prevent evaporation. Each slide was used for no more than 2 hours. All egg chambers were examined for

damage prior to imaging, using CellMask to highlight damaged areas, as damaged egg chambers do not rotate. Egg chambers were imaged with one of two laser-scanning confocal microscopes running Zen 2.3 acquisition software, either a Zeiss LSM 800 with a 40x/1.3 NA EC Plan-NEOFLUAR objective, or a Zeiss LSM 880 with 40x/1.3 Plan-APOCHROMAT objective. Time-lapse movies were performed by capturing single confocal slices near the basal epithelial surface every 60 seconds. To calculate epithelial migration rates, kymographs were generated from the time-lapse image stacks in Fiji (ImageJ) (Schindelin et al., 2012; Schneider et al., 2012) by drawing a single line across several cell diameters in the direction of migration. The migration rate for each epithelium was then determined by measuring the slope of 3-4 kymograph lines and averaging the values. Please see (Barlan et al., 2017) for an illustration of this technique.

Fixed image acquisition and microscopy

Ovaries were dissected in live imaging media, as described above. To isolate individual ovarioles, the muscle sheaths were either removed with forceps during dissection or by gentle pipetting post-fixation. In all cases, egg chambers at stage 10 or older were discarded. Egg chambers were fixed for 15 minutes in 4% EM grade formaldehyde (Polysciences) in PBT (PBS + 0.1% Triton X-100), the one exception is the use of 4% formaldehyde in Schneider's medium when immunostaining for Lar. To stain F-actin, egg chambers were washed 3x in PBT, incubated in TRITC Phalloidin (1:200 for 25 minutes, Sigma) or AlexaFluor-647 phalloidin (1:50 overnight or 1:30 for 3 hours, Invitrogen), then washed 3x in PBT and mounted with one drop of SlowFade Antifade (Invitrogen) onto a slide with a 22 x 50mm No. 1.5 coverslip. For antibody staining, egg chambers were fixed as above, washed 4x in either PBT, PBT2 or PBT3

(PBS + 0.1%, 0.2% or 0.3% Triton X-100, respectively), and incubated at 4°C overnight with the primary antibody. Then egg chambers were washed 4x, incubated with secondary antibodies conjugated to AlexaFluor-555, or -647 (Invitrogen, 1:200) for 2-3 hours at room temperature, washed 4X and mounted as above. Anti-Lar (9D82B3, 1:200 concentrate) and anti-SCAR (P1C1, 1:200 concentrate) are from the Developmental Studies Hybridoma Bank, anti-ß-Galactosidase is from Promega (Z378A, 1:200), anti-myc is from Cell Signaling Technologies (71D10, 1:200) and anti-HA is from Rockland Inc. (600-401-384, 1:250). Anti-PlexA is a gift from Takaki Komiyama (Sweeney et al., 2007), and was pre-absorbed overnight on egg chambers expressing *UAS-PlexA-RNAi* to reduce background signal prior to tissue staining and used at 1:1000. Tissue was imaged with one of the two scanning confocal microscopes described above, using the same objectives or a 63x/1.4 NA Plan-APOCHROMAT objective. For all images a single confocal slice is shown. All image processing was done in Fiji (ImageJ) (Schindelin et al., 2012; Schneider et al., 2012) and utilized the ScientiFig Plugin (Aigouy and Mirouse, 2013) for image overlays.

Quantification of egg aspect ratio

Ovaries were dissected in freshly made Robb's minimal saline and fixed in Robb's containing 8% EM grade formaldehyde (Polysciences) for 5 minutes. The tissue was washed 3x in PBT, then disrupted with pipetting to remove the muscle sheath. Tissue was stained with phalloidin (1:200) and DAPI (1 µg/ml, Sigma) for 20 minutes. Stage 14 egg chambers and mature eggs were mounted and imaged on one of the two scanning confocal microscopes described above, using a 20x/0.8 NA Plan-APOCHROMAT objective. Aspect ratios were calculated by dividing the length of each egg by its width, which were both measured in Fiji (ImageJ) (Schindelin et al.,

2012; Schneider et al., 2012); dorsal appendages were not included in the measurements. To obtain brightfield images of eggs, ovaries were dissected as described above, and eggs were imaged in Robb's media on a Leica MZ FLIII microscope with a Canon Rebel Camera. Image processing was done in Fiji (ImageJ) (Schindelin et al., 2012; Schneider et al., 2012).

Measurements of global stress fiber alignment

Egg chambers were fixed, stained with phalloidin, and imaged as described above. The orientation of stress fibers in an individual cell was determined by using the Measure function of the OrientationJ plugin (Rezakhaniha et al., 2012) for Fiji (ImageJ) (Schindelin et al., 2012; Schneider et al., 2012) after manually selecting a circular region of interest at the basal surface of each cell, excluding cell boundaries. To determine the tissue-level stress fiber alignment (the order parameter) for a given egg chamber, a single imaging plane was used and the orientation of the stress fibers in each cell was compared to all neighboring cells using a custom Python script as previously described (Cetera et al., 2014; Isabella and Horne-Badovinac, 2015).

COMETtail analysis

Flp out clones, as described above, were used to express *UAS-Col4a1-mRFP* in either control or mutant backgrounds. For COMETtail analysis, however, only adult flies were heat shocked (incubated on yeast at 37°C for 1 hour, followed by a 1 hour recovery period at 25°C followed by another hour at 37°C) and dissected 12 hours after the start of the incubation period. Clones were identified by intracellular accumulation of *UAS-Col4a1-mRFP* within the secretory pathway of expressing cells. A COMETtail was scored as being "present" in the BM if it extended more than one cell length away from the clone. Some diffusion can occur even when

there is no migration, as was occasionally seen in the *fat2*$^{N103\text{-}2}$ condition, which is non-migratory (Barlan et al., 2017).

in vitro binding assay

To test binding between Plexin A and the five *Drosophila* semaphorins, we applied the Extracellular Interactome Assay (ECIA) (Özkan et al., 2013), which is an avidity-based high-throughput interaction detection assay. The ectodomains of PlexA and the five semaphorins were cloned into expression plasmids that produce soluble bait and prey, with an Fc tag for capture on Protein A-coated plates and with a pentamerized Alkaline Phosphatase (AP_5) tag for detection of binding, respectively. For higher expression levels, the original metallothionein promoter in the ECIA expression plasmids (Carrillo et al., 2015; Özkan et al., 2013) were replaced with the highly active, constitutive Actin5c promoter. The bait and prey were expressed in and secreted from *Drosophila* S2 cells, and the binding of the prey to bait was detected using the BluePhos colorigenic substrate (KPL) for Alkaline Phosphatase with absorbance at 650 nm.

Quantification of protein localization

Relative levels of Sema-5c-3xGFP and BAC-PlexA-myc at the leading versus trailing edges of cells were quantified in Fiji (ImageJ) (Schindelin et al., 2012; Schneider et al., 2012). A 10-pixel wide line was drawn along leading-trailing cell-cell interfaces at the basal surface of epithelia that were mosaic for the tagged protein. The Measure function was then used to obtain an average fluorescence intensity over each line. The leading versus trailing edge of each clone was determined using leading-edge protrusions, which were marked by Phalloidin. Lines were drawn over 3 categories of cell-cell interfaces: leading edges of the clones, trailing edges of the clones,

and cell-cell interfaces outside of the clone (background staining). For each epithelium, the intensities from all the measurements within a single category were averaged together to obtain a single value for each epithelium in each category (leading edge, trailing edge, and background); the background level was used to normalize the data. In an individual epithelium, the same number of cell-cell interfaces was quantified across all categories.

BAC-PlexA-myc mosaic epithelia were generated by creating Flp FRT clones of *BAC-PlexA-myc* in an epithelium that was null for *PlexA*. It is necessary to use a *PlexA* null background when examining clones of *BAC-PlexA-myc* in order to maintain the endogenous level of PlexA in the cells being analyzed (when extra copies of PlexA are expressed, its planar polarity is lost). The mosaic tissue was then simultaneously immunostained with anti-PlexA and anti-myc to boost the signal.

Quantification of protein colocalization

Line scans were generated by manually drawing a 10-pixel wide line over leading-trailing cell-cell interfaces at the basal epithelial surface using Fiji (ImageJ) (Schindelin et al., 2012; Schneider et al., 2012). Each line scan spanned 5-8 cells. The PlotProfile function was used to obtain fluorescence intensities for each point along the line, and the data were normalized. Prism (GraphPad) was used to plot them against each other and calculate a Pearson correlation coefficient. *BAC-PlexA-myc* was always used with a PlexA deficiency in the background to maintain endogenous levels of PlexA, for the reason described above.

Quantification of protein levels

Levels of Sema-5c-3xGFP in *PlexA RNAi* epithelia were quantified at cell-cell interfaces at the basal surface of stage 7 epithelia within a region of uniform size across all samples. Each cell was manually outlined with a 10-pixel wide line in Fiji (ImageJ) (Schindelin et al., 2012; Schneider et al., 2012); Phalloidin was used to mark cell outlines. The Convert to Mask function was used to create a mask from these outlines. The Multiply function within Image Calculator was then used on the mask and the original image. This creates a new image in which only the pixels contained within the mask are present. The Measure function was used to obtain average fluorescence intensity across the multiplied image and data were normalized.

Quantification of protrusions

For quantification of protrusion levels, analysis was performed on stage 8 epithelia stained with Phalloidin, as described above. Protrusions were scored by eye and binned into one of three categories based on comparison to controls: normal, weak, or severely depleted. Protrusions were scored as weak if they were reduced in either number or intensity.

For quantification of protrusion orientation, analysis was performed on stage 6 epithelia stained for Phalloidin. A 48 X 38 μm region of the basal surface (approximately 70 cells) was chosen for each sample, and a 10-pixel wide line was manually drawn over all leading-trailing cell-cell interfaces in that region using FIJI (ImageJ) [64, 65]. The average fluorescence intensity along each line was then calculated using the Measure function. For a single epithelium, the measurements from all leading-trailing interfaces were averaged together to generate a single value. Keeping the lines along the leading-trailing interfaces as a guide, a 10-pixel wide line was then manually drawn over all intervening, lateral interfaces. The average fluorescence intensity

of these lines was measured and averaged in the same way as the leading-trailing interfaces to produce a single value for a given epithelium. Epithelia whose protrusions were not well preserved though dissection and fixation protocols were excluded from the analysis.

The analysis of protrusion orientation was performed at stage 6 because most *Sema-5c* epithelial are migrating at this stage as shown by COMETtail analysis, which allows a leading-trailing cell interface to be defined by tissue movement. An egg chamber had to have a COMETtail to be included in the analysis. It is important to realize, however, that our quantification method underestimates the extent to which protrusions are mis-oriented in the mutant condition; the measurements along leading-trailing cell-cell interfaces cannot distinguish between a normally oriented protrusion emanating from the leading edge and a mis-oriented protrusion emanating from the trailing edge.

Generation of *Sema-5c-3xGFP* transgenic line

The *Sema-5c-3xGFP* line was generated by using CRISPR-Cas9 mediated homologous recombination following the general design strategies described by (Gratz et al., 2013; Gratz et al., 2014). The target sequence selected for gRNA production was 5'-GTTGCCTAGCGGGTCACGAC**CGG**-3', where the underlined sequence represents the region that was cloned into the pU6-Bbsl-chiRNA plasmid, which contains the *Drosophila* snRNA:U6:96Ab promoter for *in vivo* transcription, and the bold sequence represents the adjacent PAM motif.

For homologous recombination, the donor plasmid contained three tandem copies of GFP coding sequence followed by a floxed 3xP3-DsRed module (Gratz et al., 2014) for screening insertion events. This entire cassette was flanked by approximately 2 kb homology arms that

contained sequence that matched either side of the target locus. The insertion was made after position 13,696 in the *Sema-5c* gene, immediately before the stop codon, which corresponds to amino acid 1093 of the Sema-5c protein (according to isoform A sequence).

Injections were performed by Genetivision Inc. into transgenic embryos expressing Cas9 under the *nanos* promoter. Resulting adults were mated to balancer flies and progeny were screened for founders using DsRed expression in the adult eye with a Leica MZ FL III microscope. Founders were used to establish stocks and crossed to *Cre*-expressing flies to excise the DsRed module. Insertions were verified by sequencing. Two independent lines were derived and no differences were observed between them.

Generation of *UAS-Sema-5c-GFP* transgenic line

Sema5c full-length cDNA without a stop codon was amplified from clone RE68041 and inserted into pENTR™/D-TOPO™ and then transferred to the *Drosophila* Gateway Collection™ vector pTWG for C-terminal GFP tagging. *UASt-Sema5c-GFP* flies were generated using P element injection by GenetiVision. Insertions were verified by sequencing. Two independent lines were derived and no differences were observed between them.

Quantification and statistical analysis

All data were obtained from at least two independent experiments, and several females were analyzed each time. All data were highly reproducible. No statistical method was used to predetermine sample size. The sample size for each experiment can be found in the figure panel or in the figure legend. A Student's t-test was used to determine if two data sets were significantly different. This analysis was performed using Prism software, version 6 (GraphPad).

These tests are appropriate because all data obtained follow an approximately normal distribution. These experiments were not randomized, nor was the data analysis performed blind. Egg chambers damaged by the dissection process were not included in the analysis.

Table 2.1 Experimental genotypes for "Planar polarized Semaphorin-5c and PlexinA promote the collective migration of epithelial cells in *Drosophila*"

Figure	Panel	Genotype
2.1	D	*w;; FRT80B*
		w;; Sema-5c^{K175}, FRT80B
	E	*w;; FRT80B*
		w;; Sema-5c^{K175}, FRT80B
		w;; Df(3L)BSC840/+
		w;; Df(3L)BSC840/Sema-5c^{K175}, FRT80B
2.2		*w;; FRT80B*
		w;; Sema-5c^{K175}, FRT80B
2.3	A-D	*w;; FRT80B*
		w;; Sema-5c^{K175}, FRT80B
2.4	A-E, J	*hsFlp/w; UAS-Col4a1-RFP/act5c>>Gal4, UAS-GFP*
	F, G, J	*hsFlp/w; UAS-Col4a1-RFP/act5c>>Gal4, UAS-GFP; fat2^{N103-2}, FRT80B*
	H-J	*hsFlp/w; UAS-Col4a1-mRFP/act5c>>Gal4, UAS-GFP; Sema-5c^{K175}, FRT80B*
2.5	A	*w*
		w;; Sema-5c-3xGFP
	B-C	*w/+; e22cc-Gal4, UAS-Flp/+; Sema-5c-3xGFP, FRT80B/FRT80B*
	D	*w/+; e22cc-Gal4, UAS-Flp/+; Sema-5c^{K175}, FRT80B/ubi-eGFP, FRT80B*
	E-H	*hsFlp/ w; UAS-Col4a1-mRFP/act5c>>Gal4, UAS-GFP*
	I-L	*hsFlp/ w; UAS-Col4a1-mRFP/act5c>>Gal4, UAS-GFP; Sema-5c^{K175}, FRT80B*
2.6	A-F	*w;; Sema-5c-3xGFP*
	G-I	*w/+; e22cc-Gal4, UAS-Flp/+; Sema-5c-3xGFP, FRT80B/FRT80B*
	J	*hsFlp/w; act5c>>gal4/+; UAS-Sema-5c-GFP/+*
	K	*hsFlp/w;; act5c>>gal4, UAS-RFP/UAS-Sema-5c-GFP*
2.7	A	*hsFlp/w; UAS-Sema-5c-GFP/+; act5c>>Gal4/+*
	B-C	*hsFlp/w; act5c>>Gal4, UAS-GFP/+; UAS-Sema-5c-GFP/+*

Table 2.1 continued

2.8	A	*w; traffic jam-Gal4/+; UAS-Dicer-2/+*
		w; traffic jam-Gal4/+; UAS-Dicer-2/UAS-PlexB RNAi^{GD14473}
		w; traffic jam-Gal4/UAS-PlexB RNAi^{GD1350}; UAS-Dicer-2/+
	B	*w; traffic jam-Gal4/+*
		w; traffic jam-Gal4/UAS-PlexA RNAi^{GD14483}
		w; traffic jam-Gal4/+; UAS-Dicer-2/+
		w/y, sc, v^{1}; traffic jam-Gal4/+; UAS-PlexA RNAi$^{TRiP.HM05221}$/UAS-Dicer-2
	C	*hsFlp/w; UAS-PlexA RNAi^{GD14483}/+; act5c>>Gal4, UAS-GFP/+*
		*hsFlp/ y, sc, v^{1}; UAS-Dicer-2/+**;** UAS-PlexA RNAi$^{TRiP.HM05221}$ /act5c>>Gal4, UAS-GFP*
	D	*w^{1118}*
	E-F	*yw hsFlp;; BAC-PlexA-myc, ubiGFP, h, FRT80B/FRT80B, e ca; Df(4)C3/PlexA^{MB09499}*
2.9	A	*w; traffic jam-Gal4/+*
		w; traffic jam-Gal4/UAS-PlexA RNAi^{GD14483}
	B-D	*w; traffic jam-Gal4/+; UAS-Dicer-2/+*
		w/ y, sc, v^{1}; traffic jam-Gal4/+; UAS-PlexA RNAi$^{TRiP.HM05221}$/UAS-Dicer-2
	E	*w;; BAC-PlexA-myc/+; Df(4)C3/+*
	F-H	*yw hsFlp;; BAC-PlexA-myc, ubiGFP, h, FRT80B/FRT80B, e ca; Df(4)C3/PlexA^{MB09499}*
2.10	C	*w; e22cc-Gal4, UAS-Flp/+; Sema-5c^{K175}, FRT80B/ubi-eGFP, FRT80B*
	D	*hsFlp/w; UAS-PlexA RNAi^{GD14483}/act5c>>Gal4, UAS-LacZ; Sema-5c-3xGFP/+*
	E-H	*hsFlp/w; act5c>>Gal4, UAS-LacZ/+; UAS-Sema-5c-GFP/+*
		hsFlp/w; act5c>>Gal4, UAS-GFP/UAS-PlexA RNAi^{GD14483}
		hsFlp/w; UAS-PlexA RNAi^{GD14483}/+; UAS-Sema-5c-GFP/act5c>>Gal4
2.11	A-B	*w; traffic jam-Gal4/+; Sema-5c-3xGFP/+*
		w; traffic jam-Gal4/ UAS-PlexA RNAi^{GD14483}; Sema-5c-3xGFP/+
	C-G	*w;; BAC-PlexA-myc, Sema-5c-3xGFP/+; Df(4)C3/+*
	H-K	*w; traffic jam-Gal4/UAS-RFP-RNAi; UAS-Sema-5c-GFP/+*
		w; traffic jam-Gal4/UAS-HA-PlexA
		w; traffic jam-Gal4/UAS-HA-PlexA; UAS-Sema-5c-GFP/+
2.12	A-D	*w^{1118}*
		w/+; Lar^{Bola2}/+
		Lar^{Bola1}/Lar^{Bola2}
		w;; Sema-5c^{K175}, FRT80B

Table 2.1 continued

2.12	E-I	*w; Lar^{Bola2}/+; $Sema\text{-}5c^{K175}$, FRT80B*
		w;; Sema-5c-3xGFP
	J	*w; $Lar^{13.2}$, FRT40A /ubi-mRFP, FRT40A; Sema5c-3xGFP /T155-Gal4, UAS-Flp*
2.13	A	*w^{1118}*
		w^{1118}/+; Lar^{Bola1}/+
		w;; $Sema\text{-}5c^{K175}$, FRT80B
		w; Lar^{Bola1}/+; $Sema\text{-}5c^{K175}$, FRT80B
	B	*w^{1118}*
		w^{1118}/+; $Lar^{13.2}$ FRT40A/+
		w;; $Sema\text{-}5c^{K175}$, FRT80B
		w; $Lar^{13.2}$ FRT40A/+; $Sema\text{-}5c^{K175}$, FRT80B
	C	*w^{1118}*
		Lar^{Bola1}/Lar^{Bola2}
	D	*w^{1118}*
		w/+; Lar^{Bola2}/+
		w;; $Sema\text{-}5c^{K175}$, FRT80B
		w; Lar^{Bola2}/+; $Sema\text{-}5c^{K175}$, FRT80B
	E	*w^{1118}*
		w;; $fat2^{N103.2}$, FRT80B/+
		w;; $Sema\text{-}5c^{K175}$, FRT80B
		w; $fat2^{N103\text{-}2}$, $Sema\text{-}5c^{K175}/Sema\text{-}5c^{K175}$, FRT80B
	F	*w; traffic jam-Gal4/+; UAS-Dicer-2/+*
		w; traffic jam-Gal4/Lar^{Bola2}; UAS-Dicer-2/+
		w/ y, sc, v^{1}; traffic jam-Gal4/+; UAS-Dicer-2/UAS-PlexA $RNAi^{TRiP.HM05221}$
		w; traffic jam-Gal4/Lar^{Bola2}; UAS-Dicer-2/UAS-PlexA $RNAi^{TRiP.HM05221}$
	G	*w; e22cc-Gal4, UAS-Flp/+; $Sema\text{-}5c^{K175}$, FRT80B/Ubi-eGFP, FRT80B*
	H	*hsFlp/w; UAS-PlexA $RNAi^{GD14483}$/+; act5c>>Gal4, UAS-GFP/+*
	I	*w; ubi-mRFP, FRT40A/$Lar^{13.2}$, FRT40A; T155-Gal4, UAS-Flp/+*

Table 2.2 Experimental conditions for "Planar polarized Semaphorin-5c and PlexinA promote the collective migration of epithelial cells in *Drosophila*"

Figure	Panel	Females on yeast		
		Adult age (days)	Temp (°C)	Duration (days)
2.1	D-E	1-2	25	2
2.2	A	1-2	25	2
2.3	A-D	1-2	25	2
2.4	A-E	1-2	25 (post heat shock)	0.5
2.5	A	1-2	25	2
	B-C	1-3	29	3
	D	1-3	29	3
	E-L	1-2	25 (post heat shock)	0.5
2.6	A-F	1-2	25	2
	G-I	1-3	29	3
	J-K'	1-2	29 (post heat shock)	1
2.7	A	1-2	29 (post heat shock)	2
	B-C	1-2	29 (post heat shock)	1
2.8	A-B	1-3	29	3
	C	1-2	29 (post heat shock)	1
	D	1-2	25	2
	E-F	1-2	25 (post heat shock)	2
2.9	A-D	1-3	29	3
	E	1-2	25	2
	F-H	1-2	25 (post heat shock)	2
2.10	C	1-2	29	3
	D	1-2	29 (post heat shock)	1
	E-H	1-2	29 (post heat shock)	1.5
2.11	A-B	1-2	29	3
	C-G	1-2	25	2
	H-K	1-2	29	2
2.12	A-I	1-2	25	2
	J	1-3	25	2
2.13	A-E	1-2	25	2
	F	1-3	29	3
	G	1-2	29	3
	H	1-2	29 (post heat shock)	1
	I	1-3	29	4

CHAPTER 3: INVESTIGATING THE ROLE OF THE ACTIN DISASSEMBLY FACTOR MICAL IN THE FOLLICULAR EPITHELIUM

3.1 PREFACE

Mical is an actin disassembly factor that interacts with PlexA (Hung et al., 2010; Terman et al., 2002), suggesting it could play a role in follicle cell migration downstream of Sema-5c – PlexA signaling. Data from a former undergraduate student in the lab, Will Menegas, provided a few pieces of evidence to support this model and part of my early work included following up on these results. Much of my data indicate that Mical could indeed act downstream of PlexA; however, complications arose with some of the reagents that made it unfeasible for me to include any of the Mical data in my paper or for me to draw any strong conclusions about its function at this time. Despite this, some interesting models can be draw from this work and I am providing all of the data here for the benefit future researchers who are interested in the role of Mical in the egg chamber.

3.2 INTRODUCTION

MICAL family proteins directly link Semaphorin-Plexin signaling to disassembly of the actin cytoskeleton (Hung et al., 2010). *Drosophila* Mical, and its mammalian homologs MICAL-1, 2 and 3, are oxidoreductase (Redox) enzymes that disassemble F-actin (Hung and Terman, 2011). They do this though a Redox domain at their N-terminus which enables them to bind to and oxidize actin monomers; this severs the actin filaments and decreases subsequent polymerization (Hung and Terman, 2011; Hung et al., 2010; Hung et al., 2011; Terman et al., 2002). At their C-

terminus, MICAL family proteins contain a Plexin-interacting Region which enables them to associate with the cytoplasmic domain of class A plexins (Terman et al., 2002).

MICAL family proteins play a role in a variety of contexts (Frémont et al., 2017; Hung and Terman, 2011), but it was particularly interesting when *Drosophila* Mical was shown to disassemble F-actin downstream of semaphorin-plexin signaling (Hung et al., 2010). It was well established that semaphorin signaling affected the actin cytoskeleton, but a direct link between actin regulation and semaphorins had been missing. In *Drosophila,* Mical acts downstream of Sema-1a – PlexA signaling during both axon guidance and extension of the bristle process (Hung et al., 2010; Terman et al., 2002). Mammalian MICALs also act downstream of semaphorins and plexins and disassembles F-actin (Giridharan et al., 2012; Morinaka et al., 2011; Schmidt et al., 2008).

Mical is a good candidate to act downstream of Sema-5c – PlexA signaling in the follicular epithelium. In the previous chapter, I showed that Sema-5c and PlexA promote follicle cell migration, but what factors act downstream of PlexA remained unexplored. Since cell migration involves dynamic regulation of the actin cytoskeleton, it is possible that Sema-5c – PlexA signaling exerts effects on actin through Mical. Previous work in the lab, using RNAi and overexpression constructs, suggested that Mical localizes to the trailing edge of each cell, loss of Mical disrupts egg chamber elongation, and that Mical disassembles the basal stress fibers. These data indicated that Mical may play a role in follicle cell migration.

I brought new reagents to this project to further characterize the role of Mical, investigate its localization, and probe whether it may be acting downstream of Sema-5c and PlexA during follicle cell migration. I also repeated the previous experiments to validate these earlier findings. While many of my results are suggestive of Mical acting downstream of PlexA, and indicate

models by which this could work, I also uncovered complications with the reagents that were being used. Thus, I am not able to draw any strong conclusions at this time. In the results section I will present the data in an agnostic manner, and then in the discussion I will address the issues that arose and how they may be addressed going forward.

3.3 RESULTS

Loss of Mical reduces egg chamber elongation

To determine if Mical acts downstream of Sema-5c - PlexA signaling in the egg chamber, I first tested if loss of Mical affects egg chamber elongation. Driving *Mical-RNAi* in the follicle cells results in eggs with aspect ratios that are lower than controls (Figures 3.1A and 3.1B). A previously published *Mical* null condition also causes a similar phenotype (Figure 3.1B). This condition places a *Mical* allele with a premature stop codon over a deficiency that removes *Mical* and I will refer to it as *Mical (-/-)* (Hung et al., 2010). These data show that Mical plays a role in egg chamber elongation.

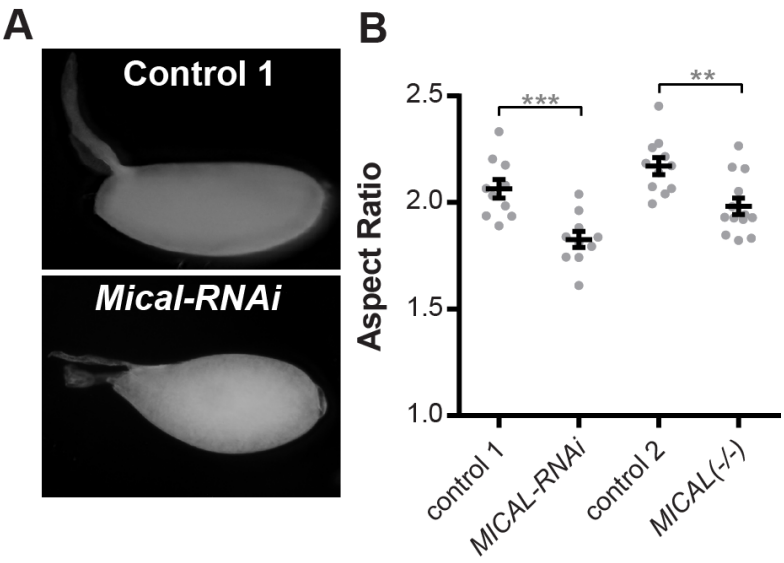

Figure 3.1. Loss of Mical disrupts egg chamber elongation (A) Representative images of eggs from a control female and a female expressing *Mical-RNAi* in the follicular epithelium. (B) Egg aspect ratio measurements (length/width) showing that eggs from females expressing *Mical-RNAi* in the follicular epithlium and females that are *Mical (-/-)* are significantly rounder than controls. Mean ± SEM. Unpaired t test. **p< 0.01; ***p<0.001.

Loss of Mical partially disrupts follicle cell migration

Next, I tested if Mical plays a role in follicle cell migration. Since follicle cell migration is tightly linked to global stress fiber alignment (Cetera et al., 2014), I first examined if loss of Mical affects this alignment. At stage 7, global stress fiber alignment is not affected by loss of Mical, the stress fibers remain aligned in the direction of migration (Figure 3.2A). Next I examined migration of *Mical (-/-)* tissue by live imaging and found that loss of Mical appears to have a variable effect on the rate of follicle cell migration. At stage 7, some *Mical (-/-)* epithelia exhibit slower migration, while some are not different from controls (Figure 3.2B). Overall, this shows that Mical is involved in follicle cell migration but is not strictly required for motility.

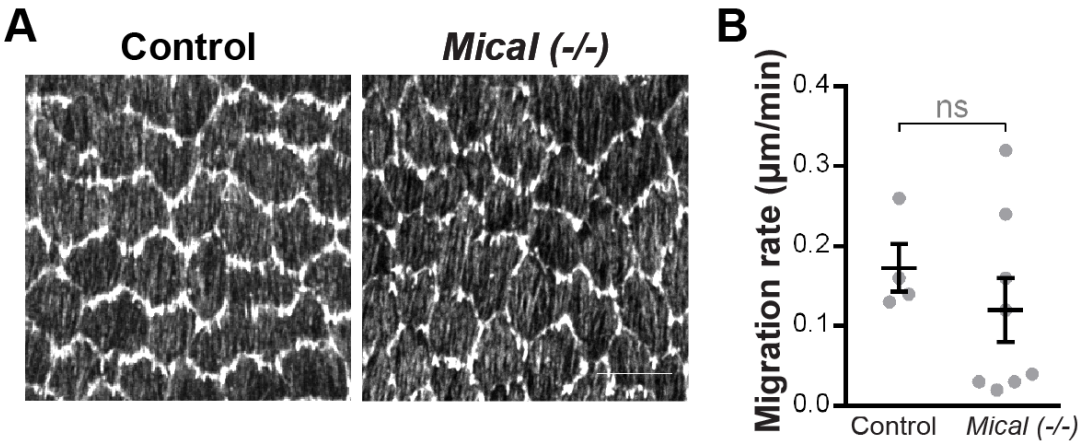

Figure 3.2. Loss of Mical affects cell migration but not global stress fiber alignment
(A) Images of the basal epithelial surface of control and *Mical (-/-)* epithelia showing that loss of Mical does not affect global stress fiber alignment. (B) Migration rates of control and *Mical (-/-)* epithelia showing that, although the difference is not statistically significant, loss of Mical decreases the migration rate in a subset of egg chambers. Mean ± SEM. Unpaired t test. ns, not significant. Scale bars, 10 µm.

UAS-GFP-Mical is enriched at the rear of each cell and this localization depends on PlexA

To further investigate Mical's role in the follicle cells, I examined its localization pattern. When driven in the follicle cells, UAS-GFP-Mical localizes to the apical and lateral sides of each follicle cell, and forms puncta at the basal surface (Figures 3.3A-C). Mosaic expression of this

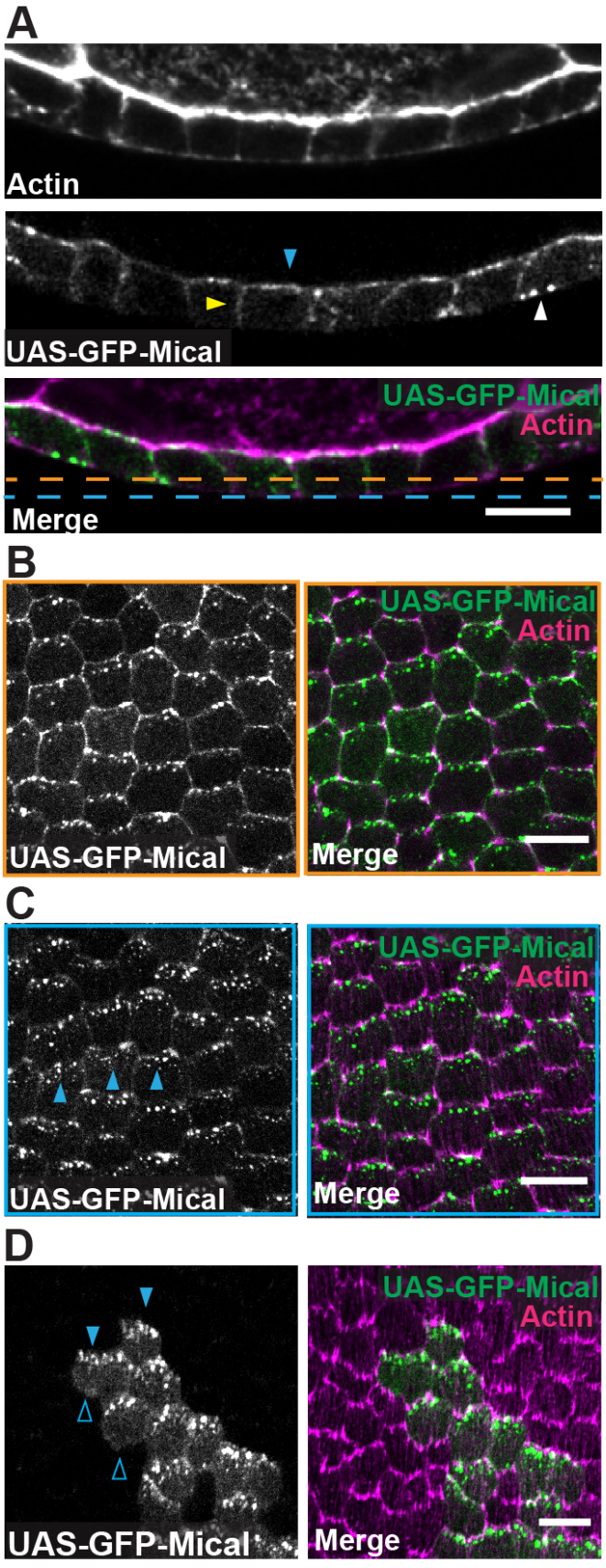

transgene reveals that this basal population localizes specifically to the rear of each migrating cell (Figure 3.3D).

Since Mical binds to and colocalizes with PlexA (Hung et al., 2010; Terman et al., 2002), it is possible that Mical is recruited to the basal surface via an interaction with PlexA. Upon driving *PlexA-RNAi* in the follicle cells, the basal

Figure 3.3. When expressed in the follicle cells, a *GFP-Mical* transgene localizes to the trailing edge of each cell (A) Image of a sagittal section through an egg chamber expressing UAS-GFP-Mical in the follicle cells showing that it localizes to the apical surface, lateral cell-cell interfaces, and intercellular puncta. (B-C) Images of a single basal epithelial surface taken at two different planes, corresponding approximately at the planes shown with the dashed lines in (A) showing that slightly off the basal surface, UAS-GFP-Mical localizes to cell-cell interfaces (B), while at the basal surface it is present in puncta that appear at one side of each cell (C). (D) Image of the basal surface of a *UAS-GFP-Mical* mosaic epithelium showing that UAS-GFP-Mical is enriched at the trailing edge of each cell and is absent from the leading edge. Leading edge determined by presence of leading edge protrusions. Scale bars, 10 µm.

population of UAS-GFP-Mical is reduced, suggesting that this could be the case (Figure 3.4). This phenotype does not appear to be due to lower levels of *UAS-GFP-Mical* expression in the *PlexA-RNAi* background because the lateral and apical populations of UAS-GFP-Mical don't appear reduced.

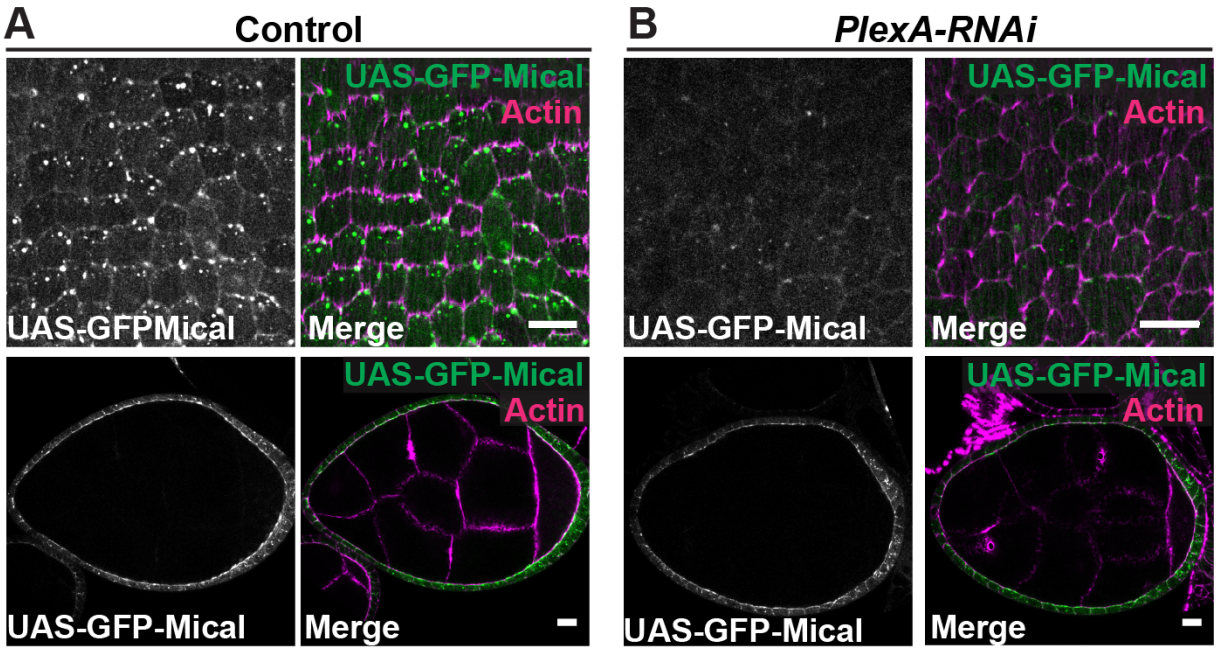

Figure 3.4. Loss of PlexA disrupts the basal localization of UAS-GFP-Mical (A) Images of the basal epithelial surface and a sagittal cross section from the same egg chamber expressing *UAS-GFP-Mical* in the follicle cells. (B) Images of the basal epithelial surface and a sagittal cross section from the same egg chamber expressing *UAS-GFP-Mical* and *UAS-PlexA-RNAi* in the follicle cells. Levels of UAS-GFP-Mical are greatly reduced at the basal epithelial surface in (B) compared to (A) while the levels of UAS-GFP-Mical in the sagittal cross sections are not greatly changed. Scale bars, 10 μm.

It is also possible that a PlexA-Mical interaction requires the active form of PlexA, and thus Mical's basal localization could also be dependent on Sema-5c. In *Sema-5c* epithelia, the basal localization of UAS-GFP-Mical is not reduced (Figure 3.5), suggesting its interaction with PlexA does not require PlexA to be activated by Sema-5c. This result also suggests that loss of UAS-GFP-Mical from the basal surface of *PlexA-RNAi* epithelia is not due to a general disruption of follicle cell migration, further suggesting it is due to a specific interaction with

PlexA. Together, these data suggest that Mical plays a role at the rear of each follicle cell and is recruited to this location by PlexA.

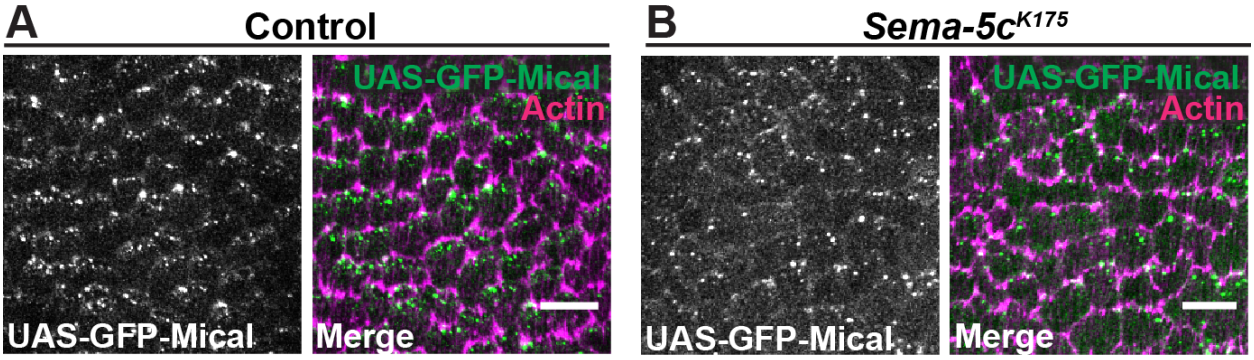

Figure 3.5. Loss of Sema-5c does not affect the basal localization of UAS-GFP-Mical (A) Image of the basal epithelial surface of a control egg chamber expressing *UAS-GFP-Mical* in the follicle cells. (B) Image of the basal epithelial surface of a *Sema-5c* egg chamber expressing *UAS-GFP-Mical* in the follicle cells. UAS-GFP-Mical is present at the basal surface in both conditions. Scale bars, 10 μm.

Immunostaining reveals that Mical is on lateral membranes and not dependent on PlexA

After the studies of UAS-GFP-Mical localization, I obtained an antibody to see if these overexpression results could be validated. Immunostaining reveals that *Mical* is expressed specifically in the follicle cells, and not the germ cells, during rotation stages (Figure 3.6A). A cross section through the egg chamber shows that Mical localizes to lateral cell-cell interfaces, and appears enriched at the apical junctional region (Figure 3.6A). This lateral localization extends down to the basal surface, such that an image at the basal plane shows Mical outlining the cortex of each cell, notably it is not planar polarized (Figure 3.6B). Antibody staining in *PlexA* or *Sema-5c* mosaic tissue reveals that Mical does not require either of these factors to localize to the basal surface (Figures 3.6C and 3.6D). Overall, these data show that Mical

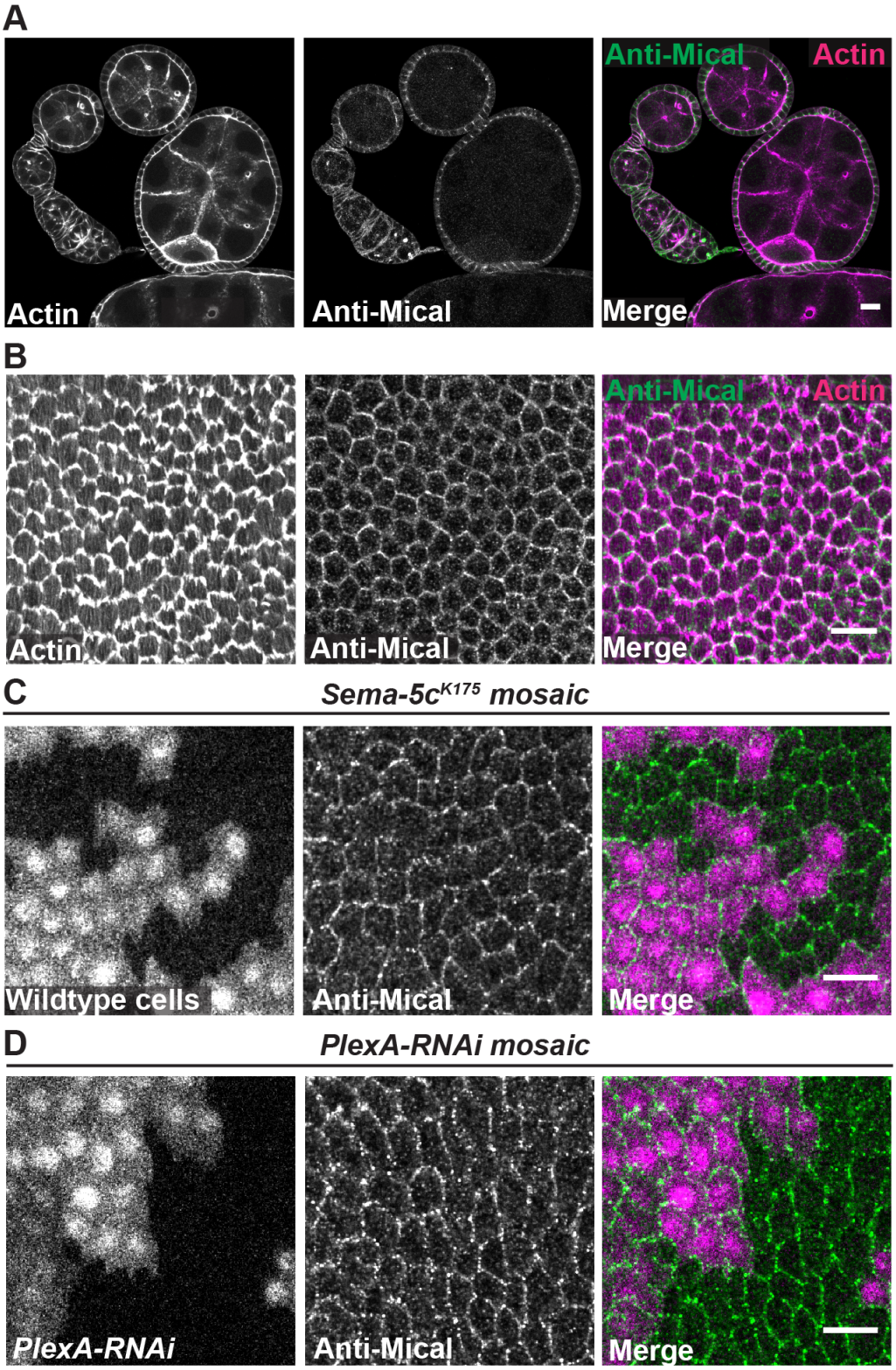

Figure 3.6. Mical localizes to basal surface of the follicular epithelium.

Figure 3.6. continued (A) Image of a sagittal section through an ovariole with Mical immunostaining showing Mical is highly expressed in the follicle cells with very little signal in the germ cells. In the follicle cells, Mical localizes to lateral cell-cell interfaces. (B) Mical immunostaining at the basal epithelial surface showing that Mical localizes to cell-cell interfaces. (C) Mical immunostaining at the basal surface of a *Sema-5c* mosaic epithelium showing that localization of Mical to the basal surface is not affected by loss of Sema-5c. (D) Mical immunostaining at the basal surface of *PlexA-RNAi* mosaic epithelium showing that localization of Mical to the basal surface is not affected by loss of PlexA. Scale bars, 10 μm.

is expressed in the right time and place to play a role in follicle cell migration, and that this localization does not depend on PlexA or Sema-5c. This conflict with the overexpression data will be further explored in the discussion.

At stage 8, Mical immunostaining reveals an interesting pattern at the anterior-most cells of the follicular epithelium; Mical becomes enriched at the trailing edge of each cell (Figure 3.7). Upon loss of Sema-5c, this trailing-edge enrichment of Mical spreads across the tissue (Figure 3.8). This is suggestive of a connection between Mical and Sema-5c that is ripe for further exploration.

Mical may act on the stress fibers

Manipulating levels of Mical in the follicle cells reveals that Mical may specifically affect the stress fibers. Stress fiber levels in *Mical* overexpression clones are greatly reduced compared to those in the neighboring wildtype cells, while the cortical actin remains intact (Figures 3.9A). If this represents the activity of endogenous Mical, then I would expect loss of Mical to cause an increase in stress fiber levels. This is seen upon driving *Mical-RNAi* (Figures 3.9B), but not in *Mical (-/-)* epithelia (Figure 3.2). This discrepancy indicates that further validation of these

reagents is required before conclusions can be drawn about the effect of Mical on the stress fibers.

Validation of Mical transgenic lines

These conflicting stress fiber results prompted a further validation of the *Mical-RNAi* and *Mical (-/-)* transgenic lines with the newly-acquired Mical antibody. Antibody staining revealed that Mical is strongly depleted from the basal surface in *Mical (-/-)* tissue, while driving *Mical-RNAi* does not have this effect (Figure 3.10). This validates the *Mical (-/-)* condition but not the *Mical-RNAi*.

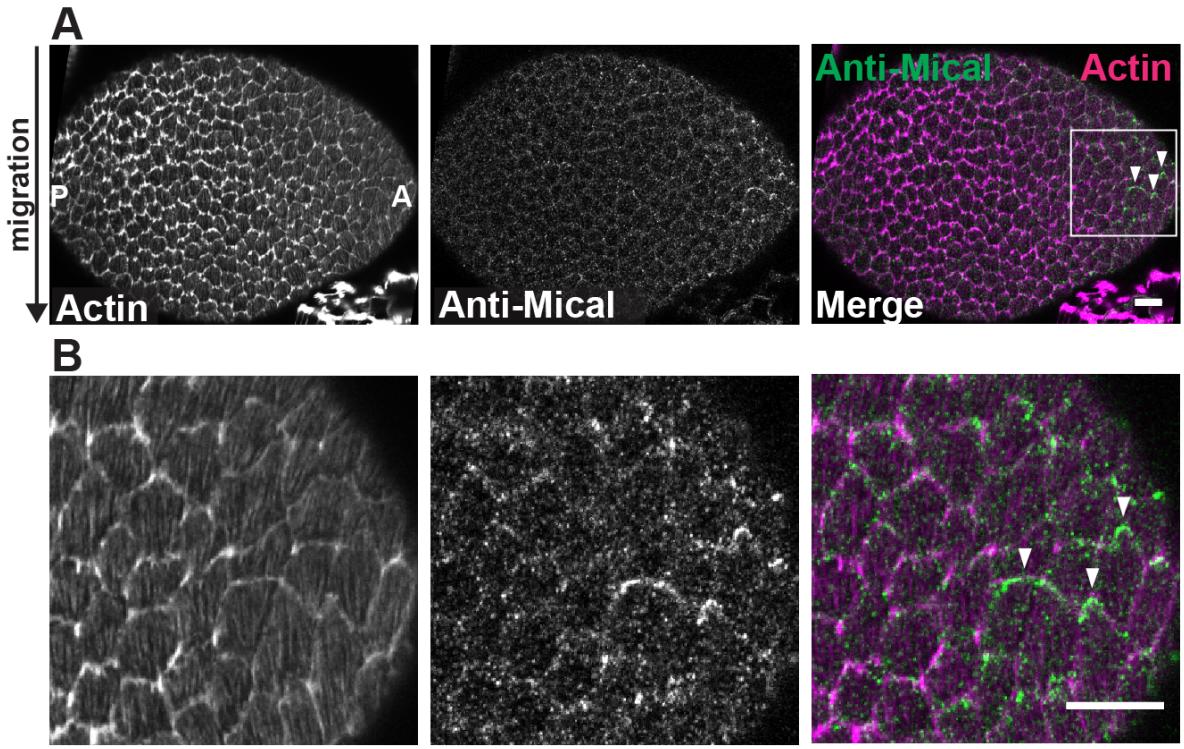

Figure 3.7. Mical localizes to the trailing edge of a subset of follicle cells at stage 8 (A-B) Image of Mical immuostaining at the stage 8 basal epithelial surface showing that at the anterior tip of the egg chamber Mical becomes enriched at the trailing edge, white triangles. Images oriented with the direction of migration going down, A and P indicate the anterior-posterior axis. (B) Zoom of the boxed region in (A). Scale bar, 10 µm.

3.4 DISCUSSION

Much of the data presented here are suggestive that Mical plays a role in the follicular epithelium. However, conflicting data from different reagents need to be resolved before any strong conclusions can be drawn. Here I will address these complications and what studies could help address them going forward.

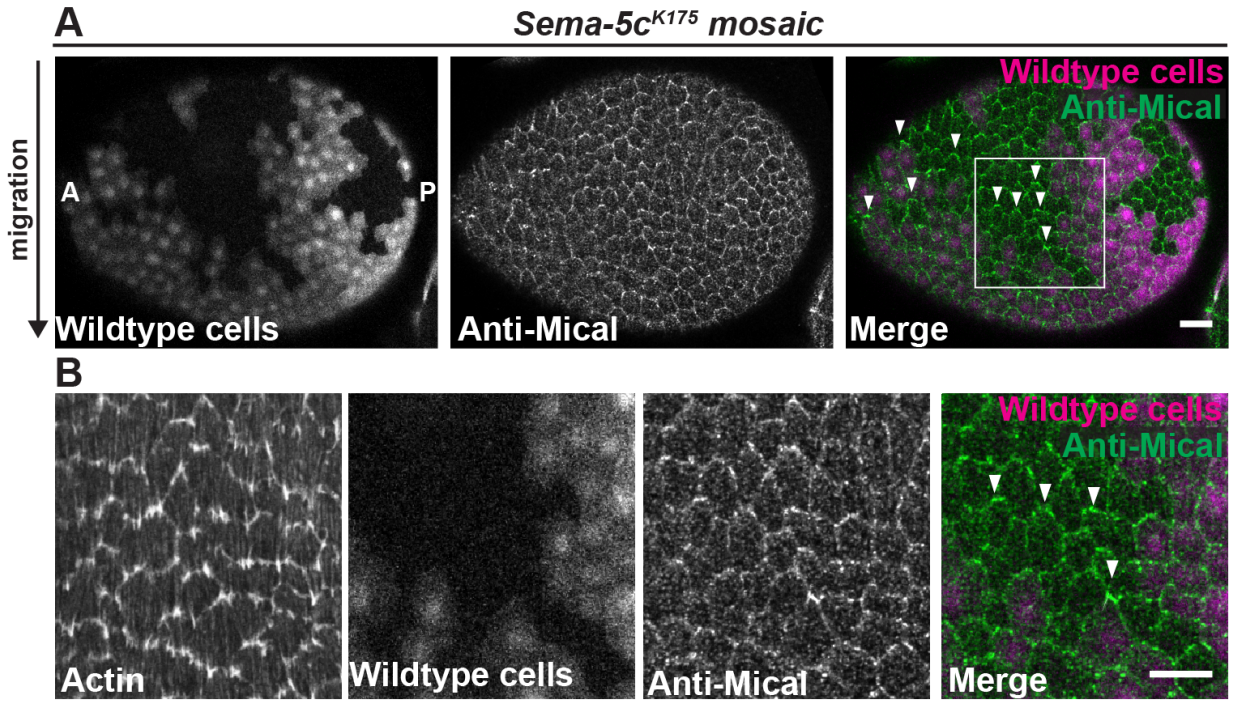

Figure 3.8. In stage 8 *Sema-5c* epithelia, Mical localizes to the trailing edge across the tissue (A-B) Image of Mical immuostaining at the stage 8 basal surface of *Sema-5c* mosaic epithelia. The trailing edge enrichment of Mical seen at the anterior in stage 8 controls now spreads toward the center of the egg chamber, white triangles. (B) Zoom of the boxed region in (A). Images oriented with the direction of migration going down, A and P indicate the anterior-posterior axis. Scale bar, 10 μm.

Does Mical function downstream of PlexA during follicle cell migration?

Since Mical acts downstream of Sema-1a - PlexA signaling in the *Drosophila* bristle (Hung et al., 2010), it was a good candidate to act downstream of Sema-5c – PlexA signaling in the follicle cells. While some of the data presented here suggest that Mical could be downstream of

PlexA, other aspects of my results call these pieces of data into question. Here I will address the data that support this idea, and then those that conflict with it.

Loss of Mical partially disrupts follicle cell migration, which supports it acting downstream of PlexA during this process. Loss of Mical does not disrupt migration to the same extent as loss of Sema-5c or PlexA, but multiple factors can act downstream of PlexA, so it is possible that all of the downstream players need to be knocked out before a significant loss of migration is to be seen. Additionally, PlexA and Sema-5c play a larger role during early migration stages compared to later migration stages, so it is possible that examining earlier stages of *Mical (-/-)* epithelial could reveal a stronger migration phenotype.

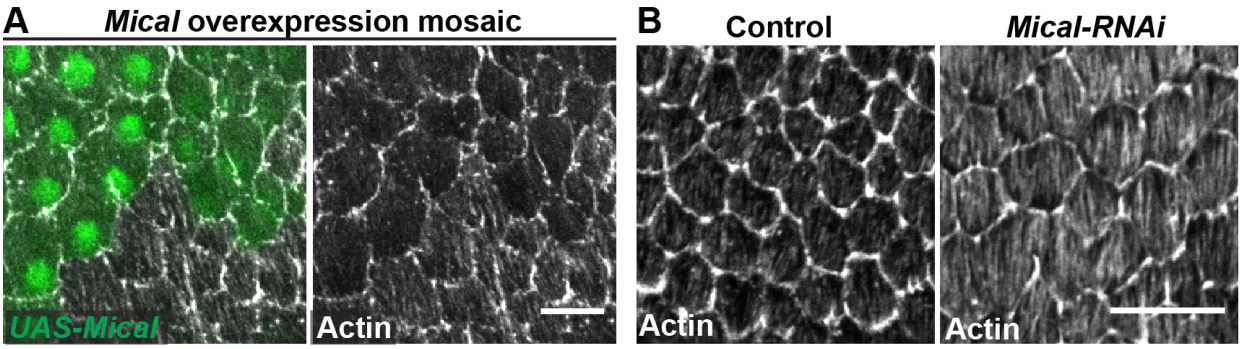

Figure 3.9. Mical may act on the basal stress fibers (A) Image of the basal epithelial surface of a *UAS-Mical* mosaic epithelium showing that overexpression of Mical causes depletion of the basal actin bundles. (B). Image of the basal epithelial surface of an egg chamber expressing *Mical-RNAi* in the follicle cells showing that *Mical-RNAi* causes an increase in stress fiber levels, as assessed by Phalloidin staining. Scale bars, 10 µm.

Localization of UAS-GFP-Mical also provides support for an interaction with PlexA. If Mical acts downstream of PlexA, I predicted it would localize to the same subcellular region as PlexA, the trailing edge, and possibly be dependent on PlexA for this localization. Expressing *UAS-GFP-Mical* in the follicle cells revealed both of these phenotypes. At the basal surface,

UAS-GFP-Mical appears in puncta that are localized toward the rear of each cell and this basal localization is depleted upon driving *PlexA-RNAi*.

The immunostaining also provides some evidence in support of Mical acting downstream of Sema-5c – PlexA signaling. Antibody staining reveals that the basal localization of Mical changes in *Sema-5c* epithelia. In controls, the Mical antibody localizes evenly around the cell cortex at the basal surface, but in *Sema-5c* epithelia Mical becomes slightly enriched at the trailing edge of cell. This phenotype was observed at stage 8, but as the current analysis was limited to this stage; this phenotype may be present in earlier stages as well. This change in localization suggests there could be a link between Mical localization and Sema-5c activity.

Together these localization data are consistent with a model in which PlexA sequesters Mical at the trailing edge of each cell, then upon Sema-5c activation of PlexA, Mical is released to act on the local actin cytoskeleton. In this case, loss of Sema-5c could cause Mical to accumulate on PlexA at the trailing edge of each cell. This could lead to increased levels of Mical at the trailing edge of each cell, which is seen in the immunostaining of *Sema-5c* epithelia. Following this model, Mical localization to the basal surface would be dependent on PlexA but

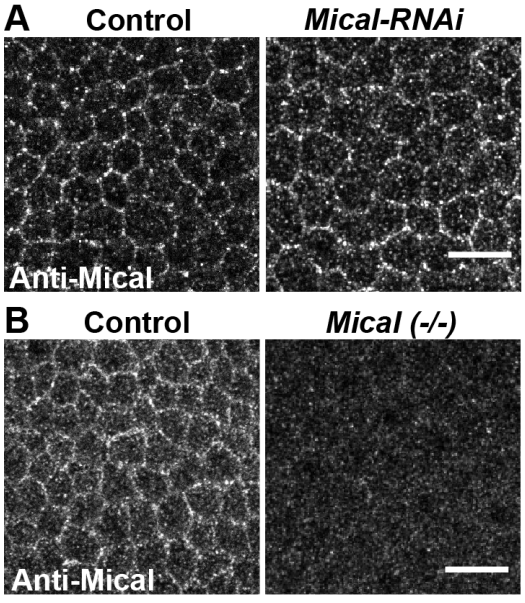

Figure 3.10. Validation of Mical reagents (A) Images of Mical immunostaining at the basal epithelial surface in control and *Mical-RNAi* epithelia showing that Mical levels are not altered by *Mical-RNAi.* (B) Images of Mical immunostaining at the basal epithelial surface in control and *Mical (-/-)* epithelia showing that Mical levels are reduced in *Mical (-/-)* tissue. Scale bars, 10 μm.

not on Sema-5c, which is consistent with the UAS-GFP-Mical results. This model also explains how the puncta of UAS-GFP-Mical become enriched at the rear of each cell.

However, there are results from Mical immunostaining that do not fit with this model. The Mical antibody localizes evenly around the cell cortex at the basal surface; there are no puncta that are enriched at the rear of each cell as with UAS-GFP-Mical. Also, its basal localization does not depend on PlexA, which further contrasts with UAS-GFP-Mical. However, since the antibody localizes to cell-cell interfaces at the basal surface, this distribution would overlap with that of PlexA. It is possible that Mical is only active when it is in contact with PlexA and the remaining Mical is either inactive or playing a role in another process. Despite these data, the more confounding result is that Mical immunostaining at the basal surface is not affected by loss of PlexA. I validated the Mical antibody, the signal is greatly reduced in *Mical (-/-)* epithelia, which suggests that this result is representative of true Mical localization and calls into question the results obtained with UAS-GFP-Mical. However, the results using UAS-GFP-Mical were repeated on two separate occasions and consistent results obtained, which confirms that loss of PlexA does affect localization of UAS-GFP-Mical.

The large question that remains to be resolved is determining if localization of UAS-GFP-Mical is representative of endogenous Mical. It is possible that the puncta of UAS-GFP-Mical visible at the basal surface are truly there, but are normally quite small. Thus, they may not be sufficiently amplified by antibody staining and only when Mical is overexpressed, and accumulates in those puncta, do they become visible. If this is the case, then it explains why no effect on Mical immunostaining is seen in *PlexA-RNAi* epithelia. However, it is also possible that these puncta are an overexpression artifact. Endogenously tagging Mical could help to resolve

these questions and will be an important step to verifying its localization and its interaction with PlexA.

Is Mical disassembling actin in the follicle cells?

Since Mical disassembles F-actin, it could play a role in follicle cell migration by affecting actin dynamics. In mammalian cells, MICAL shows a preference for disassembling stress fibers over cortical actin (Giridharan et al., 2012), and *Drosophila* Mical disassembles bundled actin, both *in vitro* and *in vivo* (Hung et al., 2010). Thus, if Mical disassembles actin in the follicle cells, it could act on the stress fibers. However, Mical also affects growth cone morphology and when expressed in neurons it localizes to the growth cone (Hung et al., 2010), which suggests it can also act on actin-rich protrusive structures.

Data from Mical overexpression and RNAi knockdown both support a role for Mical acting on the follicle cell stress fibers. In clones of *UAS-Mical*, stress fiber levels are greatly reduced compared to wildtype neighbors which shows that, when expressed in the follicle cells, Mical can disassemble the stress fibers. If endogenous Mical also displays this activity, then removing Mical could cause an increase in stress fiber levels, which was seen upon driving *Mical-RNAi*. These data, along with the localization of UAS-GFP-Mical to the rear of each cell suggested that Mical could drive migration by disassembling stress fibers at the trailing edge of each cell.

Examination of *Mical (-/-)* epithelia does not support a role for Mical in disassembling the stress fibers. No change in stress fiber levels was seen in *Mical (-/-)* tissue. Since immunostaining validated the *Mical (-/-)* condition but not the *Mical-RNAi,* this calls into question the data obtained with *Mical-RNAi*. This result is further confounded by the fact that

driving *Mical-RNAi* in the follicle cells reduces egg chamber elongation. One explanation for this is that this RNAi has an off-target effect on another gene that also affects actin levels and egg chamber elongation. However, it is also possible that the *Mical (-/-)* condition is not a true null, which is why no effect on stress fibers was seen; examining additional Mical alleles, or using CRISPR/Cas9 technology to make a true null, could test this. A third possibility is that loss of Mical doesn't affect stress fibers, it affects a different population of actin, such as protrusions, which was not examined in the current analysis. Going forward, examination of additional actin structures in *Mical (-/-)* epithelial could reveal if a different actin population is affected. Protrusions are a particularly interesting candidate for Mical to act on, as my data for Sema-5c – PlexA signaling in the follicle cells suggests that they inhibit protrusion formation, which could be accomplished by Mical disassembling these actin-based structures.

Could Mical play additional roles in the follicular epithelium?

It is possible that Mical plays roles in the follicle cells that are independent of Sema-5c – PlexA activity. Interestingly, antibody staining revealed that Mical becomes enriched at the trailing edge of follicle cells at the anterior end of stage 8 egg chambers, suggesting Mical may be required for a specific role in the anterior-most cells starting at stage 8. These cells are starting to change morphology and become stretch cells (Horne-Badovinac and Bilder, 2005), which suggests Mical could play a role in actin dynamics as the cells transition from cuboidal to squamous. Characterization of *Mical (-/-)* epithelia during post-migration stages will determine if Mical is involved in processes outside of follicle cell migration.

Mical could also act downstream multiple semaphorins in the follicle cells. In the *Drosophila* bristle, Mical acts downstream of Sema-1a. According to data from the

modENCODE: *Drosophila* transcriptome, Sema-1a and Sema-1b are expressed in the ovary, so it is possible that Mical may act downstream of class 1 semaphorins in the follicle cells as well. However, it would first need to be determined what role, if any, class 1 semaphorins play in egg chamber.

Conclusions

Overall, many of these results are suggestive of a role for Mical in follicle cell migration downstream of Sema-5c and PlexA. A few different models can be drawn from the current data and investigating them further will be an interesting area for future work. However, some data present complications that will need to be resolved for this work to proceed.

3.5 METHODS

Drosophila Genetics

Full genotypes for each experiment and the conditions at which the females were cultures are provided in Table 3.1. All stock are as described in Chapter 2 with the following additions: *UAS-Mical-RNAi* (v20673, CG33208) is from the Vienna Drosophila Resource Center. *UAS-GFP-Mical, UAS-Mical, Df(3R)swp2,* and $Mical^{K1496}$ were gifts from Johnathan Terman.

Time lapse video and fixed image acquisition and microscopy

Time lapse videos, fixed imaging, and staining were performed as described in Chapter 2 with the following additions: The Mical antibody (rabbit #3835), a gift from Alex Kolodkin (received on 4/6/16), which was made against last 395 amino acids of Mical (Mical-CT) and originally

used in (Terman et al., 2002). This antibody was pre-absorbed overnight on Mical (-/-) egg chambers to reduce background signal prior to tissue staining and used at 1:4000 in PBT3.

Quantification of egg aspect ratio

Egg aspect ratios were quantified as described in Chapter 2.

Validation of *UAS-Mical-RNAi* and *Mical (-/-)*

To control for variability in antibody staining, control and experimental conditions for each set of validations were stained in the same tube, controls were distinguished by the protein trap Indy-GFP, from FlyTrap (Buszczak et al., 2006), which has been used to visualize follicle cell membranes (Cetera et al., 2014).

Table 3.1: Experimental genotypes and conditions for "Investigating the role of the actin disassembly factor Mical in the follicular epithelium"

Figure	Panel	Females on yeast	
		Genotype	Temp (ºC), Duration (days)
3.1	A	*tj/+*	29, 3
		tj/Mical-RNAi ^{CG33208}	29, 3
	B	*tj/+*	29, 3
		tj/Mical-RNAi ^{CG33208}	29, 3
		Df(3R)swp2/+	25, 3
		Mical^{K1496}/ Df(3R)swp2	25, 3
3.2	A	*Mical^{K1496}/ +*	25, 3
		Mical^{K1496}/ Df(3R)swp2	25, 3
	B	*Mical^{K1496}/ +*	25, 2
		Mical^{K1496}/ Df(3R)swp2	25, 2
3.3	A-C	*tj/+; UAS-GFP-Mical/+*	22, 2
	D	*hsFLP/+; UAS-GFP-MICAL/act5c>>Gal4, UAS-RFP*	25, 2, post heat shock
3.4	A	*tj/+; UAS-GFP-Mical/+*	29, 3
	B	*tj/UAS-PlexA-RNAi^{GD14483}; UAS-GFP-Mical/+*	29, 3
3.5	A	*tj/+; UAS-GFP-Mical/+*	25, 2

Table 3.1 continued

3.5	B	*tj/+; UAS-GFP-Mical, Sema-5c^{K175}, FRT80B*/ Sema-5c^{K175}, FRT80B*	25, 2
3.6	A, B	*w^{1118}*	25, 3
	C	*w/+; e22c-Gal4, UAS-Flp/+;Sema-5c^{K175}, FRT80B/ubi-eGFP, FRT80B*	29, 3
	D	*hsFLP/+; UAS-PlexA-RNAi^{GD14483}/act5c>>Gal4, UAS-GFP*	29, 2, post heat shock
3.7	A, B	*w^{1118}*	25, 3
3.8	A, B	*w/+; e22c-Gal4, UAS-Flp/+;Sema-5c^{K175}, FRT80B/ubi-eGFP, FRT80B*	29, 3
3.9	A	*hsFLP/+; UAS-MICAL/act5c>>Gal4, UAS-GFP*	25, 2, post heat shock
	B	*tj/+*	29, 3
		tj/Mical-RNAi ^{CG33208}	29, 3
3.10	A	*indy-GFP*	29, 3
		tj/Mical-RNAi ^{CG33208}	29, 3
	B	*indy-GFP*	25, 2
		Mical^{K1496}/ Df(3R)swp2	25, 2

*This line was built by recombining the *UAS-GFP-Mical* transgene and *Sema-5c^{K175}, FRT80B*. The position of *UAS-GFP-Mical* is unknown and its location relative to *Sema-5c^{K175}* has not been determined. Additionally, I have not confirmed whether the FRT80B site is present is this new line.

CHAPTER 4: CONCLUSIONS AND FUTURE DIRECTIONS

4.1 PREFACE

In section 4.2 I will discuss the conclusions that can be drawn from my work on the function of Sema-5c in epithelial migration. In section 4.3 I will address the remaining questions that arise from these results.

4.2 CONCLUSIONS

During my dissertation work, I examined how Sema-5c, a transmembrane semaphorin, promotes collective migration of follicle cells in *Drosophila* and what factors it interacts with during this process. Transmembrane semaphorins are good candidates to coordinate cell behavior during collective motility, but the mechanisms by which they operate during cell migration *in vivo* are poorly understood. Sema-5c is understudied compared to the other fly semaphorins, despite being the only *Drosophila* semaphorin with direct homologs in vertebrates. Thus, studying the role of Sema-5c during follicle cell migration was a great opportunity to utilize a highly-tractable system to explore the role of a conserved transmembrane semaphorin in collective movement.

This work was motivated by an interest in understanding how individual cells coordinate their behavior for collective motility. During collective cell migration, cells influence the behavior of their neighbors to keep everyone moving in the same direction. This likely involves signaling between neighboring cells, but few such cell-cell signaling systems have been identified. Semaphorin signaling is well known to guide the migration of individual cells, suggesting that transmembrane semaphorins could also provide guidance cues within a group of

collectively migrating cells, but exactly how they would be deployed to accomplish this task was unclear.

My work on the role of Sema-5c in follicle cell migration reveals a model for how transmembrane semaphorins can drive collective movement. My data suggest that Sema-5c promotes epithelial migration by providing a repulsive cue for neighboring cells, similar to the role of CIL in collective movement. During these studies, I identified that PlexA is the likely receptor for Sema-5c in the follicle cells and uncovered a point of convergence between Sema-5c – PlexA activity and the Fat2 – Lar signaling system. Characterizing *Sema-5c* epithelia also uncovered unexpected features of follicle cell migration that further our understanding of this system.

Follicle cell migration can begin late in development from a disordered state

I showed that the follicle cells can begin migrating late in development, which is in contrast to the wildtype case in which migration starts as soon as an egg chamber forms (Cetera et al., 2014; Chen et al., 2016). Live imaging of *Sema-5c* epithelia suggested they were non-migratory, but the global alignment of stress fibers suggested that the migration might just be delayed. In *Sema-5c* epithelia, global stress fiber alignment starts high but decreases over time, reaching a low point at stage 5, and then recovers by stage 7. Since migration is required to maintain global stress fiber alignment (Cetera et al., 2014), this strongly suggested that migration is disrupted in *Sema-5c* epithelia prior to stage 5. I thus developed COMETtail method to further test this hypothesis. This showed that COMETTails are not present in a majority of stage 5 *Sema-5c* epithelia, but are present in all cases examined by stage 7. Together these data show that loss of

Sema-5c delays the onset of follicle cell migration. Going forward, it will be interesting to determine why migration is able to initiate at later stages.

The delayed onset of migration in *Sema-5c* epithelia is interesting because it coincides with a lack of tissue-level order. Studies of collective cell migration suggest that organization across a cohort is a prerequisite for collective movement, all cells must have their polarities aligned so they can move in the same direction as neighboring cells. Thus, a lack of global order would suggest that the tissue would be unable to migrate. However, my work shows that this is not the case in the follicle cells, they can begin migration even from a disordered state. This was unexpected, as the follicle cells normally have a high degree of tissue-level organization prior to the onset of migration (Cetera et al., 2014). This suggests that the ability of the follicular epithelium to break symmetry and polarize is more robust than previously appreciated.

My studies of *Sema-5c* epithelia highlight a few points that should be taken into account in future studies of follicle cell migration. First, the follicle cells can migrate extremely slowly, so slowly that it cannot be captured by current live imaging techniques. Such migration can only be revealed in fixed tissue by COMETtail analysis or a similar method that was recently published (Chen et al., 2017). Despite being slow, this migration is still sufficient to promote egg chamber rotation and likely feeds into tissue morphogenesis, so it is important that future studies are aware of this cryptic migration. Second, my work shows that migratory phenotypes can differ between early and late migration stages. This implies that examining a single stage of follicle cell migration is likely not sufficient to capture all the developmental dynamics of the tissue and future studies need to take multiple stages into consideration.

Sema-5c is planar polarized and likely signals in a directional manner between follicle cells

Sema-5c may provide a directional signal within the follicular epithelium that promotes its migration. At the basal epithelial surface, Sema-5c localizes specifically to leading edge of each cell. Such a planar polarized distribution has not, to my knowledge, been described for a semaphorin before. This suggested that Sema-5c could signal between neighboring cells within the tissue, specifically from the leading edge of each cell to the trailing edge of the cell ahead. And indeed, overexpression of Sema-5c revealed that it has short-range non-cell-autonomous activity, which supports it signaling between neighboring cells. Together these data suggest that by being deployed in a planar polarized manner, Sema-5c provides a directional signal between neighboring follicle cells.

This presumptive activity of Sema-5c displays some interesting similarities and differences to the planar cell polarity (PCP) pathway. The core PCP pathway has been well-studied in the *Drosophila* wing, where a set of core PCP proteins localize to the apical junctional region of the epithelial cells of the wing (Goodrich and Strutt, 2011; Humphries and Mlodzik, 2018; Munoz-Soriano et al., 2012). A majority of these proteins are specifically located at just one side of each cell, with one subset at the proximal side and one subset at the distal side, thus each of these complexes adopt a planar polarized distribution across the wing. The asymmetric distribution of core proteins enables them to form heterophilic interactions across cell-cell boundaries and leads to the generation of a trichome just at the distal side of each cell. This pathway sets up a global directional cue across the epithelium, which is demonstrated by the fact that loss of a core PCP protein from a clone of cells in the wing causes the wildtype cells, both those adjacent to the clone and those multiple cell lengths away, to change the orientation of their trichomes. Similar to the core PCP proteins, in the follicular epithelium, Sema-5c is 1)

planar polarized across an epithelium, localizing to just one side of each cell, 2) may form heterophilic interactions across cell-cell boundaries though its interaction with PlexA, 3) causes a phenotype at only one side of each cell, in this case suppression of protrusions at the trailing edge of the cell ahead, and 4) Sema-5c plays a role in setting up global organization across a tissue, as loss of Sema-5c results in a loss of global stress fiber alignment in the follicular epithelium. However, in contrast to the core PCP pathway, Sema-5c's role in achieving global order appears to be through providing an extremely short-range cue, just between directly adjacent cells. Going forward, it will be interesting to determine how such a short-range cue is able to feed into global tissue order. It is possible that Sema-5c's ability to promote cell migration will feed into the propagation of its cue across the tissue, as previous work form our lab shows that cell migration plays an important role in tissue-level organization of the follicular epithelium (Cetera et al., 2014).

Sema-5c may promote collective motility by acting as a repulsive cue for neighboring cells

Sema-5c may promote follicle cell migration through contact inhibition of locomotion (CIL). CIL describes the phenomenon when two migrating cells collide, collapse their protrusions at the point of contact, and repolarize to migrate away from one another (Stramer and Mayor, 2016). CIL is proposed to play a role in collective motility by helping to polarize a group of cells; it inhibits protrusions at points of cell contact, which could direct leader cells to protrude away from follower cells and help to set a direction for migration (Stramer and Mayor, 2016). A characteristic phenotype of losing CIL is that each cell's protrusions become randomly oriented instead of just extending from the leading edge (Carmona-Fontaine et al., 2008).

Studies of Sema-5c revealed two phenotypes that suggest that Sema-5c – based CIL could be operating during follicle cell migration. First, overexpression studies revealed that Sema-5c supresses protrusions in neighboring cells. Second, examination of stage 6 *Sema-5c* epithelia showed that protrusions are often mis-oriented. Interestingly, I also predicted that protrusion levels would be increased in Sema-5c epithelia, and the lack of this phenotype suggests another factor may be acting redundantly with Sema-5c. These data, together with the directional signaling of Sema-5c described above, suggest a model in which Sema-5c acts at the leading edge of each cell to suppress protrusions at the trailing edge of the cell ahead. This could cause each cell to migrate away from the leading edge Sema-5c, thus maintaining the polarity of each cell relative to its neighbors in the tissue and setting a uniform direction for migration. In this scenario, Sema-5c is acting as a repulsive cue, similar to its role during axon guidance.

A CIL-based mechanism could be required specifically in the follicle cells because it provides a means by which to orient the polarity of all cells in the absence of an external migratory cue. Collectively migrating cells are often organized by chemotactic cue in the environment or by a free leading edge. However, in the follicle cells, neither of those is present, so the cells need another means by which to collectively polarize. Semap-5c-based CIL could play a role in this process by providing a repulsive cue at the leading edge of each cell, which directs the cell ahead to migrate away. When extended across an epithelium, this could organize the polarity of each cell in the tissue relative to its neighbors. Overall, this suggests that Sema-5c could play a role in orienting the polarity of each follicle cell so they can collectively migrate without an external cue.

PlexA is likely a receptor for Sema-5c

My data show that, in the follicular epithelium, Sema-5c likely signals to PlexA. I found that PlexA is required in the follicle cells for their migration and loss of PlexA disrupts global stress fiber alignment in a similar manner to loss of Sema-5c. Sema-5c and PlexA also bind *in vitro* and interact *in vivo*. And finally, PlexA is enriched at each cell's trailing edge, a location where it could receive a Sema-5c signal coming from the leading edge of the cell behind. These data are consistent with a model in which Sema-5c signals from the leading edge of each cell to activate PlexA at the trailing edge of the cell ahead. In this model, Sema-5c and PlexA interact *in trans*, as semaphorins and plexins are well established to do.

In *Drosophila,* PlexA interacts with Mical and a few pieces of my data are suggestive of Mical playing a role downstream of PlexA in the follicle cells. Mical is in interesting candidate because it directly links semaphorin-plexin signaling to the actin cytoskeleton (Hung et al., 2010). I showed that loss of Mical disrupts follicle cell migration, that UAS-Mical-GFP is enriched at the trailing edge of each cell, and that this localization depends on PlexA. These data are consistent with Mical interacting with PlexA during follicle cell migration. However, experiments with a Mical antibody did not recapitulate these localization results, which prevents me from drawing any strong conclusions at this time. Future work will be required to resolve these inconsistencies and may reveal additional factors that act downstream of PlexA.

Multiple guidance cues converge to promote epithelial migration

The activity of Sema-5c and PlexA displays many parallels with Fat2 and Lar, suggesting that there could be cross-talk between these two signaling systems. During follicle cell migration, Fat2 and Lar are planar polarized at the basal surface and provide short-range signals between

leading-trailing cell-cell interfaces to drive motility (Barlan et al., 2017). Sema-5c and PlexA are also planar polarized at the basal surface of the follicular epithelium during migration, and my data suggest that they similarly signal between the leading and trailing edges of neighboring cells to promote movement. Thus, I explored whether there were any connections between the two signaling systems.

I found that Sema-5c interacts with Lar and that this interaction likely takes place during follicle cell migration. Sema-5c and Lar genetically interact, loss of one copy of *Lar* rescues some *Sema-5c* phenotypes, which suggests that Sema-5c has an antagonistic effect on Lar. Their distributions at the basal surface also show a high degree of overlap, suggesting they could colocalize in a signaling complex. And finally, loss of Lar reduces the levels of Sema-5c at the basal surface, suggesting they bind to each other, either directly or indirectly, and this interaction stabilizes Sema-5c at the membrane. However, their mode of physically interaction remains unknown. My data further suggest that this interaction takes place during follicle cell migration and starts during early rotation stages, as global stress fiber alignment is higher in *Lar (-/+); Sema-5c (-/-)* epithelial than in *Sema-5c (-/-)* epithelia at both stages 5 and 7. It is possible that loss of *Lar* rescues *Sema-5c* epithelia by preventing the delayed onset of migration that normally occurs. Although live imaging suggests that any migration which is recovered will still be slow, it seems possible that an early recovery of slow migration could account for the rescue of *Sema-5c* phenotypes.

A connection between semaphorins and Lar-family proteins has only recently been uncovered, and those interactions are very different from my findings. My data show that Sema-5c and Lar interact in an epithelial context and suggests that they do so *in cis*. Previously, semaphorins and Lar-family RPTPs were shown to interact *in trans* in the nervous systems of *C.*

elegans and mice; Lar acts with a plexin to amplify the signal from a secreted semaphorin (Nakamura et al., 2017). My work now suggests that there may be cross talk between semaphorins and Lar family proteins in other contexts.

Sema-5c, PlexA, Fat2, and Lar are all known for their roles in nervous system development (Avilés and Goodrich, 2017; Han et al., 2016; Kolodkin and Tessier-Lavigne, 2011). During this process, cues in the environment steer protrusive growth cones toward their targets, similar to guiding a migrating cell. Now it is apparent that neuronal guidance cues can also be deployed in an epithelial context to promote migration by providing short-range cues that coordinate behavior between neighboring cells.

Broad relevance of my work

I showed that Sema-5c and PlexA promote collective motility by acting within the migrating cells themselves. This is in contrast to the previously described roles of semaphorins during cell migration. Semaphorins are well-established to act as cues in the migratory environment, where they repel plexin-expressing cells. For example, secreted semaphorins line the migratory route of collectively migrating neural crest cells to keep them on the correct path. Transmembrane semaphorins can play a similar role. When they guide migration in developing tissues, the transmembrane semaphorin and its plexin receptor are each expressed in a different population of cells, then signaling between these populations causes one population to migrate away from the other (Kerjan et al., 2005; Toyofuku et al., 2004b). In contrast, my data shows that Sema-5c and PlexA are expressed within the migratory follicle cells and are required for their motility. These data show that signaling from transmembrane semaphorins can guide cell migration from within the migrating cells themselves. This expands our understanding of how transmembrane

semaphorins can promote motility and is likely to inform future work on the role of semaphorins during development.

My work also presents a model for how transmembrane semaphorins could guide movement from within the migrating cells: by being deployed in a planar polarized manner so they can signal directionally between neighboring cells. At the basal surface of the follicular epithelium, Sema-5c localizes specifically to the leading edge of each cell while PlexA is primarily enriched at the trailing edge. This suggests that Sema-5c signals from the leading edge of each cell to PlexA at the trailing edge of the cell ahead, in a uniform direction across the epithelium. This is in contrast to previous work on the role of transmembrane semaphorins in epithelial tissues, in which it appears that semaphorin-plexin signaling is isotropic across the tissue plane (Xia et al., 2015; Yoo et al., 2016). Such isotropic signaling would not be conducive to collective motility, as it doesn't enforce any higher-level organization between neighboring cells. On the other hand, a directional signal is well-poised to guide all cells to move in the same direction as their neighbors and thus coordinate collective motility. An important point raised by my finding is that examining the subcellular localization of semaphorins and plexins, which is not often done, can reveal important aspects of their role in tissues. As the expression of both transmembrane semaphorins and their plexin receptors within a single epithelium is not unusual (Xia et al., 2015; Yoo et al., 2016), and three of the five classes of mammalian semaphorins are transmembrane proteins (Yazdani and Terman, 2006), the mode of semaphorin-plexin signaling seen in follicle cells could apply to other epithelial contexts, if not additional cases of collective migration.

4.3 FUTURE DIRECTIONS

My work gives rise to many interesting avenues to explore in future research, here I will discuss the next steps for advancing these studies.

Does basement membrane structure play a role in the recovery of motility in *Sema-5c* epithelia?

As described in Chapter 2, in a majority of *Sema-5c* epithelia, the timing of migration onset coincides with changes in the basement membrane that may create a more favorable environment for motility. I showed that loss of Sema-5c largely inhibits follicle cell migration in a majority of epithelia until approximately stage 5, but then the tissue can migrate, albeit slowly. As the egg chamber develops, the stiffness of the basement membrane increases, with the matrix being stiffer at stages 5-6 than at stages 3-4 (Crest et al., 2017). Since stiffer matrices promote cell migration (Mason et al., 2012), the improved migratory ability of *Sema-5c* epithelia could be due to a change in matrix stiffness. Even in wildtype egg chambers the rate of follicle cell migration increases after stage 5 (Cetera et al., 2014), which suggests that the follicle cells could respond to changes in basement membrane stiffness.

I hypothesize that the recovery of migration in *Sema-5c* epithelia is due to an increase in matrix stiffness, and in the absence of this increase, the migration will no longer recover. Work from a former graduate student in the lab, Adam Isabella, suggests that matrix stiffness could be decreased by overexpressing SPARC, which blocks the incorporation of Collagen IV, a major basement membrane protein, into the matrix (Isabella and Horne-Badovinac, 2015). I predict that overexpressing SPARC in *Sema-5c* epithelia will disrupt the recovery of motility and global stress fiber alignment. It would also be interesting to see if increasing matrix stiffness has an

effect on the motility of *Sema-5c* epithelia, perhaps it could result in migration speeds that are closer to wildtype. Stiffness can be increased by overexpressing Ehbp1 (Crest et al., 2017), which increases formation of basement membrane fibrils (Isabella and Horne-Badovinac, 2016).

It is important to note that determining how *Sema-5c* epithelia recover motility does not explain why the rate of follicle cell migration is so slow once it recovers. My data show that Sema-5c signaling is required for the follicle cells to achieve a wildtype migration rate and elucidating the mechanism behind this activity will require future studies on what factors act downstream of Sema-5c.

What factors act downstream of PlexA?

I presented many pieces of evidence that suggest Sema-5c is a ligand for PlexA, thus determining what factors act downstream of PlexA is the next step in elucidating the mechanism underlying Sema-5c – PlexA activity in the follicle cells. In *Drosophila*, two factors that act downstream of PlexA, Mical, an actin disassembly factor (Hung et al., 2010), and Rap1, a small GTPase of the Ras Family (Yoo et al., 2016), are good candidates.

In Chapter 3, I presented data that are suggestive of Mical playing a role downstream of PlexA, but future studies are required. It is possible that the *Mical* mutant allele is a hypomorph, as the early stop codon occurs after a majority of the redox domain. Thus, a critical next step for future studies will be to use CRISPR/Cas9 to make a new null allele. This allele could be made on a FRT to enable the production of fully mutant epithelia, eliminating the use of the *Mical* deficiency, which takes out additional genes. Another an important next step is to endogenously tag Mical so that it's subcellular localization and the dependence of this localization on PlexA can be verified. And finally, examining if loss of Mical affects actin-based structures at the basal

surface, namely stress fibers or protrusions, will help determine if it is active during follicle cell migration. Making null clones of Mical could be ideal for these studies so that there is an internal control when staining for levels of F-actin.

Recent work on Rap1 suggests it is also a good candidate to act downstream of PlexA. The intracellular region of plexins contains a Ras GAP domain and *Drosophila* PlexA has GAP activity for Rap1 (Yoo et al., 2016). Interestingly, during migration of the border cells in the *Drosophila* egg chamber, Rap1 regulates protrusion formation to promote directional migration (Chang et al., 2018). Expression of constitutively active Rap1 in the border cells leads to mis-oriented protrusions, increased Rac activity, and increased levels of Ena, an actin filament elongation factor. Expression of dominant negative Rap1 results in a loss of protrusions and decreases Rac activity. Rap1 also suppresses Hippo signaling, which inactivates Ena. Together these data suggest that Rap1 can promote directional migration and protrusion formation though Ena. During follicle cell migration, Ena is present at the tips of filopodia and is required for their formation (Cetera et al., 2014). Based on these studies, I hypothesize that PlexA could inhibit filopodia formation at the trailing edge of each cell through its GAP activity for Rap1. Upon loss of Sema-5c or PlexA, Rap1 would be overactive, leading to increased protrusive activity and mis-oriented protrusions that disrupt collective migration, as we observe. To test whether Rap1 acts downstream of Sema-5c and PlexA, I propose reducing Rap1 activity in *Sema-5c* or *PlexA-RNAi* epithelia. If my hypothesis is correct, then in the absence of Rap1 activity, mis-oriented protrusions would not form and I would predict a rescue of the onset or rate of migration. In addition, expressing a constitutively active Rap1 in these backgrounds should make the phenotypes worse. It would also be interesting to see if overexpression of Rap1 alone causes an increase in mis-oriented protrusions or affects migration. Overall, determining if Mical, Rap1, or

another factor, acts downstream of PlexA will help elucidate the Sema-5c –PlexA signaling pathway the operates during follicle cell migration.

Does PlexA localize Sema-5c to the basal surface via a *trans* interaction?

I presented multiple pieces of evidence that suggest Sema-5c signals though PlexA across cell-cell interfaces, which supports a *trans* interaction, but I have not definitively shown a *trans* interaction *in vivo*. The majority of the time, semaphorins-plexin interactions occur *in trans* and crystallography studies show that semaphorins and plexins bind *in trans* via their extracellular sema domains (Janssen et al., 2010; Liu et al., 2010). However, semaphorins and plexins can interact *in cis* (Battistini and Tamagnone, 2016; Jongbloets and Pasterkamp, 2014) and since there is a population of PlexA at the leading edge of each follicle cell, where Sema-5c localizes, it is possible that Sema-5c and PlexA have a *cis* interaction as well.

One of the strongest pieces of evidence that shows Sema-5c and PlexA interact *in vivo* is that PlexA is required for Sema-5c to localize to the basal surface, as this population of Sema-5c is reduced upon loss of PlexA. It is possible to test if PlexA localizes Sema-5c to the basal surface via a *trans* interaction by making clones of *PlexA-RNAi* in a *Sema-5c-3xGFP* background. If PlexA stabilizes Sema-5c-3xGFP *in trans*, then control cells immediately behind a *PlexA-RNAi* clone should be missing Sema-5c-3xGFP from their leading edge, because there is no PlexA at the trailing edge of the cell ahead to stabilize Sema-5c-3xGFP at the membrane. Additionally, *PlexA-RNAi* cells at the front of the clone should retain Sema-5c-3xGFP at their leading edge because there is PlexA at the trailing edge of the control cells in front of them. This result would verify that Sema-5c and PlexA interact *in trans* in the follicle cells. It is also possible that the opposite result could occur, Sema-5c-3xGFP is present at the leading edge of

the cells behind the clone but absent from the leading edge of the clone itself. This would suggest that either PlexA stabilizes Sema-5c-3xGFP *in cis* or that PlexA plays a role in recruiting Sema-5c to the basal surface, not stabilizing it once it is there. Either of these results would be informative because they reveal information about how Sema-5c and PlexA interact in the follicle cells.

Do Sema-1a and/or Sema-1b act redundantly with Sema-5c?

In Chapter 2, I proposed that Sema-5c promotes migration by acting as a repulsive cue for neighboring cells, and my data suggest that there may be another factor acting redundantly with Sema-5c during this process. According to my model, Sema-5c's repulsive activity inhibits protrusion formation, and I showed that overexpression of Sema-5c-GFP has just this effect. This implies that loss of Sema-5c should cause an increase in protrusions, however I have not found that to be the case. Clones of *Sema-5c* mutant cells do not appear to have any difference in protrusion levels compared to neighboring control cells. This suggests that another factor is acting redundantly with Sema-5c and only by knocking out both of them will an increase in protrusion levels be revealed. Two additional pieces of evidence further suggest that there may be redundancy between Sema-5c and another factor. First, global stress fiber alignment in *PlexA-RNAi* epithelia does not recover to the same extent as in *Sema-5c* epithelia and *PlexA-RNAi* eggs are slightly rounder. Second, the basal surface distributions of PlexA and Sema-5c only partially overlap, so there is a population of PlexA that is available to interact with another protein.

Sema-1a and Sema-1b are good candidates to act redundantly with Sema-5c for two main reasons. First, they are both known ligands for PlexA in *Drosophila* (Winberg et al., 1998). Second, I have preliminary data from protein trap lines which suggests that at least Sema-1b and

possibly Sema-1a are expressed in the follicle cells. Notably, the signal from these transgenes is quite dim so further work is required to validate this result, but data from the modENCODE *Drosophila* transcriptome project shows that Sema-1a and Sema-1b are expressed in the ovary, so it is likely that the signal from the protein trap lines is valid. Additionally, it is interesting to note that another paper examining PlexA signaling in *Drosophila* found that knockdown of Sema-1a and Sema-1b did not produce as strong of a phenotype as knockdown of PlexA (Yoo et al., 2016), which suggests that there are multiple contexts in which the *Drosophila* transmembrane semaphorins may act redundantly.

To test if Sema-1a and/or Sema-1b act redundantly with Sema-5c in the follicle cells we can look for genetic interactions. First, the Sema-1a/b protein trap lines can be used to validate RNAi knockdown of these proteins. Then, driving RNAi against Sema-1a, Sema-1b or both in the background of *Sema-5c* would reveal if they genetically interact. Sema-1a/b can act redundantly so it is possible that knocking down both simultaneously will be required. I predict that knocking them down would further inhibit elongation and recovery of global stress fiber alignment of *Sema-5c* tissue. It would also be interesting to knock Sema-1a/b down in the background of *Sema-5c* mosaic epithelia to see if this reveals increased protrusions in the *Sema-5c* cells. A former postdoc in the lab, Kari Barlan, built a line which makes this experiment feasible. It is also possible that Sema-1a/b act with PlexA independently of Sema-5c, so testing if knockdown of them alone affects elongation will also be required. Determining if Sema-1a/b act redundantly with Sema-5c will be important to know going forward.

Examining what connects Sema-5c to Lar

Since a *cis* interaction between a semaphorin and a Lar family protein has not previously been seen, it will be interesting to determine how these proteins interact at a molecular level. I showed that Sema-5c and Lar colocalize in the follicle cells and that Lar is required for Sema-5c localization to the basal surface. Since both of these proteins localize to the leading edge of each cell, these data suggest that they physically interact *in cis*. It is possible that they directly interact, via their extracellular or intracellular domains. However, it is also possible that a cofactor is involved, which bridges a connection between them. Class 5 semaphorins and Lar both bind heparan sulfate proteoglycans (Johnson et al., 2006; Kantor et al., 2004) and Syndecan is a particularly good candidate for binding to both of them, as it has been shown to be a ligand for Lar (Fox and Zinn, 2005) and was a strong candidate to interact with Sema5A in mouse (Kantor et al., 2004). Furthermore, unpublished data from our lab shows that Syndecan is planar polarized at the basal surface of the follicular epithelium, which places it in the right location to bind to Sema-5c and Lar. I have built lines to test whether this localization is specific to the leading or trailing edge. To test if Syndecan links Sema-5c to Lar, I propose altering Syndecan levels and then examining the localization of Sema-5c and Lar. If my hypothesis is correct, then loss of Syndecan will disrupt the localization of Sema-5c to the basal surface, while overexpression Syndecan could increase the colocalization of Sema-5c and Lar. If Sema-5c and Lar are connected via Syndecan, this provides a starting point for investigating how Sema-5c and Lar affect each other's activity.

Does loss of one copy of Lar rescue early migration of Sema-5c epithelia?

I am very interested to know how losing one copy of *Lar* increases elongation and global stress fiber alignment of *Sema-5c* epithelia. Since follicle cell migration is tightly correlated with global stress fiber alignment and egg chamber elongation, both of these results could be explained by a rescue of motility. Because *Lar (-/+); Sema-5c (-/-)* epithelia have higher global stress fiber alignment at stage 5 than *Sema-5c (-/-)* epithelia, I hypothesize that loss of Lar enables migration to initiate earlier. I further predict that any migration that takes place will be very slow, since live imaging of stage 7 *Lar (-/+); Sema-5c (-/-)* in Chapter 2 revealed no increase in migration speed compared to *Sema-5c (-/-)* epithelia. Thus, the COMETtail method I developed to visualize slow migration would be ideal for testing this hypothesis. It if turns out that loss of *Lar* does enable migration to initiate earlier in *Sema-5c* epithelia, it would suggest that Sema-5c promotes migration partially by antagonizing Lar or that Lar has an inhibitory effect on motility.

Overall, the genetic and physical interaction between Sema-5c and Lar presents a point of convergence between two signaling systems that act at leading-trailing cell-cell interfaces during follicle cell migration, those of Sema-5c – PlexA and Fat2 – Lar. This highlights the complexity of coordinating dynamics between neighboring cells during migration. It also opens the door to a new area of investigation on how these pathways interact that will contribute to our understanding of what drives collective movement.

APPENDIX A: EXAMINATION OF BASEMENT MEMBRANE FIBRILS IN *SEMAPHORIN-5C* EGG CHAMBERS

Introduction

Egg chamber elongation is proposed to occur though the formation of a "molecular corset" composed of stress fibers and basement membrane fibrils, as described in Chapter 1 (Gutzeit et al., 1991). At the basal surface of the follicular epithelium, stress fibers are aligned perpendicular to the axis of elongation such that they result in a circumferential arrangement around the outer surface of the egg chamber (Cetera et al., 2014; Gutzeit et al., 1991). Additionally, fibrils of basement membrane proteins are also aligned in this direction (Gutzeit et al., 1991; Isabella and Horne-Badovinac, 2016). As the egg chamber grows, the stress fibers and basement membrane fibrils are thought to channel growth along the anterior-posterior axis by resisting expansion perpendicular to this plane. In egg chambers that fail to elongate this circumferential organization of the stress fibers and basement membrane fibrils is often affected (Bateman et al., 2001; Cetera et al., 2014; Frydman and Spradling, 2001; Gutzeit et al., 1991; Haigo and Bilder, 2011; Horne-Badovinac et al., 2012; Isabella and Horne-Badovinac, 2016; Lewellyn et al., 2013; Viktorinova et al., 2009). The formation of the basement membrane fibrils depends on follicle cell migration (Isabella and Horne-Badovinac, 2016; Lewellyn et al., 2013). In epithelia where migration is slow, the basement membrane contains fewer fibrils and they are not well aligned. When migration is blocked entirely, fibrils fail to form and instead basement membrane proteins accumulate at cell-cell interfaces at the basal surface.

It is interesting that *Sema-5c* mutant egg chambers fail to elongate properly even though many recover their stress fiber alignment. One hypothesis for why elongation fails is that slow

migration is insufficient to polarize the basement membrane; since migration is disrupted in *Sema-5c* epithelia, it is likely that fibril formation is also be affected.

Here I show that loss of Sema-5c results in a range of fibril phenotypes and present data that suggest these phenotypes may need to be validated with additional tools for visualizing basement membrane proteins.

Results

The basement membrane fibrils are best visualized using a GFP protein trap in in the Col 4a2 chain Viking (Col IV-GFP) (Isabella and Horne-Badovinac, 2016). Placing this transgene in the *Sema-5c* background reveals a wide range of fibril phenotypes at stage 7 (Figure 1). Some of the time the fibrils appear unchanged compared to controls, but in the majority of cases there appears to be fewer fibrils in the *Sema-5c* egg chambers. Also, in a small proportion, there are regions of the basement membrane in which Col IV-GFP accumulates at cell-cell interfaces but does not surround entire cells. These data show that loss of Sema-5c disrupts fibril formation.

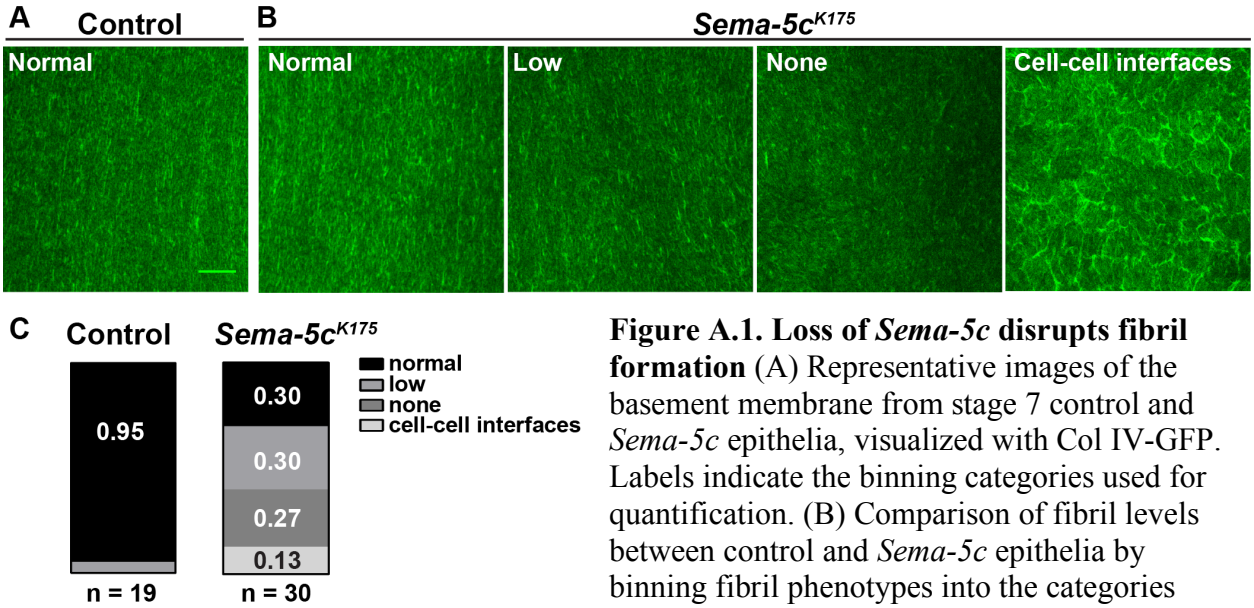

Figure A.1. Loss of *Sema-5c* disrupts fibril formation (A) Representative images of the basement membrane from stage 7 control and *Sema-5c* epithelia, visualized with Col IV-GFP. Labels indicate the binning categories used for quantification. (B) Comparison of fibril levels between control and *Sema-5c* epithelia by binning fibril phenotypes into the categories indicated in (A). Scale bar, 10 µm.

During these experiments, I noticed that when Col IV-GFP was in the background, the eggs produced by *Sema-5c* females appeared rounder than usual. A rotation student who I was mentoring at the time, Sonja Lazarevic, tested if there may be an interaction between the *Col IV-GFP* transgene and *Sema-5c*. When *Col IV-GFP* is present, *Sema-5c* eggs are rounder than usual, however, she also found that the *Col IV-GFP* transgene alone causes eggs to be slightly rounder than controls (Figure 2). This shows that the *Col IV-GFP* transgene generally has a low-level effect on egg chamber elongation, and that this effect may be magnified by loss of Sema-5.

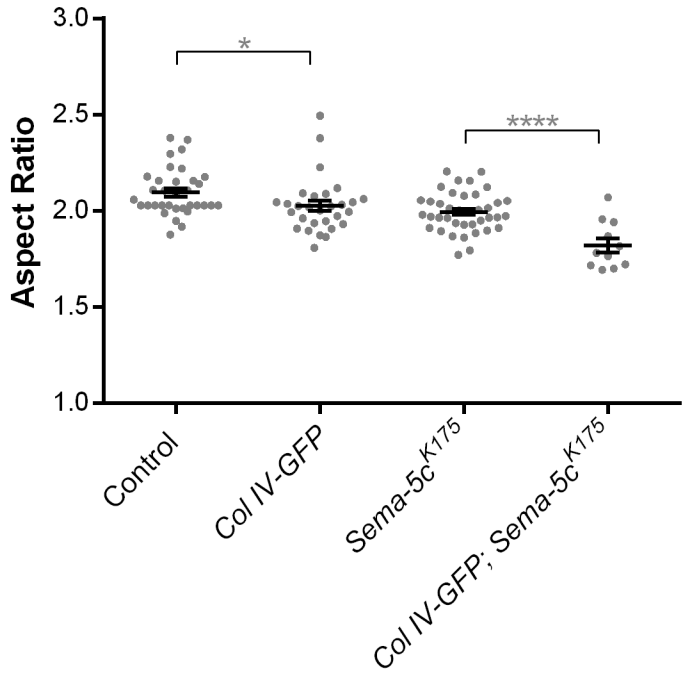

Figure A.2. Collagen IV-GFP affects egg chamber elongation
Egg aspect ratio measurements showing that Col IV-GFP reduces elongation of both control and *Sema-5c* egg chambers. Mean ± SEM. Unpaired t test. *p<0.05, ****p<0.0001.

Discussion

I hypothesized that fibril formation would be disrupted in *Sema-5c* egg chambers since *Sema-5c* females produce round eggs and *Sema-5c* epithelia have disrupted migration, both of which are linked to disruptions in fibril formation. I visualized the fibrils with a widely-used Col IV-GFP protein trap, however during these studies I noticed that this further disrupts elongation of eggs produced by *Sema-5c* females. This raises the concern that the fibril phenotypes I observed could

be affected by this interaction. Since *Sema-5c* epithelia already have compromised migration, a slight alteration to a major component of the basement membrane could hurt their ability to recover motility and thus the fibril phenotypes in this background would not be representative. Elongation of control egg chambers was also affected by *Col IV-GFP,* but not to the same extent as *Sema*-5c tissue was affected. This makes unclear how to interpret the interaction between *Sema-5c* and *Col IV-GFP,* but a few experiments could help clarify these results. First, it would be ideal to visualize the fibrils using another basement membrane protein to both confirm these fibril phenotypes and test if elongation of *Sema-5c* egg chambers is affected by multiple transgenes or if this is specific to Col IV-GFP. Perlecan and Laminin are two good candidates since they are also components of the fibrils and GFP-tagged versions of the Perlecan homolog Trol and the Laminin ß subunit LanB1 can both be used to visualize fibrils (Isabella and Horne-Badovinac, 2016). If one of these transgenes is sufficient for fibril visualization and does not affect elongation, then this issue is resolved. However, if such a tool is not found, it is still possible to test if Col IV-GFP is a viable tool in this background. Measuring aspect ratios across stages in *Col IV-GFP* egg chambers compared to controls would reveal if the effect of this transgene on elongation occurs during or after follicle cell migration. If it is a post-migration effect, then this makes it less concerning when interpreting the *Sema-5c* phenotypes. A final control would be to determine to what extent Sema-5c activity is affected by this transgene. Examining if migration and global stress fiber alignment are further reduced in this background, compared to loss of Sema-5c alone, could reveal if Col IV-GFP interferes with Sema-5c function. If Col IV-GFP does appear to affect recovery of *Sema-5c* epithelia, this potentially uncovers an interesting aspect of the *Sema-5c* phenotype. In Chapter 4, I hypothesized that recovery of *Sema-5c* epithelia may be related to changes in the basement membrane that coincide

with the recovery. If Col IV-GFP hinders recovery, it suggests that the basement membrane may indeed play a key role in this process.

With this caveat in mind, the fibril phenotypes exhibited upon loss of *Sema-5c* suggest that the majority of *Sema-5c* epithelia are not migrating well enough for fibril formation to proceed normally. This decrease in fibril formation could weaken the molecular corset (Isabella and Horne-Badovinac, 2016) and is consistent with the decreased elongation seen in the *Sema-5c* egg chambers. Since *Sema-5c* epithelia are migrating extremely slowly, this raises the interesting possibility that migration speed or duration could play a role in fibril formation, which would be interesting to investigate going forward. Perhaps the range of fibril phenotypes seen in the *Sema-5c* basement membranes reflects a variation in the duration of migration, with those that start to migrate early in stage 5 having more fibrils that those that don't recover motility until late stage 6. It is also possible that, although the *Sema-5c* epithelia are migrating very slowly, there could still be a range in their migration rates and the slightly faster ones form more fibrils while the slower ones form fewer. A particularly interesting case are the *Sema-5c* basement membranes in which Col IV-GFP accumulates at cell-cell interfaces. This phenotype has been previously seen when the follicular epithelium is not migrating (Isabella and Horne-Badovinac, 2016; Lewellyn et al., 2013). But in this case, the phenotype is not as severe as when migration is fully blocked, the cells aren't entirely surrounded by thick rings of Col IV-GFP and the amount that has accumulated is wispy with lots of variation in thickness. Thus, it appears that it may be possible that *Sema-5c* epithelia could still be moving even as Col IV-GFP is accumulating at cell-cell interfaces. This suggests that the rate of migration may need to reach a certain threshold in order for fibril formation to occur. Going forward, analyzing fibril fraction (Isabella and Horne-

Badovinac, 2016) would be a nice way to compare phenotypes between multiple migratory conditions when exploring the role of migration speed in fibril formation.

Overall, these data suggest that that basement membrane likely plays a role in the elongation defect of *Sema-5c* egg chambers. Additionally, they reveal that loss of Sema-5c presents an interesting background in which to examine parameters that feed into proper fibril formation.

Methods

Drosophila Genetics

Experimental genotypes and the conditions for culturing females are provided in the table below. All stock are as described in Chapter 2 with the following addition: *vkg-GFP* is from FlyTrap (Buszczak et al., 2006).

Fixed image acquisition and microscopy

Fixed imaging was performed as described in Chapter 2.

Quantification of egg aspect ratio

Egg aspect ratios were measured and quantified as described in Chapter 2.

Quantification of fibril levels

Fibrils were binned by eye into four categories. Three of the categories, normal, low, and none were based on fibril density compared to wildtype images. The fourth category, accumulation at

cell-cell interfaces, was created for basement membranes with this specific phenotype because it cannot fully be captured by the previous three categories.

Table A.1. Experimental genotypes and conditions for "Appendix A: Examination of basement membrane fibrils in *Semaphorin-5c* egg chambers"

Figure	Panel	Females on yeast	
		Genotype	**Temp (ºC), Duration (days)**
1	A, C	*vkg-GFP/+; FRT80B/FRT80B*	25, 2
	B, C	*vkg-GFP/+; Sema-5c^{K175}, FRT80B / Sema-5c^{K175}, FRT80B*	25, 2
2	A	*FRT80B/FRT80B*	25, 2
		vkg-GFP/ vkg-GFP; FRT80B/FRT80B	25, 2
		Sema-5c^{K175}, FRT80B / Sema-5c^{K175}, FRT80B	25, 2
		vkg-GFP/ vkg-GFP; Sema-5c^{K175}, FRT80B /Sema-5c^{K175}, FRT80B	25, 2

APPENDIX B: FURTHER INVESTIGATION OF THE CONVERGENCE BETWEEN SEMA-5C, PLEXA, FAT2 AND LAR

Introduction

My data suggest that there may be a convergence between Sema-5c – PlexA activity and the Fat2 – Lar signaling system. Both of these systems operate along leading-trailing cell-cell interfaces at the basal epithelial surface where they likely provide short ranges cues to drive follicle cell migration (Barlan et al., 2017). Not only are there many parallels between these systems, but Sema-5c and Lar genetically interact and Lar promotes Sema-5c's localization to the basal surface. These connections raise the question of how the activity of Sema-5c – PlexA and Fat2 – Lar impinge on one another. Could all four factors at times converge in one signaling complex?

I initially explored a role for PlexA and Fat2 with genetic interaction studies, as that is how the connection between Sema-5c and Lar was uncovered. This did not reveal any interaction between PlexA and Lar or Fat2 and Sema-5c. However, as this assay only examines final egg shape, there may be more subtle interactions between these factors that were missed. Here I will present two additional results that suggest that the interaction between Sema-5c and Lar is not entirely independent of PlexA and Fat2.

Results

In Chapter 2, I showed that, at the basal epithelial surface, the distribution of Sema-5c overlaps with that of Lar more frequently (average Pearson coefficient of 0.72) than with PlexA (average Pearson coefficient of 0.25). This suggests that either Sema-5c interacts independently with PlexA and with Lar, or that a complex of Lar and Sema-5c forms transient interactions with

PlexA. To test these hypothesis, I compared the distributions of PlexA and Lar at the basal surface (Figure 1). This reveals that they have almost the same correlation as PlexA and Sema-5c (average Pearson coefficient of 0.24). This suggests that either PlexA and Lar form an independent complex or that Sema-5c, PlexA and Lar occasionally exist in a single signaling center.

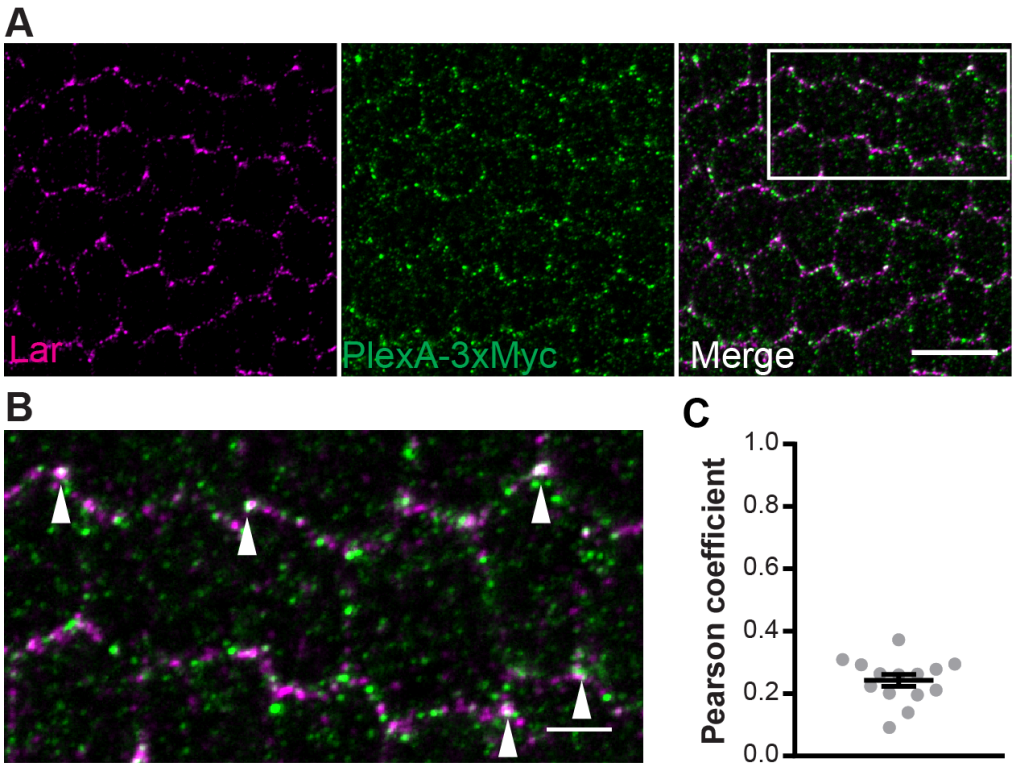

Figure B.1. The distribution of PlexA occasionally overlaps with that of Lar (A) Image of the basal epithelial surface of a *BAC-PlexA-myc* epithelium immunostained for Lar. (B) Zoom of the boxed region in (A), puncta of PlexA and Lar occasionally colocalize (white triangles). (C) Pearson correlation coefficient for BAC-PlexA-myc and Lar at the basal epithelial surface. Mean ± SEM. Scale bars, 10 μm (A), 3 μm (B).

In Chapter 2, I also showed that loss of one copy of a *fat2* did not rescue elongation of *Sema-5c* egg chambers. However, this experiment was done using the null allele $fat2^{N103\text{-}2}$, and I

found that using a different *fat2* allele, *fat2*^{58D} (Viktorinova et al., 2009), does cause a partial rescue (Figure 2). This suggests that *fat2* may feed into Sema-5c activity.

Discussion

Overall, these results are suggestive of a connection between PlexA and Lar as well as a link between Sema-5c and Fat2, which raises the possibility that the Sema-5c – PlexA and Fat2 – Lar signaling systems may converge more than was previously thought.

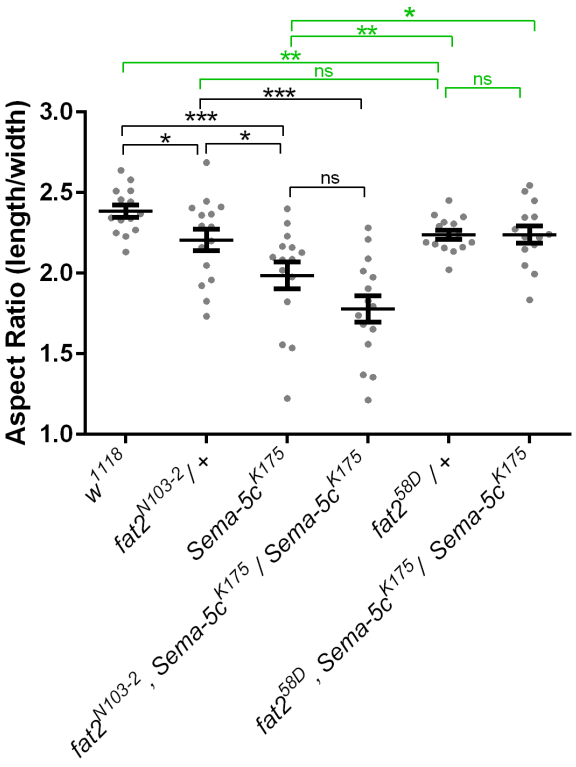

Figure B.2. Two alleles of *fat2* have differing effects on elongation of *Sema-5c* egg chambers Egg aspect ratios showing that *fat*$^{N103-2}$ does not affect elongation of Sema-5c egg chambers but *fat2*^{58D} partially rescues their elongation. Black asterisks compare to *fat2*$^{N103-2}$ conditions, green asterisks compare to *fat2*^{58D} conditions. Mean ± SEM. Unpaired t test. * $p < 0.05$, **$p < 0.01$, *** $p<0.001$. ns, not significant.

My localization data show that at the basal surface, the distributions of PlexA and Lar overlap to the same extent as those of PlexA and Sema-5c. Interestingly, the distribution of Sema-5c at the basal surface displays a higher correlation with Lar than with PlexA. These data are consistent with a model in which Sema-5c and Lar interact more often and form transient

interactions with PlexA. This model also fits with my earlier data showing that Sema-5c and Lar both localize to the leading edge while PlexA is primarily enriched at the trailing edge of the cell ahead, and is consistent with the idea that the repulsive nature of semaphorin-plexin signaling necessitates that their interaction be transient, as proposed in Chapter 2. Although I cannot currently rule out the possibility that PlexA and Lar interact separately, it seems more likely that PlexA would interact with Lar via Sema-5c since semaphorins have been shown to interact with Lar family proteins in other systems (Nakamura et al., 2017). This could be tested by examining the localization of Sema-5c, Lar and PlexA in a single epithelium. If overlap between them is seen in fixed tissue, then live imaging could be used to further explore the dynamics of their interactions.

It was initially puzzling that one *fat2* loss of function condition partially rescues elongation of Sema-5c egg chambers while another does not. However, evidence from a former post-doc in the lab, Kari Barlan, suggests $fat2^{58D}$, an allele in which part of the 5' end of the coding sequence is removed, is not a null allele as previously believed; sequencing data suggest that it may have a cryptic start site which causes it to be missing the first 5 cadherin repeats. This still remains to be verified, but since $fat2^{58D}$ is able to partially rescue elongation of *Sema-5c* egg chambers while $fat2^{N103\text{-}2}$ does not, this further suggests there is indeed a difference between these two alleles. Since loss of one copy of Lar and the $fat2^{58D}$ condition both rescue elongation of Sema-5c egg chambers, it suggests that $fat2^{58D}$ may not be able to interact with Lar, and thus it causes a similar effect to loss of one copy of Lar. This could be a less severe effect than a *fat2* null condition, which would block all of Fat2's functions, since previous work suggests that Fat2 interacts with other factors besides Lar (Barlan et al., 2017). Overall, this data suggests that Sema-5c interacts with the Fat2-Lar signaling system, over Sema-5c and Lar acting

independently of Fat2. Going forward, it will be interesting to explore how these players interact and what downstream effects result. To start, it would be useful to determine to what extent the localization of all these players is dependent one another. For example, it seems likely that loss of Fat2 would affect localization of Sema-5c, since Sema-5c depends on Lar and Lar requires Fat2 (Barlan et al., 2017). However, it is an open question how PlexA and Fat2 will affect each other.

Methods

Drosophila Genetics

Experimental genotypes and the conditions for culturing females are provided in the table below. All stock are as described in Chapter 2 with the following addition: $fat2^{58D}$ is from Christian Dahmann.

Fixed image acquisition and microscopy

Fixed imaging and staining were performed as described in Chapter 2.

Quantification of protein colocalization and egg aspect ratio

Egg aspect ratio and protein colocalization were measured and quantified as in Chapter 2.

Table B.2. Experimental genotypes and conditions for "Appendix B: Further examination of the convergence between Sema-5c, PlexA, Fat2 and Lar"

Figure	Panel	Females on yeast	
		Genotype	**Temp (ºC), Duration (days)**
1	A-C	*BAC-PlexA-myc/+; Df(4)C3/+*	25, 2
2		w^{1118}	25, 2
		$fat^{N103\text{-}2}$, *FRT80B/+*	25, 2

Table B.2. continued

2		*Sema-5c^{K175}, FRT80B*	25, 2
		fat^{N103-2}, Sema-5c^{K175}, FRT80B /Sema-5c^{K175}, FRT80B	25, 2
		fat2^{58D} /+	25, 2
		fat2^{58D}, Sema-5c^{K175}, FRT80B /Sema-5c^{K175}, FRT80B	25, 2

REFERENCES

Aigouy, B. and Mirouse, V. (2013). ScientiFig: a tool to build publication-ready scientific figures. *Nat. Methods* 10, 1048–1048.

Alto, L. T. and Terman, J. R. (2017). Semaphorins and their signaling mechanisms. In *Semaphorin Signaling* (ed. Terman, J. R.), pp. 1–25. New York, NY: Springer Science.

Artigiani, S., Conrotto, P., Fazzari, P., Gilestro, G. F., Barberis, D., Giordano, S., Comoglio, P. M. and Tamagnone, L. (2004). Plexin-B3 is a functional receptor for Semaphorin 5A. *EMBO Rep.* 5, 710–714.

Aurich, F. and Dahmann, C. (2016). A mutation in fat2 uncouples tissue elongation from global tissue rotation. *Cell Rep.* 14, 2503–2510.

Avilés, E. C. and Goodrich, L. V. (2017). Configuring a robust nervous system with Fat cadherins. *Semin. Cell Dev. Biol.* 69, 91–101.

Ayoob, J. C. (2006). *Drosophila* Plexin B is a Sema-2a receptor required for axon guidance. *Development* 133, 2125–2135.

Bahri, S. M., Chia, W. and Yang, X. (2001). Characterization and mutant analysis of the *Drosophila sema 5c* gene. *Dev. Dyn.* 221, 322–330.

Barberis, D., Artigiani, S., Casazza, A., Corso, S., Giordano, S., Love, C. A., Jones, E. Y., Comoglio, P. M. and Tamagnone, L. (2004). Plexin signaling hampers integrin-based adhesion, leading to Rho-kinase independent cell rounding, and inhibiting lamellipodia extension and cell motility. *FASEB J.* 18, 592–594.

Barlan, K., Cetera, M. and Horne-Badovinac, S. (2017). Fat2 and Lar define a basally localized planar signaling system controlling collective cell migration. *Dev. Cell* 40, 467–477.

Bateman, J., Reddy, R. S., Saito, H. and Van Vactor, D. (2001). The receptor tyrosine phosphatase Dlar and integrins organize actin filaments in the *Drosophila* follicular epithelium. *Curr. Biol.* 11, 1317–1327.

Battistini, C. and Tamagnone, L. (2016). Transmembrane semaphorins, forward and reverse signaling: have a look both ways. *Cell. Mol. Life Sci.* 73, 1609–1622.

Buszczak, M., Paterno, S., Lighthouse, D., Bachman, J., Planck, J., Owen, S., Skora, A. D., Nystul, T. G., Ohlstein, B., Allen, A., et al. (2006). The Carnegie Protein Trap Library: A Versatile Tool for Drosophila Developmental Studies. *Genetics* 175, 1505–1531.

Cai, D., Chen, S.-C., Prasad, M., He, L., Wang, X., Choesmel-Cadamuro, V., Sawyer, J. K., Danuser, G. and Montell, D. J. (2014). Mechanical Feedback through E-Cadherin Promotes Direction Sensing during Collective Cell Migration. *Cell* 157, 1146–1159.

Carmona-Fontaine, C., Matthews, H. K., Kuriyama, S., Moreno, M., Dunn, G. A., Parsons, M., Stern, C. D. and Mayor, R. (2008). Contact inhibition of locomotion in vivo controls neural crest directional migration. *Nature* 456, 957–961.

Carmona-Fontaine, C., Theveneau, E., Tzekou, A., Tada, M., Woods, M., Page, K. M., Parsons, M., Lambris, J. D. and Mayor, R. (2011). Complement Fragment C3a Controls Mutual Cell Attraction during Collective Cell Migration. *Dev. Cell* 21, 1026–1037.

Carrillo, R. A., Özkan, E., Menon, K. P., Nagarkar-Jaiswal, S., Lee, P.-T., Jeon, M., Birnbaum, M. E., Bellen, H. J., Garcia, K. C. and Zinn, K. (2015). Control of synaptic connectivity by a network of *Drosophila* IgSF cell surface proteins. *Cell* 163, 1770–1782.

Casazza, A., Fazzari, P. and Tamagnone, L. (2007). Semaphorin signals in cell adhesion and cell migration: functional role and molecular mechanisms. In *Semaphorins: Receptor and Intracellular Signaling Mechanisms,* (ed. Pasterkamp, R. Jeroen), pp. 90–108. New York, NY: Landes Bioscience and Springer Science.

Cetera, M. and Horne-Badovinac, S. (2015). Round and round gets you somewhere: collective cell migration and planar polarity in elongating Drosophila egg chambers. *Curr. Opin. Genet. Dev.* 32, 10–15.

Cetera, M., Ramirez-San Juan, G. R., Oakes, P. W., Lewellyn, L., Fairchild, M. J., Tanentzapf, G., Gardel, M. L. and Horne-Badovinac, S. (2014). Epithelial rotation promotes the global alignment of contractile actin bundles during *Drosophila* egg chamber elongation. *Nat. Commun.* 5, 5511.

Cetera, M., Lewellyn, L. and Horne-Badovinac, S. (2016). Cultivation and live imaging of *Drosophila* ovaries. In *Drosophila* (ed. Dahmann, C.), pp. 215–226. New York, NY: Springer.

Chagnon, M. J., Uetani, N. and Tremblay, M. L. (2004). Functional significance of the LAR receptor protein tyrosine phosphatase family in development and diseases. *Biochem. Cell Biol.* 82, 664–675.

Chang, Y.-C., Wu, J.-W., Hsieh, Y.-C., Huang, T.-H., Liao, Z.-M., Huang, Y.-S., Mondo, J. A., Montell, D. and Jang, A. C.-C. (2018). Rap1 Negatively Regulates the Hippo Pathway to Polarize Directional Protrusions in Collective Cell Migration. *Cell Rep.* 22, 2160–2175.

Chen, D.-Y., Lipari, K. R., Dehghan, Y., Streichan, S. J. and Bilder, D. (2016). Symmetry breaking in an edgeless epithelium by Fat2-regulated microtubule polarity. *Cell Rep.* 15, 1125–1133.

Chen, D.-Y., Crest, J. and Bilder, D. (2017). A cell migration tracking tool supports coupling of tissue rotation to elongation. *Cell Rep.* 21, 559–569.

Cheung, K. J., Padmanaban, V., Silvestri, V., Schipper, K., Cohen, J. D., Fairchild, A. N., Gorin, M. A., Verdone, J. E., Pienta, K. J., Bader, J. S., et al. (2016). Polyclonal breast cancer

metastases arise from collective dissemination of keratin 14-expressing tumor cell clusters. *Proc. Natl. Acad. Sci.* 113, E854–E863.

Chlasta, J., Milani, P., Runel, G., Duteyrat, J.-L., Arias, L., Lamiré, L.-A., Boudaoud, A. and Grammont, M. (2017). Variations in basement membrane mechanics are linked to epithelial morphogenesis. *Development* 144, 4350–4362.

Crest, J., Diz-Muñoz, A., Chen, D.-Y., Fletcher, D. A. and Bilder, D. (2017). Organ sculpting by patterned extracellular matrix stiffness. *eLife* 6, e24958.

Das, T., Safferling, K., Rausch, S., Grabe, N., Boehm, H. and Spatz, J. P. (2015). A molecular mechanotransduction pathway regulates collective migration of epithelial cells. *Nat. Cell Biol.* 17, 276–287.

Davidson, L. A., Hoffstrom, B. G., Keller, R. and DeSimone, D. W. (2002). Mesendoderm Extension and Mantle Closure in Xenopus laevis Gastrulation: Combined Roles for Integrin α5β1, Fibronectin, and Tissue Geometry. *Dev. Biol.* 242, 109–129.

De Pascalis, C. and Etienne-Manneville, S. (2017). Single and collective cell migration: the mechanics of adhesions. *Mol. Biol. Cell* 28, 1833–1846.

Deb Roy, A., Yin, T., Choudhary, S., Rodionov, V., Pilbeam, C. C. and Wu, Y. I. (2017). Optogenetic activation of Plexin-B1 reveals contact repulsion between osteoclasts and osteoblasts. *Nat. Commun.* 8, 15831.

Delon, I. and Brown, N. H. (2009). The integrin adhesion complex changes its composition and function during morphogenesis of an epithelium. *J. Cell Sci.* 122, 4363–4374.

Donà, E., Barry, J. D., Valentin, G., Quirin, C., Khmelinskii, A., Kunze, A., Durdu, S., Newton, L. R., Fernandez-Minan, A., Huber, W., et al. (2013). Directional tissue migration through a self-generated chemokine gradient. *Nature* 503, 285–289.

Doxzen, K., Vedula, S. R. K., Leong, M. C., Hirata, H., Gov, N. S., Kabla, A. J., Ladoux, B. and Lim, C. T. (2013). Guidance of collective cell migration by substrate geometry. *Integr. Biol.* 5, 1026.

Duan, Y., Wang, S.-H., Song, J., Mironova, Y., Ming, G., Kolodkin, A. L. and Giger, R. J. (2014). Semaphorin 5A inhibits synaptogenesis in early postnatal- and adult-born hippocampal dentate granule cells. *eLife* 3, e.04390.

Duchek, P. and Rørth, P. (2001). Guidance of cell migration by EGF receptor signaling during Drosophila oogenesis. *Science* 291, 131–133.

Duda, D. G., Duyverman, A. M. M. J., Kohno, M., Snuderl, M., Steller, E. J. A., Fukumura, D. and Jain, R. K. (2010). Malignant cells facilitate lung metastasis by bringing their own soil. *Proc. Natl. Acad. Sci.* 107, 21677–21682.

Duffy, J. B., Harrison, D. A. and Perrimon, N. (1998). Identifying loci required for follicular patterning using directed mosaics. *Development* 125, 2263–2271.

Duhart, J. C., Parsons, T. T. and Raftery, L. A. (2017). The repertoire of epithelial morphogenesis on display: progressive elaboration of *Drosophila* egg structure. *Mech. Dev.* 148, 18–39.

Eickholt, B. J., Mackenzie, S. L., Graham, A., Walsh, F. S. and Doherty, P. (1999). Evidence for collapsin-1 functioning in the control of neural crest migration in both trunk and hindbrain regions. 9.

Ewald, A. J., Brenot, A., Duong, M., Chan, B. S. and Werb, Z. (2008). Collective epithelial migration and cell rearrangements drive mammary branching morphogenesis. *Dev. Cell* 14, 570–581.

Fox, A. N. and Zinn, K. (2005). The Heparan Sulfate Proteoglycan Syndecan Is an In Vivo Ligand for the Drosophila LAR Receptor Tyrosine Phosphatase. *Curr. Biol.* 15, 1701–1711.

Frémont, S., Romet-Lemonne, G., Houdusse, A. and Echard, A. (2017). Emerging roles of MICAL family proteins – from actin oxidation to membrane trafficking during cytokinesis. *J. Cell Sci.* jcs.202028.

Friedl, P. and Gilmour, D. (2009). Collective cell migration in morphogenesis, regeneration and cancer. *Nat. Rev. Mol. Cell Biol.* 10, 445–457.

Friedl, P., Locker, J., Sahai, E. and Segall, J. E. (2012). Classifying collective cancer cell invasion. *Nat. Cell Biol.* 14, 777–783.

Frydman, H. M. and Spradling, A. C. (2001). The receptor-like tyrosine phosphatase Lar is required for epithelial planar polarity and for axis determination within *Drosophila* ovarian follicles. *Development* 128, 3209–3220.

Gaggioli, C., Hooper, S., Hidalgo-Carcedo, C., Grosse, R., Marshall, J. F., Harrington, K. and Sahai, E. (2007). Fibroblast-led collective invasion of carcinoma cells with differing roles for RhoGTPases in leading and following cells. *Nat. Cell Biol.* 9, 1392–1400.

Gammill, L. S., Gonzalez, C., Gu, C. and Bronner-Fraser, M. (2006). Guidance of trunk neural crest migration requires neuropilin 2/semaphorin 3F signaling. *Dev. Camb. Engl.* 133, 99–106.

Gerhardt, H., Golding, M., Fruttiger, M., Ruhrberg, C., Lundkvist, A., Abramsson, A., Jeltsch, M., Mitchell, C., Alitalo, K., Shima, D., et al. (2003). VEGF guides angiogenic sprouting utilizing endothelial tip cell filopodia. *J. Cell Biol.* 161, 1163–1177.

Giordano, S., Corso, S., Conrotto, P., Artigiani, S., Gilestro, G., Barberis, D., Tamagnone, L. and Comoglio, P. M. (2002). The Semaphorin 4D receptor controls invasive growth by coupling with Met. *Nat. Cell Biol.* 4, 720–724.

Giridharan, S. S. P., Rohn, J. L., Naslavsky, N. and Caplan, S. (2012). Differential regulation of actin microfilaments by human MICAL proteins. *J. Cell Sci.* 125, 614–624.

Goodrich, L. V. and Strutt, D. (2011). Principles of planar polarity in animal development. *Development* 138, 1877–1892.

Gratz, S. J., Cummings, A. M., Nguyen, J. N., Hamm, D. C., Donohue, L. K., Harrison, M. M., Wildonger, J. and O'Connor-Giles, K. M. (2013). Genome engineering of *Drosophila* with the CRISPR RNA-guided Cas9 nuclease. *Genetics* 194, 1029–1035.

Gratz, S. J., Ukken, F. P., Rubinstein, C. D., Thiede, G., Donohue, L. K., Cummings, A. M. and O'Connor-Giles, K. M. (2014). Highly specific and efficient CRISPR/Cas9-catalyzed homology-directed repair in *Drosophila*. *Genetics* 196, 961–971.

Gu, C. and Giraudo, E. (2013). The role of semaphorins and their receptors in vascular development and cancer. *Exp. Cell Res.* 319, 1306–1316.

Gutzeit, H. O. (1990). The microfilament pattern in the somatic follicle cells of mid-vitellogenic ovarian follicles of *Drosophila*. *Eur. J. Cell Biol.* 53, 349–356.

Gutzeit, H. O., Eberhardt, W. and Gratwohl, E. (1991). Laminin and basement membrane-associated microfilaments in wild-type and mutant *Drosophila* ovarian follicles. *J. Cell Sci.* 100, 781–788.

Haas, P. and Gilmour, D. (2006). Chemokine Signaling Mediates Self-Organizing Tissue Migration in the Zebrafish Lateral Line. *Dev. Cell* 10, 673–680.

Haigo, S. L. and Bilder, D. (2011). Global tissue revolutions in a morphogenetic movement controlling elongation. *Science* 331, 1071–1074.

Hamm, M. J., Kirchmaier, B. C. and Herzog, W. (2016). Sema3d controls collective endothelial cell migration by distinct mechanisms via Nrp1 and PlxnD1. *J. Cell Biol.* 215, 415–430.

Han, K. A., Jeon, S., Um, J. W. and Ko, J. (2016). Emergent synapse organizers: LAR-RPTPs and their companions. In *International Review of Cell and Molecular Biology* (ed. Jeon, Kwang W.), pp. 39–65. Elsevier.

Horne-Badovinac, S. (2014). The *Drosophila* egg chamber--a new spin on how tissues elongate. *Integr. Comp. Biol.* 54, 667–676.

Horne-Badovinac, S. (2017). Fat-like cadherins in cell migration—leading from both the front and the back. *Curr. Opin. Cell Biol.* 48, 26–32.

Horne-Badovinac, S. and Bilder, D. (2005). Mass transit: Epithelial morphogenesis in the *Drosophila* egg chamber. *Dev. Dyn.* 232, 559–574.

Horne-Badovinac, S., Hill, J., Gerlach, G., Menegas, W. and Bilder, D. (2012). A screen for round egg mutants in *Drosophila* identifies tricornered, furry, and misshapen as regulators of egg chamber elongation. *G3* 2, 371–378.

Huber, A. B., Kolodkin, A. L., Ginty, D. D. and Cloutier, J.-F. (2003). Signaling at the growth cone : Ligand-Receptor Complexes and the Control of Axon Growth and Guidance. *Annu. Rev. Neurosci.* 26, 509–563.

Hulpiau, P. and van Roy, F. (2011). New insights into the evolution of metazoan cadherins. *Mol. Biol. Evol.* 28, 647–657.

Humphries, A. C. and Mlodzik, M. (2018). From instruction to output: Wnt/PCP signaling in development and cancer. *Curr. Opin. Cell Biol.* 51, 110–116.

Hung, R.-J. and Terman, J. R. (2011). Extracellular inhibitors, repellents, and Semaphorin/Plexin/MICAL-mediated Actin filament disassembly. *Cytoskeleton* 68, 415.

Hung, R.-J., Yazdani, U., Yoon, J., Wu, H., Yang, T., Gupta, N., Huang, Z., van Berkel, W. J. H. and Terman, J. R. (2010). Mical links semaphorins to F-actin disassembly. *Nature* 463, 823–827.

Hung, R.-J., Pak, C. W. and Terman, J. R. (2011). Direct redox regulation of F-actin assembly and disassembly by Mical. *Science* 334, 1710–1713.

Isabella, A. J. and Horne-Badovinac, S. (2015). Dynamic regulation of basement membrane protein levels promotes egg chamber elongation in *Drosophila*. *Dev. Biol.* 406, 212–221.

Isabella, A. J. and Horne-Badovinac, S. (2016). Rab10-mediated secretion synergizes with tissue movement to build a polarized basement membrane architecture for organ morphogenesis. *Dev. Cell* 38, 47–60.

Janssen, B. J. C., Robinson, R. A., Pérez-Brangulí, F., Bell, C. H., Mitchell, K. J., Siebold, C. and Jones, E. Y. (2010). Structural basis of semaphorin–plexin signalling. *Nature* 467, 1118–1122.

Johnson, K. G., Tenney, A. P., Ghose, A., Duckworth, A. M., Higashi, M. E., Parfitt, K., Marcu, O., Heslip, T. R., Marsh, J. L., Schwarz, T. L., et al. (2006). The HSPGs Syndecan and Dallylike bind the receptor phosphatase LAR and exert distinct effects on synaptic development. *Neuron* 49, 517–531.

Jongbloets, B. C. and Pasterkamp, R. J. (2014). Semaphorin signaling during development. *Development* 141, 3292–3297.

Kantor, D. B., Chivatakarn, O., Peer, K. L., Oster, S. F., Inatani, M., Hansen, M. J., Flanagan, J. G., Yamaguchi, Y., Sretavan, D. W., Giger, R. J., et al. (2004). Semaphorin 5A Is a bifunctional axon guidance cue regulated by heparan and chondroitin sulfate proteoglycans. *Neuron* 44, 961–975.

Kerjan, G., Dolan, J., Haumaitre, C., Schneider-Maunoury, S., Fujisawa, H., Mitchell, K. J. and Chédotal, A. (2005). The transmembrane semaphorin Sema6A controls cerebellar granule cell migration. *Nat. Neurosci.* 8, 1516–1524.

Kolodkin, A. L. and Tessier-Lavigne, M. (2011). Mechanisms and molecules of neuronal wiring: a primer. *Cold Spring Harb. Perspect. Biol.* 3, a001727–a001727.

Kolodkin, A. L., Matthes, D. J., O'Connor, T. P., Patel, N. H., Admon, A., Bentley, D. and Goodman, C. S. (1992). Fasciclin IV: Sequence, expression, and function during growth cone guidance in the grasshopper embryo. *Neuron* 9, 831–845.

Kruger, R. P., Aurandt, J. and Guan, K.-L. (2005). Semaphorins command cells to move. *Nat. Rev. Mol. Cell Biol.* 6, 789–800.

Ladoux, B. and Mège, R.-M. (2017). Mechanobiology of collective cell behaviours. *Nat. Rev. Mol. Cell Biol.* 18, 743–757.

Lebreton, G. and Casanova, J. (2014). Specification of leading and trailing cell features during collective migration in the Drosophila trachea. *J. Cell Sci.* 127, 465–474.

Lewellyn, L., Cetera, M. and Horne-Badovinac, S. (2013). Misshapen decreases integrin levels to promote epithelial motility and planar polarity in *Drosophila*. *J. Cell Biol.* 200, 721–729.

Li, X. and Lee, A. Y. W. (2010a). Semaphorin 5A and plexin-B3 inhibit human glioma cell motility through RhoGDIalpha-mediated inactivation of Rac1 GTPase. *J. Biol. Chem.* 285, 32436–32445.

Li, X. and Lee, A. Y. W. (2010b). Semaphorin 5A and Plexin-B3 inhibit human glioma cell motility through RhoGDIα-mediated inactivation of Rac1 GTPase. *J. Biol. Chem.* 285, 32436–32445.

Li, X., Law, J. W. S. and Lee, A. Y. W. (2012). Semaphorin 5A and Plexin-B3 regulate human glioma cell motility and morphology through Rac1 and the Actin cytoskeleton. *Oncogene* 31, 595–610.

Lintz, M., Muñoz, A. and Reinhart-King, C. A. (2017). The Mechanics of single cell and collective migration of tumor cells. *J. Biomech. Eng.* 139,.

Liu, C.-Y. and Kao, W. W.-Y. (2015). Corneal epithelial wound healing. *Prog. Mol. Biol. Transl. Sci.* 134, 61–71.

Liu, H., Juo, Z. S., Shim, A. H.-R., Focia, P. J., Chen, X., Garcia, K. C. and He, X. (2010). Structural Basis of Semaphorin-Plexin Recognition and Viral Mimicry from Sema7A and A39R Complexes with PlexinC1. *Cell* 142, 749–761.

Luo, Y., Raible, D. and Raper, J. A. (1993). Collapsin: A protein in brain that induces the collapse and paralysis of neuronal growth cones. *Cell* 75, 217–227.

Mason, B. N., Califano, J. P. and Reinhart-King, C. A. (2012). Matrix stiffness: a regulator of cellular behavior and tissue formation. In *Engineering Biomaterials for Regenerative Medicine* (ed. Bhatia, S. K.), pp. 19–37. New York, NY: Springer.

Matsuoka, R. L., Chivatakarn, O., Badea, T. C., Samuels, I. S., Cahill, H., Katayama, K., Kumar, S. R., Suto, F., Chédotal, A., Peachey, N. S., et al. (2011). Class 5 transmembrane semaphorins control selective mammalian retinal lamination and function. *Neuron* 71, 460–473.

Mayor, R. and Etienne-Manneville, S. (2016). The front and rear of collective cell migration. *Nat. Rev. Mol. Cell Biol.* 17, 97–109.

McDonald, J. A., Pinheiro, E. M. and Montell, D. J. (2003). PVF1, a PDGF/VEGF homolog, is sufficient to guide border cells and interacts genetically with Taiman. *Dev. Camb. Engl.* 130, 3469–3478.

McDonald, J. A., Pinheiro, E. M., Kadlec, L., Schupbach, T. and Montell, D. J. (2006). Multiple EGFR ligands participate in guiding migrating border cells. *Dev. Biol.* 296, 94–103.

Meltzer, S., Yadav, S., Lee, J., Soba, P., Younger, S. H., Jin, P., Zhang, W., Parrish, J., Jan, L. Y. and Jan, Y.-N. (2016). Epidermis-derived semaphorin promotes dendrite self-avoidance by regulating dendrite-substrate adhesion in *Drosophila* sensory neurons. *Neuron* 89, 741–755.

Michaelis, U. R. (2014). Mechanisms of endothelial cell migration. *Cell. Mol. Life Sci.* 71, 4131–4148.

Montell, D. J. (2003). Border-cell migration: the race is on. *Nat. Rev. Mol. Cell Biol.* 4, 13–24.

Morinaka, A., Yamada, M., Itofusa, R., Funato, Y., Yoshimura, Y., Nakamura, F., Yoshimura, T., Kaibuchi, K., Goshima, Y., Hoshino, M., et al. (2011). Thioredoxin mediates oxidation-dependent phosphorylation of CRMP2 and growth cone collapse. *Sci. Signal.* 4, ra26.

Munoz-Soriano, V., Belacortu, Y. and Paricio, N. (2012). Planar Cell Polarity Signaling in Collective Cell Movements During Morphogenesis and Disease. *Curr. Genomics* 13, 609–622.

Nakamura, F., Okada, T., Shishikura, M., Uetani, N., Taniguchi, M., Yagi, T., Iwakura, Y., Ohshima, T., Goshima, Y. and Strittmatter, S. M. (2017). Protein tyrosine phosphatase δ mediates the Sema3A-induced cortical basal dendritic arborization through the activation of Fyn tyrosine kinase. *J. Neurosci.* 37, 7125–7139.

Oinuma, I., Ishikawa, Y., Katoh, H. and Negishi, M. (2004). The Semaphorin 4D receptor Plexin-B1 is a GTPase activating protein for R-Ras. *Science* 305, 862–865.

Oinuma, I., Katoh, H. and Negishi, M. (2006). Semaphorin 4D/Plexin-B1–mediated R-Ras GAP activity inhibits cell migration by regulating β_1 integrin activity. *J. Cell Biol.* 173, 601–613.

Özkan, E., Carrillo, R. A., Eastman, C. L., Weiszmann, R., Waghray, D., Johnson, K. G., Zinn, K., Celniker, S. E. and Garcia, K. C. (2013). An extracellular interactome of immunoglobulin and LRR proteins reveals receptor-ligand networks. *Cell* 154, 228–239.

Pasterkamp, R. J., Peschon, J. J., Spriggs, M. K. and Kolodkin, A. L. (2003). Semaphorin 7A promotes axon outgrowth through integrins and MAPKs independent of plexinC1, which was a good candidate to be it's receptor. instead it uses integrins, but sema7a has an RGD domain, a known integrin binding motif. 424, 10.

Pecot, M. Y., Tadros, W., Nern, A., Bader, M., Chen, Y. and Zipursky, S. L. (2013). Multiple interactions control synaptic layer specificity in the *Drosophila* visual system. *Neuron* 77, 299–310.

Pollitt, A. Y. and Insall, R. H. (2009). WASP and SCAR/WAVE proteins: the drivers of actin assembly. *J. Cell Sci.* 122, 2575–2578.

Prasad, M., Jang, A. C.-C., Starz-Gaiano, M., Melani, M. and Montell, D. J. (2007). A protocol for culturing *Drosophila* melanogaster stage 9 egg chambers for live imaging. *Nat. Protoc.* 2, 2467–2473.

Rezakhaniha, R., Agianniotis, A., Schrauwen, J. T. C., Griffa, A., Sage, D., Bouten, C. V. C., van de Vosse, F. N., Unser, M. and Stergiopulos, N. (2012). Experimental investigation of collagen waviness and orientation in the arterial adventitia using confocal laser scanning microscopy. *Biomech. Model. Mechanobiol.* 11, 461–473.

Ridley, A. J. (2003). Cell Migration: Integrating Signals from Front to Back. *Science* 302, 1704–1709.

Ridley, A. J. (2011). Life at the Leading Edge. *Cell* 145, 1012–1022.

Rørth, P. (2009). Collective Cell Migration. *Annu. Rev. Cell Dev. Biol.* 25, 407–429.

Rørth, P. (2012). Fellow travellers: emergent properties of collective cell migration. *EMBO Rep.* 13, 984–991.

Ruhrberg, C. and Schwarz, Q. (2010). In the beginning: generating neural crest cell diversity. *Cell Adhes. Migr.* 4, 622–630.

Sadanandam, A., Rosenbaugh, E. G., Singh, S., Varney, M. and Singh, R. K. (2010). Semaphorin 5A promotes angiogenesis by increasing endothelial cell proliferation, migration, and decreasing apoptosis. *Microvasc. Res.* 79, 1–9.

Sadeqzadeh, E., de Bock, C. E. and Thorne, R. F. (2014). Sleeping Giants: Emerging Roles for the Fat Cadherins in Health and Disease. *Med. Res. Rev.* 34, 190–221.

Scarpa, E. and Mayor, R. (2016). Collective cell migration in development. *J. Cell Biol.* 212, 143–155.

Schindelin, J., Arganda-Carreras, I., Frise, E., Kaynig, V., Longair, M., Pietzsch, T., Preibisch, S., Rueden, C., Saalfeld, S., Schmid, B., et al. (2012). Fiji: an open-source platform for biological-image analysis. *Nat. Methods* 9, 676–682.

Schmidt, E. F., Shim, S.-O. and Strittmatter, S. M. (2008). Release of MICAL Autoinhibition by Semaphorin-Plexin Signaling Promotes Interaction with Collapsin Response Mediator Protein. *J. Neurosci.* 28, 2287–2297.

Schneider, C. A., Rasband, W. S. and Eliceiri, K. W. (2012). NIH Image to ImageJ: 25 years of image analysis. *Nat. Methods* 9, 671–675.

Serini, G., Valdembri, D., Zanivan, S., Morterra, G., Burkhardt, C., Caccavari, F., Zammataro, L., Primo, L., Tamagnone, L., Logan, M., et al. (2003). Class 3 semaphorins control vascular morphogenesis by inhibiting integrin function. 424, 8.

Shaw, T. J. and Martin, P. (2016). Wound repair: a showcase for cell plasticity and migration. *Curr. Opin. Cell Biol.* 42, 29–37.

Sidhaye, J. and Norden, C. (2017). Concerted action of neuroepithelial basal shrinkage and active epithelial migration ensures efficient optic cup morphogenesis. *eLife* 6, e22689.

Squarr, A. J., Brinkmann, K., Chen, B., Steinbacher, T., Ebnet, K., Rosen, M. K. and Bogdan, S. (2016). Fat2 acts through the WAVE regulatory complex to drive collective cell migration during tissue rotation. *J. Cell Biol.* 212, 591–603.

Stramer, B. and Mayor, R. (2016). Mechanisms and in vivo functions of contact inhibition of locomotion. *Nat. Rev. Mol. Cell Biol.*

Sweeney, L. B., Couto, A., Chou, Y.-H., Berdnik, D., Dickson, B. J., Luo, L. and Komiyama, T. (2007). Temporal target restriction of olfactory receptor neurons by Semaphorin-1a/PlexinA-mediated axon-axon interactions. *Neuron* 53, 185–200.

Takamatsu, H., Takegahara, N., Nakagawa, Y., Tomura, M., Taniguchi, M., Friedel, R. H., Rayburn, H., Tessier-Lavigne, M., Yoshida, Y., Okuno, T., et al. (2010). Semaphorins guide the entry of dendritic cells into the lymphatics by activating Myosin II. *Nat. Immunol.* 11, 594–600.

Tamagnone, L. and Comoglio, P. M. (2004). To move or not to move? *EMBO Rep.* 5, 356–361.

Tanner, K., Mori, H., Mroue, R., Bruni-Cardoso, A. and Bissell, M. J. (2012). Coherent angular motion in the establishment of multicellular architecture of glandular tissues. *Proc. Natl. Acad. Sci.* 109, 1973–1978.

Terman, J. R., Mao, T., Pasterkamp, R. J., Yu, H.-H. and Kolodkin, A. L. (2002). MICALs, a family of conserved flavoprotein oxidoreductases, function in plexin-mediated axonal repulsion. *Cell* 109, 887–900.

Theveneau, E. and Mayor, R. (2012). Neural crest migration: interplay between chemorepellents, chemoattractants, contact inhibition, epithelial-mesenchymal transition, and collective cell migration. *Wiley Interdiscip. Rev. Dev. Biol.* 1, 435–445.

Theveneau, E., Marchant, L., Kuriyama, S., Gull, M., Moepps, B., Parsons, M. and Mayor, R. (2010). Collective Chemotaxis Requires Contact-Dependent Cell Polarity. *Dev. Cell* 19, 39–53.

Theveneau, E., Steventon, B., Scarpa, E., Garcia, S., Trepat, X., Streit, A. and Mayor, R. (2013). Chase-and-run between adjacent cell populations promotes directional collective migration. *Nat. Cell Biol.* 15, 763–772.

Tojkander, S., Gateva, G. and Lappalainen, P. (2012). Actin stress fibers - assembly, dynamics and biological roles. *J. Cell Sci.* 125, 1855–1864.

Toyofuku, T., Zhang, H., Kumanogoh, A., Takegahara, N., Suto, F., Kamei, J., Aoki, K., Yabuki, M., Hori, M., Fujisawa, H., et al. (2004a). Dual roles of Sema6D in cardiac morphogenesis through region-specific association of its receptor, Plexin-A1, with off-track and vascular endothelial growth factor receptor type 2. *Genes Dev.* 18, 435–447.

Toyofuku, T., Zhang, H., Kumanogoh, A., Takegahara, N., Yabuki, M., Harada, K., Hori, M. and Kikutani, H. (2004b). Guidance of myocardial patterning in cardiac development by Sema6D reverse signalling. *Nat. Cell Biol.* 6, 1204–1211.

Tran, T. S., Kolodkin, A. L. and Bharadwaj, R. (2007). Semaphorin regulation of cellular morphology. *Annu. Rev. Cell Dev. Biol.* 23, 263–292.

van Rijn, A., Paulis, L., te Riet, J., Vasaturo, A., Reinieren-Beeren, I., van der Schaaf, A., Kuipers, A. J., Schulte, L. P., Jongbloets, B. C., Pasterkamp, R. J., et al. (2016). Semaphorin 7A promotes chemokine-driven dendritic cell migration. *J. Immunol.* 196, 459–468.

Vasilyev, A., Liu, Y., Mudumana, S., Mangos, S., Lam, P.-Y., Majumdar, A., Zhao, J., Poon, K.-L., Kondrychyn, I., Korzh, V., et al. (2009). Collective cell migration drives morphogenesis of the kidney nephron. *PLoS Biol.* 7, e9.

Viktorinová, I. and Dahmann, C. (2013). Microtubule polarity predicts direction of egg chamber rotation in *Drosophila*. *Curr. Biol.* 23, 1472–1477.

Viktorinova, I., Konig, T., Schlichting, K. and Dahmann, C. (2009). The cadherin Fat2 is required for planar cell polarity in the *Drosophila* ovary. *Development* 136, 4123–4132.

Wang, X., He, L., Wu, Y. I., Hahn, K. M. and Montell, D. J. (2010). Light-mediated activation reveals a key role for Rac in collective guidance of cell movement in vivo. *Nat. Cell Biol.* 12, 591–597.

Wang, H., Lacoche, S., Huang, L., Xue, B. and Muthuswamy, S. K. (2013). Rotational motion during three-dimensional morphogenesis of mammary epithelial acini relates to laminin matrix assembly. *Proc. Natl. Acad. Sci.* 110, 163–168.

Weber, G. F., Bjerke, M. A. and DeSimone, D. W. (2012). A Mechanoresponsive Cadherin-Keratin Complex Directs Polarized Protrusive Behavior and Collective Cell Migration. *Dev. Cell* 22, 104–115.

Winberg, M. L., Noordermeer, J. N., Tamagnone, L., Comoglio, P. M., Spriggs, M. K., Tessier-Lavigne, M. and Goodman, C. S. (1998). Plexin A is a neuronal semaphorin receptor that controls axon guidance. *Cell* 95, 903–916.

Wu, Z., Sweeney, L. B., Ayoob, J. C., Chak, K., Andreone, B. J., Ohyama, T., Kerr, R., Luo, L., Zlatic, M. and Kolodkin, A. L. (2011). A combinatorial semaphorin code instructs the initial steps of sensory circuit assembly in the *Drosophila* CNS. *Neuron* 70, 281–298.

Xia, J., Swiercz, J. M., Bañón-Rodríguez, I., Matković, I., Federico, G., Sun, T., Franz, T., Brakebusch, C. H., Kumanogoh, A., Friedel, R. H., et al. (2015). Semaphorin-Plexin Signaling Controls Mitotic Spindle Orientation during Epithelial Morphogenesis and Repair. *Dev. Cell* 33, 299–313.

Yazdani, U. and Terman, J. R. (2006). The semaphorins. *Genome Biol.* 7, 211.

Yoo, S. K., Pascoe, H. G., Pereira, T., Kondo, S., Jacinto, A., Zhang, X. and Hariharan, I. K. (2016). Plexins function in epithelial repair in both *Drosophila* and zebrafish. *Nat. Commun.* 7, 12282.

Yu, H.-H. and Moens, C. B. (2005). Semaphorin signaling guides cranial neural crest cell migration in zebrafish. *Dev. Biol.* 280, 373–385.

Zang, Y., Wan, M., Liu, M., Ke, H., Ma, S., Liu, L.-P., Ni, J.-Q. and Carlos Pastor-Pareja, J. (2015). Plasma membrane overgrowth causes fibrotic collagen accumulation and immune activation in *Drosophila* adipocytes. *eLife* 4, e.07187.

Zegers, M. M. and Friedl, P. (2014). Rho GTPases in collective cell migration. *Small GTPases* 5,.